MACROPHAGE POLARIZATION AND NITRIC OXIDE MECHANISMS IN LYMPHATIC DYSFUNCTION IN A RAT MODEL OF METABOLIC SYNDROME

A Dissertation

by

SCOTT DAVID ZAWIEJA

Submitted to the Office of Graduate and Professional Studies of
Texas A&M University
in partial fulfillment of the requirements for the degree of

DOCTOR OF PHILOSOPHY

Chair of Committee,	Mariappan Muthuchamy
Committee Members,	Cynthia J. Meininger
	M. Karen Newell-Rogers
	Robert Alaniz
Head of Department,	Van Wilson

December 2014

Major Subject: Medical Sciences

ABSTRACT

Metabolic syndrome (MetSyn) is the clustering of multiple metabolic disorders that further increase the risk for cardiovascular disease and has been recently linked to poor lymphatic function. The lymphatic system plays a crucial role in maintaining oncotic balance and returning excess fluid and macromolecules back to the blood circulation. In this dissertation we addressed the role of macrophage polarization and nitric oxide mechanisms in lymphatic dysfunction in a rat model of MetSyn. We hypothesized that mesenteric lymphatic vessel dysfunction would be associated with a polarization switch of resident macrophages after induction of peritonitis or metabolic syndrome. We used an intra-peritoneal injection of lipopolysaccharide (LPS) to simulate peritonitis in the rat and a seven-week high fructose-feeding regime to induce the MetSyn. We distinguished macrophage polarization and recruitment to the lymphatic collecting vessels using immunofluorescence and a combination of CD163, CD206, and major histocompatibility complex II (MHCII) expression. We determined the intrinsic mesenteric lymphatic contractility using the isolated mesenteric lymphatic vessel isobaric preparation. LPS-induced peritonitis increased the macrophage accumulation two fold and increased both $CD163^{+}CD206^{+}$ and $CD163^{-}CD206^{+}$ cell populations and had severely impaired lymphatic contractility. We also found evidence for a phenotype switch from $CD163^{+}MHCII^{-}$ M2 macrophages to a M1 skewed $CD163^{+}MHCII^{+}$ phenotype in the MetSyn rats and impaired lymphatic contractility. Additionally, cultured lymphatic endothelial and muscle cells were found to express macrophage

maturation and expansion markers in response to LPS stimulation. We also examined the role of nitric oxide in the contractile regulation of lymphatic thoracic ducts isolated from MetSyn rats. We found a reduced flow-dependent inhibition of contractility in metabolic syndrome thoracic ducts despite a normal response to the exogenous nitric oxide donor S-nitro-N-acetylpenicillamine (SNAP). The reactive oxygen species scavenging agent 4-hydroxy-2,2,6,6-tetramethylpiperidine-N-oxyl (TEMPOL) did not restore flow sensitivity, however control vessels treated with the nitric oxide synthase inhibitor L-N^G-nitro arginine methyl ester (LNAME) had comparable flow inhibition to MetSyn thoracic ducts. Western blots of thoracic ducts revealed a 60% reduction in the expression of eNOS, which can explain the loss of shear sensitivity. Thus, this study demonstrates the mechanisms that underlie lymphatic dysfunction in the MetSyn.

DEDICATION

This dissertation is dedicated to my family, as they have been my support and anchor throughout my life.

ACKNOWLEDGEMENTS

I would like to thank my committee chair, Dr. Muthuchamy, and my committee members, Dr. Meininger, Dr. Newell, Dr. Alaniz, for their guidance and support throughout the course of this research.

I would also like to thank Dr. Gashev, Dr. Ed Childs and Dr. Zawieja for their support and advice.

I would like to thank the wonderful coworkers who have had the patience and understanding to help me along this process: Dr. Wei Wang for his humor and technical assistance, Dr. Olga Gasheva and Dr. Zhanna Nepiyushchikh for their extensive time training my hands in lymphatic functional preps, Dr. Sanjukta Chakraborty who has been instrumental in the progress of my research, Dr. Victor Chatterjee for our discussions and friendship, and Dr. Walter Cromer for his support with techniques and encouragement.

I would also like to thank the office staff for all the help with those last hour rushes. Thank you Stephanie Hilliard, Tina Mendoza, Laura Daniel, Starla Clover for your patience and support.

To all my fellow graduate students and the faculty of this department who have made this department home I thank you from the bottom of my heart.

I would like to thank Dr. Harris Granger for establishing such a productive and supportive department.

TABLE OF CONTENTS

Page

CHAPTER Page

LIST OF FIGURES

FIGURE Page

FIGURE Page

LIST OF TABLES

CHAPTER I

INTRODUCTION *

Rationale

Obesity has reached epidemic proportions as it affects over one third of the United States population. Obesity is defined as having a body mass index ≥30 (237). Obesity predisposes the patient to other metabolic related disorders such as hypertension, diabetes, stroke, kidney disease, and cardiovascular disease (CVD) and accrues an estimated $147 billion in annual medical costs (1, 114, 115). Importantly, obesity appears to be the strongest link to the development of the metabolic syndrome, which is diagnosed when the patient fulfills at least 3 of the following 5 criteria: blood pressure over 130/85, fasting blood glucose >100mg/dl, serum triglycerides >150mg/dl, HDL cholesterol <40mg/dl, and abdominal obesity (40inches men, 35inches women) (114). Patients that develop the metabolic syndrome are at a higher risk for developing fulminant type II diabetes mellitus (TIIDM), kidney failure, and are at greater risk for adverse cardiovascular events than the sum of the individual risk factors alone (175, 199). Additionally, up to 85% of patients with TIIDM also fall under the metabolic syndrome spectrum (153). While the diagnosis was initially controversial, the metabolic syndrome is now readily accepted as a disease state with appreciated risks that have spread globally in parallel with obesity. The metabolic syndrome increases the risk of developing CVD by over three fold and the associated mortality of CVD increases up to five fold higher (175). Cardiovascular impairment is the leading cause of mortality from

the metabolic syndrome with dysfunction of both the micro- and macro-vessel blood vasculature and impaired heart function (21, 46, 69, 194, 294). However, little work has addressed the impact on the lymphatic vasculature and function that is critical to maintaining tissue fluid and macromolecule homeostasis, immunity, and the prevention and resolution of edema (38).

Failure of lymphatic function results in chronic and progressive swelling termed lymphedema that can be the result of genetic abnormalities or vessel damage (256-258). Obesity is a historical risk factor for post-operative lymphedema in cancer patients (126, 208). Additionally, obesity has been characterized as a mild edematous state with excess water retention and swelling, which suggests lymphatic insufficiency (23, 272). Yet little work has been completed to increase our understanding of the role lymphatic function in metabolic syndrome. Many of these phenomena have been prescribed to venous insufficiency with little interest to lymphatic function despite the role lymphatic vessels play in maintaining fluid and macromolecule homeostasis in the tissue (225, 336). The link between obesity and lymphatic dysfunction has recently crystallized in the appearance of a previously rare medical condition called massive localized lymphedema (MLL) that affects up to 80% of morbidly obese patients (12, 18, 41, 81, 111, 144, 193, 214). MLL has dramatically risen in occurrence with the rise of the morbidly obese population, which fit the diagnosis parameters for the metabolic syndrome (86, 87). Furthermore, genetic models of lymphatic disruption or direct physical ablation often result in expansion and hypertrophy of adipose tissue or fulminant obesity (13, 125, 208, 349). Lymphatic vessels that drain adipose tissue also show reduced macromolecule

clearance in obese patients (9). This dissertation seeks to review the current literature regarding the links that exist between metabolic syndrome factors and lymphatic function, and provide the independent research carried out to further address this association.

Hyperglycemia and the Insulin Resistant State in Metabolic Syndrome

Circulating blood glucose concentration is maintained at approximately 5mM (90mg/dl) by the action of two different peptide hormones, insulin and glucagon. They are produced by beta cells and alpha cells, respectively, found in the islet of Langerhans of the pancreas. Insulin is released when blood glucose concentrations are high and promotes glucose uptake and inhibits gluconeogenesis, the endogenous production of glucose by the liver. In contrast, glucagon stimulates gluconeogenesis and is critical for preventing fasting blood glucose levels from dropping too low. The metabolic syndrome state is characterized as a chronic hyperinsulinemic and hyperglycemic state especially in the post-prandial, or fed, state (21). Glucose levels rise in the post-prandial state from nutritional absorption and transport to the blood through the portal circulation. Insulin stimulates glucose uptake through the translocation of glucose transporter 4 (Glut4) to the cellular membrane in skeletal muscle and adipose tissue, which are responsible for approximately 80% and 5% of post-prandial glucose uptake, respectively (64).

Beta cells secrete insulin in response to an inhibition of adenosine triphosphate (ATP) sensitive potassium channels (K_{ATP}) as ATP builds up within the cell. These channels allow potassium ions to move down their concentration gradient out of the cell

and thus hyperpolarize the beta cell's membrane, making membrane potential more negative (30, 44). As glucose in the blood rises, intracellular glucose metabolism concomitantly increases in the beta cell due to transport via glucose transporter 2 (Glut2) in rodents and Glut1 in humans (62). Metabolism of the influx of glucose increases the ATP concentration within the cell, which will block the efflux of potassium out of the cell through K_{ATP} channels (44). Cellular membrane potential increases with accumulation of potassium and it reaches a threshold that stimulates plasma membrane voltage gated calcium channels to allow calcium entry into the cell (44). Calcium influx regulates the fusion of vesicles to the plasma membrane and insulin is ultimately secreted.

The metabolic syndrome is characterized as a chronic but mild inflammatory state that is propagated by over-nutrition and progressive insulin resistance. Insulin resistance is the decreased sensitivity of circulating insulin and requires a higher secretion of insulin to respond to a glucose challenge and explains why patients have both elevated insulin and glucose levels (24, 131, 134, 283, 297). Insulin resistance is mediated by a loss of insulin receptor substrate -1 (IRS-1) availability, or inhibition of insulin receptor autophosphorylation, or inhibition of phosphorylation (135, 136). The insulin receptor is a member of the receptor tyrosine kinase family that resides as a dimer on the plasma membrane and undergoes a conformational shift, and subsequently autophosphorylation, in response to binding insulin. Autophosphorylation of the insulin receptor complex results in the recruitment of the IRS-1 and IRS-2, which are themselves targets for phosphorylation. Ultimately, insulin will increase the

translocation of the glucose transporter Glut4 to the cell membrane and increase the internalization of glucose from the circulation. Disruption of this phosphorylation cascade prevents proper insulin signaling and glucose uptake by the skeletal muscle and adipose, which account for over 80% of the glucose removal in the post-prandial state and results in the post-prandial hyperglycemia in the metabolic syndrome (64). Insulin insensitivity also has a profound effect on the fasting blood sugar levels due to a loss of repression of the gluconeogenic action in the liver (117).

Insulin signals primarily through the IRS-1-mediated activation of phospho-inositide 3 kinase (PI3K) (117). PI3K converts the phosphatidylinositol (3,4)-bisphosphate (PIP2) to phosphatidylinositol (3,4,5)-trisphosphate (PIP3) (117). Protein kinase B (PKB), also known as AKT, will bind to the membrane phospholipid PIP3 resulting in its activation. Activation of AKT inhibits the tuberous sclerosis complex 1 and 2 (TSC1/2) repression of the mammalian target of rapamycin complex 1(mTORC1), which is a critical positive regulator of cellular anabolic processes (117). Insulin also inhibits the gluconeogenic action of the liver and insulin resistance results in excessive gluconeogenesis. Glucose 6-phosphatase (G6p) is a critical enzyme in the gluconeogenic process that is under transcriptional control of the forkhead box protein O1, which is inhibited and targeted for destruction by active AKT. This has been linked with nonalcoholic fatty liver disease, liver steatosis, and hepatic over production of triglyceride rich low density or very low-density lipoproteins (149, 231, 247, 261, 302).

Physiological insulin resistance is part of the negative feedback mechanism to regulate nutrient uptake of the cell as a function of its nutrient state. S6 kinase is an

effector of the mTORC1 pathway and will negatively regulate IRS-1 through phosphorylation on serine residues. Conversely, cells that are "starved" or nutrient-deficient will have high adenosine monophosphate to adenosine triphosphate levels (AMP/ATP) levels (33, 259). When cellular AMP rises, it activates the AMP kinase (AMPK) that opposes effects of AKT in regards to mTORC1 activation through activation of TSC1/2 (309). Pathophysiological insulin resistance can also be derived from cellular stress and inflammatory cytokine production (134). Liver insulin insensitivity has been linked with chronic sub-clinical inflammation, elevated fatty acid flux, and elevated expression C–reactive protein (CRP) (5, 68, 188, 231, 346). CRP is produced by hepatocytes in response to IL-6 stimulation of toll like receptor (TLR) activation, including activation by dietary endotoxin (96, 275, 290). Rodent models of metabolic syndrome have demonstrated a critical role for dietary endotoxin transport through the portal circulation in the pathogenesis of liver inflammation and damage in obesity and metabolic syndrome models (96, 157, 275, 290, 299, 325). CRP is a potent inflammatory molecule that is part of the acute phase response and has been linked with TIIDM, stroke, atherosclerosis, and insulin resistance in muscle and endothelial cells (236, 252, 347). Hepatocytes and liver macrophages, Kupffer cells, have an elevated production of IL-6 in models of obesity and metabolic syndrome (60, 78, 282). IL-6 specifically activates expression of suppressor of cytokine signaling 3 (SOCS3), which acts to prevent the autophosphorylation of the insulin receptor and phosphorylation of the IRS-1, thereby contributing to insulin resistance (148, 162, 243). Tumor necrosis factor-α (TNFα) is another inflammatory cytokine that has potent insulin desensitizing

actions through inhibitory phosphorylation of IRS-1 at the serine residues (131). Inflammation within the adipose tissue is a large source of TNFα production in obesity and metabolic syndrome and exacerbates the insulin resistance in the adipose tissue (134, 135, 137).

Obesity and Adipose Inflammation in the Metabolic Syndrome

The strongest risk factor correlated with the development of metabolic syndrome is obesity and the expansion of adipose tissue, particularly the visceral fat in the abdominal cavity (114). Excess nutrient storage and adipose dysfunction are hallmarks of the metabolic syndrome and inflammatory state (19, 140, 341). Adipose tissue is primarily composed of adipocytes volumetrically, but is also host to fibroblast, pre-adipocytes, innate and adaptive immune cells, and cells from the microvasculature. Adipocytes are the body's main site of energy storage in the form of vesicles filled with triglycerides and cholesterol and play a key role in the regulation of satiety and energy flux (4).

Adipocytes respond to insulin stimulation with glucose uptake through Glut4 translocation and also fatty acid uptake through translocation of fatty acid transport protein 1 (FATP1) to the outer membrane (339). While the liver is the primary site of *de novo* lipogenesis, a modest amount occurs in the adipose tissue as well (71). However, the glucose uptake in response to insulin stimulation is primarily intended to provide the substrate for glyceroneogenesis. The adipocytes utilize glycerol for esterification of absorbed fatty acids into triglycerides that are stored in specialized vacuoles called lipid

droplets. Fatty acids can be absorbed basally by diffusion through the cell membrane but translocation of FATP1 to the membrane increases fatty acid capture and absorption. Cleavage of circulating triglycerides to glycerol and fatty acids is performed by lipoprotein lipase, which is also under regulation by insulin (289, 304). Peroxisome proliferator activated receptor gamma (PPARγ) and sterol regulatory element binding protein 1c (SREBP1c) are two critical regulators of fatty acid uptake and storage and adipocyte development that is positively regulated by insulin (333). PPARγ positively correlates with the expansion of the adipose tissue and the differentiation of the pre-adipocytes into mature adipocytes (147, 313). However, therapeutic activation of PPARγ restores insulin sensitivity, reduces adipose inflammation, while further increasing fat expansion in the metabolic syndrome. SREBP1c expression is blunted in models of obesity and insulin resistance in the adipose tissue (273). Reduction in the expression of adipocyte SREBP1c results in poor fatty acid uptake and storage in models of metabolic dysfunction (49, 168). Consistent oversaturation of nutrients to the storage capacity in regards to the underlying dysfunction in the adipocytes results in aberrant adipogenesis (lipomas), ectopic fatty acid uptake, and triglyceride accumulation in the liver and skeletal muscle (170, 172).

Adipocytes also provide the necessary fatty acids for global cellular metabolism through a process of lipolysis that breaks down stored triglyceride and releases non-esterified fatty acids. Lipolysis is heavily regulated by insulin through its negative regulation of hormone sensitive lipase (209). Hormone sensitive lipase cleaves stored triglyceride into glycerol and fatty acids and is down-regulated in the metabolic

syndrome state (146, 181, 306). Adipocytes are also the primary source of the circulating peptide hormones leptin and adiponectin. Adiponectin is negatively associated with fat mass in contrast to leptin, which is positively correlated with fat mass and obesity (151, 205). Adiponectin is a strong sensitizer of insulin signaling through its activation of AMPK and it is reduced substantially in metabolic syndrome and in the expansion of adipose tissue (150, 151, 205, 342). It can be secreted as a globular monomer that retains some signaling, but is secreted primarily as a homotrimer, multimers of trimers that have critical impacts on signaling (150, 190). The low molecular weight globular form is recognized by adiponectin receptor 1 (AdipoR1) and activates AMPK (150). Full-length adiponectin oligomers will activate peroxisome proliferator alpha (PPARα) via adiponectin receptor 2, but both receptors AdipoR1 and AdipoR2 utilize T-cadherin as a co-receptor (150, 345). AMPK and PPARα activation directly affect insulin sensitivity and fatty acid oxidation, pathways that are repressed in the metabolic syndrome state, partially due to the reduction in adiponectin levels(184).

Leptin, on the other hand, correlates strongly with body mass and expansion of the adipose tissue, and also is independently correlated with metabolic syndrome risk (95, 138). Leptin regulates satiety through its action in the hypothalamus, particularly within the arcuate nucleus. Its action is reduced in obesity and metabolic syndrome due to elevated expression of SOCS3 resulting in leptin resistance (22). SOCS3 inhibits the phosphorylation of signal transducer and activator of transcription 3, the primary downstream signaling molecule of the leptin receptor (22). In addition to its role in regulating satiety, leptin also has profound effects on the innate and adaptive arms of the

immune system (203). Macrophages exposed to leptin increase expression of inflammatory genes, such as IL-6, TNFα, and chemokine (C-C motif) ligand 2(CCL2) (98, 192). Leptin also reduces the activation and proliferation of $CD4^+CD25^+$ T regulatory cells (Tregs) (61).

IL-10 expression is lower in the lymph nodes and adipose tissue in obesity or metabolic syndrome models (185). IL-10 can inhibit T cell activation and also skew the macrophage polarization to the anti-inflammatory alternative activation state (M2). Lowered expression of IL-10 in the adipose tissue is also a characteristic of obesity and metabolic syndrome in conjunction with chronic but sub-clinical adipose inflammation (65, 141, 185). The adipose tissue is heavily invested with resident macrophages that help maintain adipose function through regulation of angiogenesis and production of anti-inflammatory markers (195, 196). Resident adipose tissue macrophages (ATMs) maintain an alternative activated phenotype (M2) that is characterized by the expression of macrophage mannose receptor (CD206), the scavenger protein CD163, and production of IL-10, transforming growth factor beta (TGFβ), and arginase (195). Maintenance of the M2 polarization is closely linked to the production of interleukin-4 (IL-4) by Th2 $CD4^+$ T cells, but more importantly from eosinophils that heavily invest normal adipose tissue as well (216, 235, 293, 337). Production of IL-4 in the adipose tissue is dramatically reduced in metabolic syndrome in association with a loss of eosinophils (293, 337). Loss of IL-4 stimulation is linked to increased adipocyte necrosis in response to nutrient overload cellular stress. Rodent models of metabolic syndrome are highly linked with an M1-skewed macrophage polarization and increased

accumulation of macrophages in the adipose tissue (42, 195, 196). While specific markers for the M1 phenotype vary by tissue bed and host species, the M1 phenotype is classically linked with elevated MHCII and inducible NOS (iNOS) expression as well as production of the inflammatory mediators IL-1β, IL-6, and TNFα (195, 196, 219). Reversal of adipose dysfunction is linked to resolution of the adipose inflammation and enhancement of the M2 polarization of ATMs (42). Chronic inflammatory stress also promotes even greater adipocyte death and turnover and results in disrupted adipogenesis by the pre-adipocyte population (286, 288). Long-term obesity models exhibit hyperplastic adipose tissue that has lost the majority of its original adipocyte pool and has been reconstituted by smaller adipocytes that have reduced function (76, 83). Elevated adipocyte death is a hallmark of overexpansion and excessive nutrient loading of adipocytes in obesity (42, 195). Excess nutrient storage in the adipocytes, however, drives adipocyte hypertrophy and then hyperplasia in response to the chronic nutrient influx (59).

Dietary endotoxin, endoplasmic reticulum stress, and poor adipose circulation increase adipocyte death and turnover. Apoptotic adipocytes are then engulfed by inflammatory ATMs that form a characteristic crown-like structure due to the large hexagonal geometry of adipocytes compared to the macrophage attempting to engulf it (222, 332). Chronic inflammatory stress also increases lipolysis resulting in a slightly elevated local non-esterified fatty acid pool that further reduces insulin sensitivity and has been linked to inflammation through ceramide production or potentially through TLR4 activation (145, 271, 277). TLR4 is a pattern recognition receptor that recognizes

LPS and has been suggested to recognize fatty acids, particularly palmitic acid although this remains controversial (224, 277). Elevated palmitic acid is linked to *de novo* production of a potent inflammatory mediator, ceramide, through action of the serine palmitoyltransferase 1 (SPT1) (145, 271). Both TLR4 activation and ceramide synthesis have been documented in the metabolic syndrome and obesity models and contribute to the chronic inflammatory state and adipose dysfunction. Genetic ablation of TLR4 or TLR2 protects mice from the development of obesity and adipose inflammation when placed on a high fat diet (128, 277). Direct infusions of endotoxin have also been linked with the development of insulin resistance, further strengthening the link between macrophage activation and adipose function (35). These studies have raised the possibility for increased sensitivity and activation in response to elevated dietary endotoxin loads (37, 173).

Dyslipidemia and Liver Dysfunction in the Metabolic Syndrome

The liver is the primary regulatory site for circulating lipids and liver dysfunction in the metabolic syndrome closely resembles and is linked to nonalcoholic fatty liver disease and liver steatosis (31, 96, 170, 247, 261). These disease states are similarly characterized by elevated hepatic production of triglyceride-rich low-density or very low-density lipoproteins that can increase the risk for endothelial dysfunction, hypertension, atherosclerosis, and severe cardiovascular events like stroke and myocardial infarctions (32, 51, 107, 108). The hepatocytes are the primary functional cells in the liver that regulate lipogenesis, the conversion of glucose into fatty acids

through *de novo* lipogenesis. Additionally, they regulate the incorporation of fatty acids into triglycerides that are packed on to lipoprotein complexes that carry the lipid stores through the circulation for peripheral metabolism. This cycling process regulates the levels of low-density and high-density lipoproteins in the circulation.

Insulin promotes *de novo* lipogenesis through increasing the expression of SREBP1c that regulates the expression of key enzymes such as acetyl-CoA carboxylase and pyruvate dehydrogenase (15, 93, 239). Pyruvate dehydrogenase activation is a regulatory step in the conversion of pyruvate into acetyl CoA, which is the building block for fatty acid synthesis. SREBP1c expression is positively regulated by insulin signaling through the IRS-1 subunit and activation of mTORC1 downstream of PI3K(180). Paradoxically, liver SREBP1c expression is up regulated in the insulin resistant state (167, 171, 229, 247) despite loss of SREBP1c expression in the adipose tissue (168).

Poor adipocyte function increases the fatty acid load on the liver and constitutive action of SREBP1c increases fatty acid storage in the hepatocytes. In addition to obesity, uric acid is also strongly correlated with hepatic fat accumulation and liver dysfunction. The high fructose model of metabolic syndrome also has a critical role for uric acid in hepatic inflammation and stress in the development and maintenance of the metabolic syndrome state (246). Hepatic stress can be induced by ATP depletion from excess fructose consumption and phosphorylation by the hepatic fructokinase. AMP levels increase as fructose is rapidly phosphorylated yet AMPK activity is paradoxically reduced. This is due to the activation of AMP deaminase by fructose-1-phosphate, which

initiates the catabolism of AMP into uric acid (176, 197). Uric acid directly inhibits AMPK function and stimulates a lipogenic profile in the hepatocyte by inducing mitochondrial stress and releasing excess citrate into the cytosol for fatty acid synthesis (40, 177). Circulating uric acid is also associated with the metabolic syndrome (154) through up regulation of CRP in the endothelial and muscle cells of the blood vasculature (154, 296). CRP expression has also been linked to dietary and portal endotoxemia and the activation of TLRs is a significant element in liver dysfunction in metabolic syndrome (213, 253, 291, 343). The majority of the dietary endotoxin is linked with the absorption of dietary fat and the formation of the chylomicrons within the enterocytes that line the intestine (105). Once the chylomicron is transported to the interstitial space, dietary endotoxin can disseminate through the lymphatic system, or the endotoxin can disassociate from the chylomicron and enter the portal circulation (105). Once in the liver it can activate the TLRs on Kupffer cells and hepatocytes, resulting in CRP, IL-6, and IL-1β signaling and inflammation (96, 253, 290, 300).

Little is known of the fate of chylomicron-bound LPS as it traverses the lymphatic system but lymphatic endothelial cells express multiple functional TLRs and high fat meals are associated with node inflammation (79, 198). The inflammation associated with dietary endotoxin is progressive with over-nutrition as insulin resistance in the intestine is linked with overproduction of apolipoprotein B (apoB) and increased gut permeability to endotoxins (35, 36, 77, 84). The enterocytes are the specialized epithelial cells that line the intestine and are the site of dietary fat absorption. Insulin

resistance in the enterocyte increases the production of the atherogenic apoB48 molecules that are correlated with elevated SREBP1c expression (77, 84, 119).

Hypertension and Endothelial Dysfunction in the Metabolic Syndrome

Hypertension in the metabolic syndrome state is linked to insulin resistance and blood vascular endothelial cell dysfunction (21, 46, 122). Vascular endothelial cells integrate multiple different signals, such as tissue metabolic demand, hormonal control, neural regulation, and mechanic forces to regulate blood flow through constriction and dilation of blood vessels in the periphery. Endothelial dysfunction is characterized by the insufficient production of dilatory mediators, specifically NO, which results in poor peripheral circulation and elevated blood pressure.

Insulin is a potent vasodilator as stimulation of the PI3K-AKT pathway results in phosphorylation of eNOS at a critical serine residue that regulates its activity (217). AKT also integrates signals from mechanical stress such as shear stress to activate NO production (70). Insulin also contributes to the maintenance of endothelial function by stimulating endothelial NOS (eNOS) expression and transcription, and arginosuccinate synthase, which is the rate-limiting step for arginine synthesis from citrulline (338). The function of eNOS is tightly regulated by phosphorylation, intracellular calcium, and availability of the substrate L-arginine (338). Proper eNOS activation also requires the presence of 5 required cofactors: tetrahydrobiopterin (BH4), heme, flavin mononucleotide, flavin adenine dinucleotide, and calmodulin.

NO is able to freely diffuse through the endothelial cell layer and induces relaxation in the smooth muscle cells. Soluble guanylate cyclase is found in the cytoplasm of the vascular smooth muscle cells and is activated by NO to increase cyclic guanosine monophosphate (cGMP) production (8, 94). This cGMP regulates the activity of protein kinase G (PKG) that, along with protein kinase A (PKA), is the major regulator for smooth muscle relaxation. There are two genes that produce PKG with PKG1 expressed in vascular smooth muscle in two isoforms (PKG1α and PKG1β). PKG mediates its vasorelaxation mechanisms through activation of K_{ATP} channels, activation of the RhoA associated kinase (ROCK) pathway, and inhibition of the inositol-3 phosphate pathway. Activation of the K_{ATP} channels hyperpolarizes the cell membrane potential and prevents action potential generation in the pacemaker cells in the vessel wall, inhibiting contraction frequency. PKG also can inhibit contraction through the inactivation of myosin light chain phosphatase (MLCP). The inhibition of the MLCP is mediated by phosphorylation of the myosin phosphatase target subunit 1 by RhoA/ROCK activation. The cGMP can also indirectly activate PKA through inhibition of phosphodiesterases that target cAMP for degradation, and competition of phosphodiesterase activity, or direct activation of PKA (189, 206, 348). PKA will also activate potassium channels and contribute to the hyperpolarization, and both PKA and PKG activation regulate lymphatic muscle relaxation (223, 260, 323).

In addition to the direct role of insulin in vasodilation, hyperglycemia is also negatively associated with poor vasodilation (29, 132, 280). BH4 is a critical cofactor for the production of NO, which regulates vasodilation, and is sensitive to the redox status

of the cell. Chronic elevations in circulating glucose increase its use as a metabolic substrate and result in high mitochondrial potential and elevated production of reactive oxygen species (ROS). BH4 production is linked to the activity of the rate-limiting enzyme GTP cyclohydrolase 1 (GTPCH1) and is critical in maintaining eNOS fidelity and function (39, 338). Oxidation of BH4 results in the complex of BH2 with eNOS and uncoupling of NO production in favor of superoxide (178). Superoxide itself is a potent ROS that can combine with NO to produce peroxynitrite, thus further lowering the bioavailability of NO. Peroxynitrite can oxidize BH4 into BH2, perpetuating the oxidative stress and reducing NO production (39, 338). Lowering mitochondrial potential or increasing the levels of BH4 through GTPCH1 expression normalize eNOS function and vasodilator capacity (52).

The pro-inflammatory CRP molecule also inhibits NO production (230, 285). As previously described, CRP is elevated in the metabolic syndrome through production by the liver and in the endothelial and smooth muscle cells of the vasculature. Uric acid has been directly linked with the production of CRP in endothelial cells and contributes to the uncoupling of eNOS through activation of the nicotinamide adenine dinucleotide phosphate (NADPH) oxidase and down-regulation of eNOS and GTPCH1 (230, 285).

Lymphatic Vasculature and Contractile Regulation

The lymphatic vasculature is the nexus of tissue fluid and protein homeostasis and antigenic detection of self and non-self molecules (351). The goal of the lymphatic system is to collect and transport lymph, the collected interstitial fluid and metabolites or

products of cellular processes, for return to the blood circulation. Without reabsorption of macromolecules the oncotic pressure of the tissue would increase leading to excessive fluid extravasation and edema. Often times this process must go against a net pressure gradient, particularly in humans where fluid must travel against a gravitational gradient to return to the blood circulation due to our upright posture (351). This is accomplished through the action of both extrinsic and intrinsic forces that regulate lymph transport. Extrinsic forces include interstitial pressure and tissue compression, such as in gastrointestinal, cardiac, or skeletal muscle contractions that affect lymphatic transport (352). The compression of tissues plays a significant role in formation of lymph by temporarily forming a positive force for fluid to enter the initial lymphatic network.

The initial lymphatics are blinded capillaries that are dispersed in the tissue and are characterized by an endothelial layer with a discontinuous basal lamina that are anchored to the extracellular matrix (43, 183). The surrounding tissue space expands with increased interstitial pressure and opens the highly permeable lymphatic endothelial capillaries (43). Primary lymphatic endothelial junctions have been characterized as button like structures with intermittent tight and adherens junctions that that allow interstitial fluid to pass through the inter-junction space (183, 344). The initial lymphatic network is characterized as a plexus that eventually feeds into larger vessels, although pressure gradients do not favor passive flow and unidirectional valves prevent backflow (17, 121, 212, 352). As the initial lymphatics coalesce into larger vessels, the basal membrane is less discontinuous and the first unidirectional valves can be observed, although these vessels lack significant muscle investiture or contractile function. These

vessels are described as “lymphatic pre-collectors” and feed into larger muscularized lymphatic collecting vessels. The lymphatic muscle cells in the collecting vessels provide the intrinsic force to propel lymph through the lymph nodes and eventually return it to the bloodstream. The lymphatic collecting vessels are circumferentially covered with unique muscle cells that display both the contractile machinery of cardiac and classical smooth muscle and have a complete basal lamina and zipper-like endothelial junctions (121, 212, 226, 344). The lymphatic system in mammals does not have a singular pumping mechanism such as the heart in the blood vasculature (352). Instead, the lymphatic collecting vessels are able to contract both tonically and phasically in coordination to regulate lymph propulsion (101, 248). This intrinsic lymph pump function is critical to global lymphatic function, but especially lymphatic vessels that drain non-compressing tissue beds or organs. Additionally, the number of valves increases in the collecting vessels demarcating a functional lymphatic unit called a lymphangion. The lymphangion is the smallest contractile unit that describes a valve region and the contracting segments upstream and downstream of it (212). Lymph is propelled from lymphangion to lymphangion using the pressure gradient generated by phasic contractions that are coordinated through both electrical and mechanical stimulation (54, 56, 57, 100, 121). Lymphatic muscle cells within a lymphangion are connected through gap junctions that allow electrical depolarization of the lymphatic muscle by the pacemaker cell to propagate and coordinate the vessel contraction (179, 207, 238, 307, 316). Adjacent lymphangions do not contract simultaneously but appear to contract in succession (354). The upstream contraction cycle will increase the stretch

and filling of the adjacent downstream lymphangion, while simultaneously closing its unidirectional lymphatic valve in response to the intra-lymphatic pressure from contraction (354). These periods of systole and diastole have parameters similar to those in cardiac contraction cycles and these parameters are utilized to assess lymphatic pump function.

The lymphatic pump is driven by the electrical depolarization of a pacemaker cell that has yet to be specifically identified but is located in the smooth muscle layer (179, 238, 307). Additionally, lymph transport can also be impeded by phasic contractions if pressure gradients favor passive lymph flow and lymphatic vessels must be able to regulate conduit function similar to the tonic constrictions and dilations observed in blood vessels (26, 100, 102, 104). Phasic contractions increase vessel resistance as a function of its diameter and potentially closure of the valve. Flow-mediated shear stress plays a significant role in the inhibition of the phasic contraction frequency (chronotropy), contraction strength (ionotropy), and regulates vessel diameter through vessel tone modulation, primarily through NO production by the endothelium (26, 100, 102-104, 317).

Proper lymph flow requires both the ability to generate force to propel lymph and to reduce resistance to lymph flow and lymphatics vessels from different tissues differ in their regulation of these processes (101). MLVs isolated from rats display a maximal contractility at a preload of 5cmH_2O while the larger thoracic ducts display maximal pump activity at a preload of 3cmH_2O (100, 101). Shear sensitivity in the thoracic duct is also much more sensitive to Flow-mediated lymph pump inhibition (100, 101).

Mechanisms of Lymphatic Contractility

Lymphatic vessels must be able to regulate vessel pumping and resistance for proper lymph flow (17, 100, 102, 248). The duality of their function is reflected in the observation that lymphatic muscle cells express both cardiac and smooth muscle contraction machinery (226, 228). Smooth muscle tonic contraction and myogenic response is ultimately linked to intracellular calcium levels that are regulated by stretch-activated calcium channels and calcium sensitivity (359). Transmembrane calcium flux, through voltage operated calcium channels, regulates the myogenic response to pressure through phosphorylation of the myosin regulatory light chain 20 (MLC_{20}) subunits of the myosin complex (270). Phosphorylation of serine 19 of the MLC_{20} results in smooth muscle force production and tonic constriction in the lymphatic collecting vessels (326). Phosphorylation of the regulatory site is balanced by myosin light chain kinase (MLCK) and MLCP (129, 130). Myosin-actin interaction is regulated by intracellular calcium that interacts with calmodulin to activate MLCK. Activation of protein kinase C (PKC) will increase the sensitivity of the smooth muscle to calcium (331) through the phosphorylation of CPI-17 that can then strongly inhibit MLCP activity (80, 163). PKC also sensitizes force production to calcium concentration in skinned lymphatic vessels, suggesting a role in the amplitude of lymphatic phasic contractions (73, 74). Contraction strength in smooth muscle is also regulated independently of calcium through ROCK activity. ROCK activation will increase phosphorylation of the inhibitory subunit of the MLCP complex, myosin phosphatase target subunit 1 (MYPT1), further increasing the MLCP/MLC ratio. Both the regulation of MLC_{20} through MLCK and MLCP has been

implicated in the tonic constriction and myogenic response in lymphatic vessel function (133, 326).

The lymphatic tissue also expresses molecular machinery found in cardiac tissue such as the cardiac actin and beta-myosin heavy chain. Cardiac muscle contractions are dependent on membrane depolarization and calcium induced calcium release from the sarcoplasmic reticulum (20).Calcium influx through voltage gated calcium L and T type channels opens sarcoplasmic reticulum (SR) stores, which further increases intracellular calcium to regulate both cardiac and lymphatic contraction amplitude. Cardiac muscle contractility is regulated by thin filament associated troponin-tropomyosin interaction (227). Calcium binds to the troponin complex, which causes a conformational shift in the tropomyosin complex and allows actin myosin cross bridging. Thus cardiac contractions are tightly regulated by excitation and calcium induced calcium store release (318). As in cardiac tissue, lymphatic muscle cells have a spike of calcium that precedes the phasic contraction (318). Lymphatic SR calcium release, both ryanodine- and IP3- sensitive, is linked to the lymphatic contraction amplitude (320). Studies from rat and guinea pig mesentery suggest that calcium spikes signifying pacemaker activation regulate chronotropy, but that basal calcium increases in lymphatic muscle over time in response to elevated pressure and may contribute to the myogenic tone activation observed over time as well (14, 54). Flow-mediated inhibition of lymphatic contraction frequency is mediated through both PKG- and PKA-mediated K_{ATP} channel activation in response to NO production (103, 104, 317, 321).

Inflammation and Lymphatic Dysfunction in the Metabolic Syndrome

Lymphedema is the hallmark of severe lymphatic dysfunction and is a chronic and debilitating disease. Lymphedema can be caused by a genetic (primary) abnormality or by lymphatic vessel damage or dysfunction (secondary). Secondary lymphedema is seen with cancer patients that have lymph node removal and radiation (254, 256). Obesity has been historically linked with risk for developing post-operative lymphedema following a mastectomy (2, 126, 166). Even moderate obesity is associated with increased water retention and mild edema (324). The rise in obesity has increased the number of lymphedema cases due to the expansion of the morbidly obese population and crystalized the connection between lymphatic dysfunction and the metabolic syndrome state. Up to 80% of morbidly obese patients were found likely to develop severe swelling in the form of lymphedema at some point in their life (86, 87). Lymphedema is a chronic progressive disease that results from obstruction or dysfunction within the lymphatic vasculature. Originally misdiagnosed as angiosarcomas, morbidly obese patients will likely develop lymphedema, characterized as massive localized lymphedema (MLL), at one point in their life, despite the majority of patients with lymphedema displaying normal lymphoscintigraphy results, suggesting there was no genetic defect or obstruction in their lymphatic network (310). MLL is predominantly unilateral with a slight preference for female patients (55%female and 45% male) (41). This disease was commonly misdiagnosed due to its low occurrence rate and its predisposing factor of morbid obesity.

Over 34% of Americans are obese and, of those, over 6% were classified as severe (BMI>40) or morbidly obese (BMI>50), putting them at risk for developing MLL. MLL is linked to the nutritional and metabolic state of the patient, as recurrence of MLL after surgical removal of the afflicted tissue bed is common and weight loss and exercise programs appear to be beneficial in its prevention (85). Macromolecule clearance is reduced in a rodent model of obesity and many of these models fit parameters for the metabolic syndrome (9). The lymphatic system has historically been linked to adipose tissue, as lymphatic vessels are often surrounded by perivascular adipose throughout the body and lymph itself has pro-adipogenic properties (123, 125). The Prospero homeobox protein 1 (Prox-1) haplotype mouse model displays poor lymphatic vessel integrity, and the surviving mice develop adult onset obesity (125). Patients with severe diabetes also have elevated lymphangiogenesis in their skin and the endothelial cells are characterized by excessive inflammatory gene expression (118). One of the critical roles of the lymphatic system is to return tissue antigens both self and non-self to the node for proper immune surveillance in the lymph node. Failures of the lymphatic system delay the appropriate immune response and can cause further damage and inflammation in even sterile injury.

Obesity has been described as a mild edematous state with chronic subclinical inflammation, and an increased risk of bacterial infections that can be explained in part by lymphatic insufficiency (139, 187). Models of inflammation in the peritoneum and intestine have demonstrated impaired lymphatic function in regards to vessel permeability and pump function (48, 204, 340). It is likely that similar inflammatory

mediators present in the metabolic syndrome state are responsible for the development of MLL and the risk associated with obesity in the development of post-operative lymphedema (254, 255). Intriguingly, secondary lymphedema is not always bilateral, suggesting that severe lymphatic dysfunction can be regionally regulated and suggesting a role for inflammation in the draining tissue. The lymphatic system production of dendritic cell chemoattractant factors and the transport of dendritic cells to the draining node have been heavily studied and are impaired in obesity (249, 250, 330). However, aside from the context of lymphangiogenesis, there is little information on the role of resident tissue macrophages and their interactions with the lymphatic system (159).

Resident tissue macrophages are found throughout the body and play critical roles in maintaining tissue function and homeostasis in addition to their immunological roles. (106). In that aspect they share a similar function as the lymphatic system that drains these organ beds and recent work has begun to suggest a more active role for the lymphatic endothelium in the response and resolution of inflammation. As discussed earlier, the metabolic syndrome is associated with an altered macrophage phenotype in the primary adipose depots, and these macrophages have poor lymphatic clearance of macromolecules. Our lab has previously shown that MLV contractility (Figure 1) is impaired in a high fructose model of metabolic syndrome that is independent of gross obesity (357).

The high fructose fed Sprague Dawley rat is a common and accepted model of metabolic syndrome due to the presence of both insulin resistance and gross dyslipidemia despite the lack of overt obesity. However, there was significant expansion

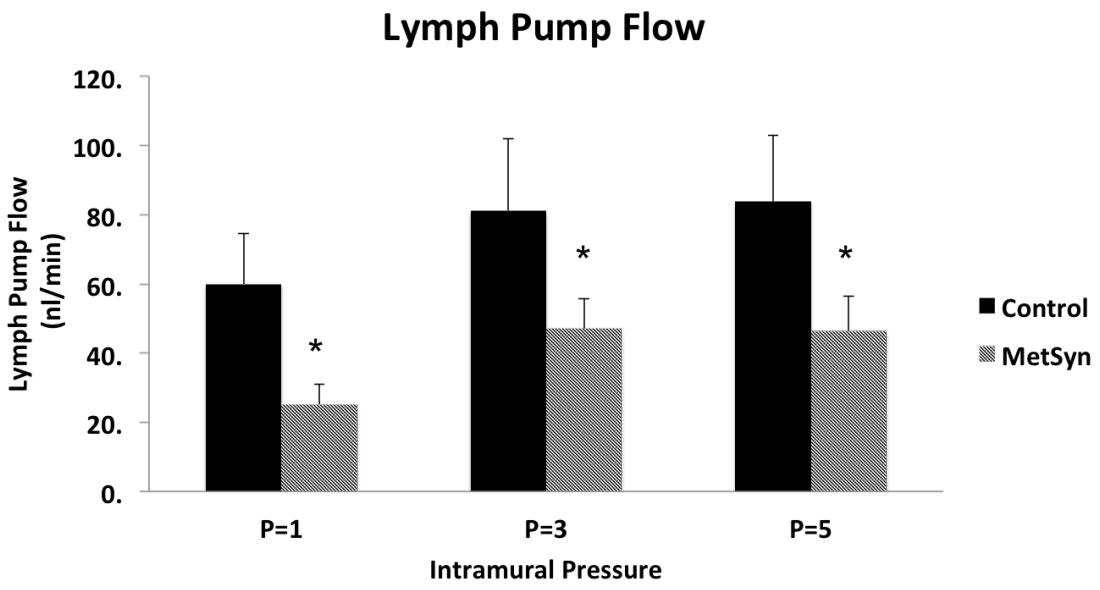

Figure 1. Impairment in the mesenteric lymphatic pump of a high fructose fed rat model of metabolic syndrome. Mesenteric vessels had significantly reduced intrinsic lymph pump flow at each pressure tested. This was significantly affected by reduced chronotropy of phasic contractions. MetSyn-metabolic syndrome * Denotes statistical difference at $p<0.05$. (357)

of the perivascular adipose tissue where the MLVs reside (Figure 2) (357). We confirmed that our 7-week feeding regime resulted in the metabolic syndrome state through elevated fasting insulin and triglyceride in addition to liver lipid disruption (Table 1) (357). This suggests that the chronic inflammatory environment in the metabolic syndrome is able to induce lymphatic dysfunction and may suggest that lymphatic contractility impairment contributes to the obesity-related lymphedema risk and massive localized lymphedema. Others have replicated these results using mouse models of metabolic syndrome (25, 330), although many questions remain. It is clear that inflammatory states are directly linked to lymphatic dysfunction but that poor lymphatic function can also contribute to or exacerbate that inflammation (350).

The Specific Aims of this Dissertation

1. To elucidate the association between macrophage polarization and the intrinsic lymphatic pump under conditions of inflammation and the metabolic syndrome. We examined the accumulation and polarization of macrophages and their spatial and temporal association with the vessels in the metabolic syndrome and an acute model of peritonitis. We then assessed the MLV contractility in response to stretch and the therapeutic potential of the anti-diabetic drug glibenclamide to restore MLV function.
2. To determine the mechanisms of dysfunction of a conduit vessel, thoracic duct, in metabolic syndrome. We examined the sensitivity to flow-mediated pump inhibition and vessel resistance to imposed flow. We tested the sensitivity of

thoracic ducts isolated from metabolic syndrome rats to the exogenous NO donor S-nitro-N-acetylpenicillamine (SNAP) and the NOS inhibitor L-N^G-nitro arginine methyl ester (LNAME). We also examined the role of endogenous production of ROS in thoracic duct regulation with the ROS scavenger 4-hydroxy-TEMPO (TEMPOL).

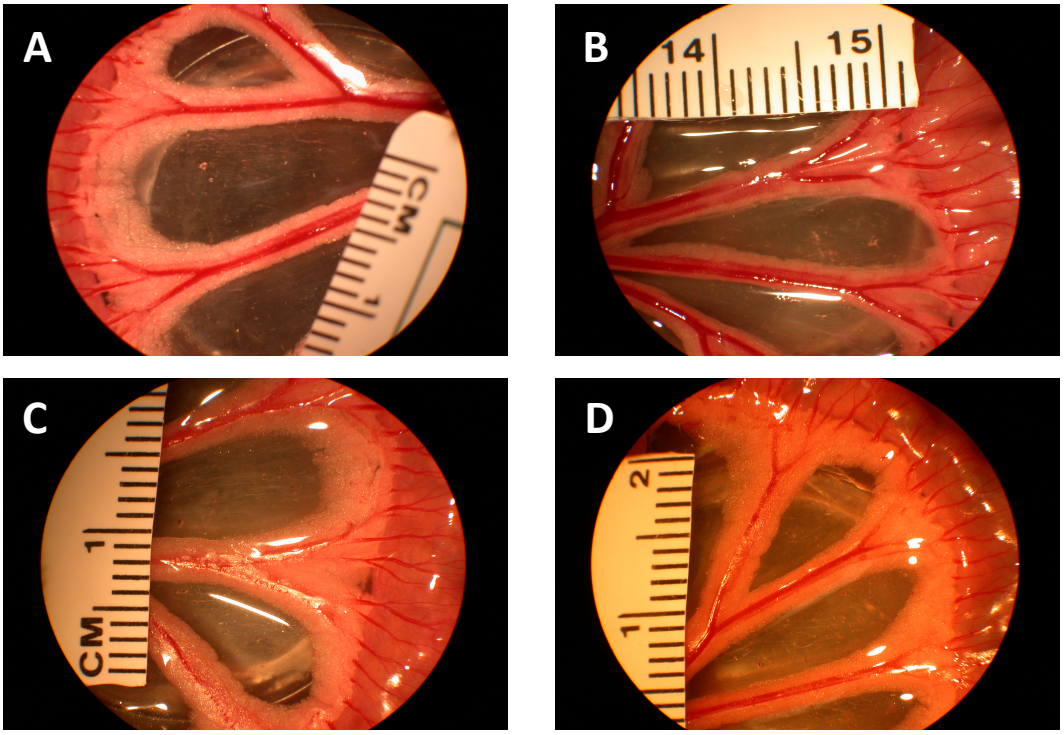

Figure 2. Seven weeks of high fructose feeding increases the perivascular adipose accumulation in the Sprague Dawley rat. Perivascular adipose in the mesentery of control rats fed normal chow for 7 weeks A, B. Perivascular adipose area increased by over 20% in the fructose-fed rats C, D. (357)

Table 1. Parameters of the high fructose feed induction of the Metabolic Syndrome

Fasting Metabolic Profile			
	Time	**Control**	**MetSyn**
Change in Body Weight(g)	Delta	86.03	103.3
p-value		**0.162**	
Insulin (ng/ul)	Wk 0	1.012	0.962
	Wk 7	0.866	1.397
p-value		0.118	**0.002**
Triglycerides (mg/dL)	Wk 0	49.5	58.9
	Wk 7	57.9	102.8
p-value		0.106	**0.014**

The high fructose model of metabolic syndrome does not cause significant weight gain compared to control chow-fed rats. Circulating insulin concentrations and triglycerides significantly increase in the fasting state in the high fructose fed rat model of metabolic syndrome. (357)

CHAPTER II

LYMPHATIC VESSEL-ASSOCIATED MACROPHAGES MATCH TISSUE RESIDENT PHENOTYPES AND ARE ASSOCIATED WITH IMPAIRMENT OF THE LYMPHATIC PUMP IN THE METABOLIC SYNDROME

Overview

The intrinsic lymphatic pump is critical to proper lymphatic function, the prevention of edema, and antigen presenting cell migration. The sub-clinical chronic inflammation observed in the metabolic syndrome (MetSyn) is both a symptom and driver of the disease state and is correlated with dietary endotoxin and macrophage inflammatory status. We have addressed the role of macrophage recruitment and investiture in the MLVs in response to both acute and chronic inflammation. We have utilized a LPS-induced peritonitis rat model and a seven-week high fructose fed rat model of MetSyn to address the association of macrophages and their polarization in lymphatic dysfunction. We found significant, yet different, alterations in macrophage polarization and investiture in response to both LPS-induced peritonitis and MetSyn. LPS-injected rats showed a two-fold increase in macrophage investiture in the perivascular adipose tissue and along the lymphatic vessel. The majority of macrophages maintained an M2 phenotype that was characterized as $CD163^{+}CD206^{+}MHCII^{-}$ and heavily invested along the lymphatic vessels. We also observed a dramatic increase in the presence of $CD163^{-}CD206^{+}$ macrophages within the vicinity of the lymphatic vessel that are not commonly observed in control rats. In contrast, MetSyn resulted in a M1-

skewed macrophage population as observed by an increase in the number of positive $CD163^{+}MHCII^{+}$ macrophages in the tissue and residing on the lymphatic vessel. Cultured lymphatic endothelial cells expressed high levels of chemokine (C-C motif) ligand 2(CCL2), and monocyte colony stimulating factor (MCSF) basally and in response to LPS stimulation. Both lymphatic muscle and endothelial cells significantly increase granulocyte/monocyte colony stimulating factor (GMCSF) expression in response to LPS stimulation. Significant impairment in MLV contractility was observed in both LPS and MetSyn models, which was primarily regulated by reduced chronotropy. Therapeutic levels (1μM) of the K_{ATP} channel blocker glibenclamide (Glib) did not significantly improve contraction frequency or lymph pump function in isolated MLVs in MetSyn. Maximal activation of lymphatic vessels with high dose (10μM) Glib also failed to consistently increase lymph pump flow despite an increase in contraction frequency. These data demonstrate that inflammatory conditions, such as LPS or MetSyn, promote macrophage polarization in the mesenteric tissue and on the lymphatic vessel that is correlated to the lymphatic dysfunction in these two models, suggesting crosstalk between the statuses of macrophages and lymphatic function.

Introduction

Obesity and its related metabolic diseases affect approximately 34% of Americans and is the strongest predictor of the MetSyn (114). Additionally, approximately 85% of the patients with type II diabetes (TIIDM) also fall under the conditions for diagnosis of MetSyn (153). The MetSyn increases the risk for cardiovascular disease greater than the sum of the parts. Patients are diagnosed with the MetSyn if they have 3 or more of the following: systolic blood pressure >135mmHg, high waist circumference (>40in male, >35in female), hypertriglyceridemia (>150mg/dl), hyperglycemia (>100mg/dl fasting glucose), and low high-density lipoprotein (<40mg/dl male, <35mg/dl female) (115). The MetSyn state is also characterized by elevated ROS, insulin resistance, adipose inflammation, and chronic but subclinical-inflammation (1, 99, 114, 195, 341).

Recent studies demonstrated a critical role for adipose tissue macrophage polarization in the pathogenesis of MetSyn. Induction of MetSyn is accompanied by increased production of inflammatory cytokines such as tumor necrosis factor alpha (TNFα), interleukin 6 (IL-6), and chemokine (C-C motif) ligand 2(CCL2) (42). The expression of these inflammatory cytokines is directly linked to the increased infiltration of macrophages and the classical (M1) polarization phenotype (195, 196). Under physiological conditions, adipose tissue macrophages demonstrate an alternative activated phenotype (M2) due to the expression of interleukin 4 by eosinophils (337). M2 macrophages produce the anti-inflammatory molecule interleukin 10 (IL-10), tumor growth factor β (TGFβ), and the interleukin 1 decoy receptor (219). Obesity reduces the

eosinophil population while simultaneously increasing the type 1 helper (Th1) $CD4^+$ effector T cell production of interferon-γ (IFNγ) (219). IFNγ is the classical stimulator of the M1 phenotype, but recent studies have also suggested that macrophage polarization is driven by the ratio of MCSF and GMCSF (91, 143, 174). Exposure of monocytes to MCSF alone results in a typical anti-inflammatory M2 polarization while GMCSF can drive the inflammatory M1 phenotype.

Obesity and TIIDM are both associated with microvascular dysfunction (2, 201, 215, 266, 324). However, much of the focus on the peripheral edema associated with obesity has been decidedly on venous insufficiency (251, 308) with little regard to lymphatic function that we know is critical to fluid homeostasis (63, 254, 310). Obesity is also a historical risk factor for developing secondary lymphedema after a mastectomy and macromolecular clearance from the adipose is reduced in obese models (2, 67, 244). The association between lymphatic dysfunction and obesity becomes clear in the morbidly obese population (10, 81, 112, 144, 160, 214) that represent at least 30% of all secondary lymphedema cases (86). The phenomena known as massive localized lymphedema (MLL) has increased with the rise in the obese and morbidly obese (BMI >50) populations (85, 87). Surgical opportunities provide relief but there is a potential of relapse if the underlying metabolic dysfunction is not addressed (85). A recent study demonstrated that human TIIDM patients have elevated lymphangiogenesis in their skin, and their lymphatic endothelial cells express a prominent inflammatory profile (118). Macromolecule clearance by the lymphatics is also reduced in obesity (9) and likely contributes to the mildly edematous state (324). Finally, lymphatic dysfunction in Prox-1

haplotypes may lead to adult onset obesity in mice (125). The lymphatic system's close association with adipose tissue underlies the connection between lymphedema, lipidemia, and adipose tissue function (124, 329).

Proper lymphatic function is critical to tissue fluid and macromolecule homeostasis and antigen delivery to the node. Lymph is comprised of the interstitial fluid, cellular metabolites, and secretions that are taken into the lymphatic vessels and transported back to the bloodstream passing through multiple nodes in the process. Failure of the lymphatic system results in a chronic and progressive disease called lymphedema that can arise from genetic complications (primary) and vessel damage or dysfunction (secondary) (254, 256). This transport of lymph is against net pressure gradient and the intrinsic lymphatic pump and unidirectional valves are critical to this process as well as the prevention of edema (17). The muscularized lymphatic collecting vessels can be described as a series of lymphangions comprised of a lymphatic valve and the contracting segments both up- and downstream that act coordinately to generate temporary pressure gradients to propel lymph (212, 352, 354). This intrinsic lymph pump is regulated by the activation of pacemaker cells found within the vessel wall that depolarize frequently and generate the phasic contractions (212, 320). The pacemaker is highly sensitive to transmural pressure fluctuations and increases the firing frequency (chronotropy) with a maximal activation achieved around a transmural pressure of 5cmH_2O in the MLV (100, 101). Depolarization of the pacemaker drives the depolarization of the lymphatic muscle cell layer and activates calcium influx through L-type channels (318). Calcium influx activates the SR release of calcium through both

ryanodine receptors and inositol-3-phosphate receptors (316). The calcium induced calcium releases by the SR and the calcium store management regulates contraction amplitude (316, 352). PKC has been shown to increase the sensitivity of lymphatic muscle to calcium and increase force production (74).

Lymphatic vessels are also self-regulating through the generation of NO in response to the shear stress of lymph propulsion (26, 104). Shear-induced NO will activate both PKA and PKG in the smooth muscle that increases adenosine triphosphate (ATP) sensitive potassium channel (K_{ATP}) channel activity, hyperpolarizing the pacemaker and reducing the contraction frequency (102, 323). Glib is an anti-diabetic drug that increases the insulin release due to increased depolarization of the beta cells in the pancreas by inhibiting K_{ATP} channels. Glib also has been documented to restore lymphatic chronotropy and function in the guinea pig model of ileitis and could potentially restore lymphatic function in the MetSyn (315). Zucker Diabetic Fatty (ZDF) rats have reduced interstitial albumin uptake by the lymphatics and treatment with rosiglitazone did not increase lymphatic function (45). Interestingly, glitazones are agonists for PPARγ and are also used to increase insulin sensitivity in diabetic patients. Glitazone therapy, however, increases both fluid retention and peripheral edema risk especially in elderly or obese individuals (88, 127, 242). Both aging and obesity are linked with impaired lymphatic function that leads to increased peripheral edema, which often occurs in the feet and ankles (158, 324) Diabetic patients treated with Glib are less likely to develop cardiopulmonary edema than patients given glitazone therapy and do not display the same edema risk (50, 233, 314).

Adipose dysfunction in MetSyn is definitively linked with the inflammatory state and polarization of adipose tissue macrophages (195, 196). Multiple studies have suggested a role for $CD11b^{+}$ macrophages in lymphatic dysfunction (164, 187), however their polarization and temporal and spatial association with the lymphatic collecting vessels has not been addressed. Macrophages can produce a multitude of vasoactive substances including substance P (7, 55) and NO (187, 191, 323), which each have potent effects on lymphatic contractility regulation (352). We have previously described a significant reduction in the intrinsic lymph pump capability of the MLV in a rat model of high fructose fed MetSyn (357). Recently, others have demonstrated a reduction in phasic activity and lymph function in genetic and diet-induced models of obesity, which also fit under the umbrella of MetSyn models (25, 262, 330). We have assessed the intrinsic pump function of the MLV both in models of LPS-induced peritonitis and high fructose fed MetSyn in the rat. We characterized the macrophage recruitment, polarization, and association of these macrophage populations with the mesenteric vessel dysfunction. Finally we assessed the role of therapeutic levels of the anti-diabetic drug Glib, a K_{ATP} channel inhibitor, on regulating lymphatic chronotropy and function in the MetSyn state.

Materials and Methods

Animal Handling

Sprague Dawley male rats weighing 250g were purchased from Charles River and given a week to acclimate. For the LPS model of peritonitis, twenty-four rats were

divided into two groups. One group was given intra-peritoneal injections of LPS at 10mg/kg daily for three consecutive days. The second group was injected with sterile phosphate buffered saline (PBS) i.p. as a vehicle control for three consecutive days. Seven rats from each group were utilized for isobaric MLV analysis. The remaining five rats from each group were utilized for immunohistochemistry (IHC) in the mesenteric tissue. Water and feed were available ad libitum except during pre-experiment (16hr) fasting.

Thirty rats weighing 180g were ordered from Charles River for the induction of the MetSyn. Twenty rats were given a high fructose feed (HFF) diet (60% fructose, ID.89247 Harlan Teklad®, 66% caloric content from fructose) for seven weeks to induce the MetSyn, while the remaining ten animals were given standard rodent chow. Water and each respective feed were available ad libitum except during pre-experiment (16hr) fasting. Ten rats from the MetSyn group and five rats from the control group were utilized for isobaric functional analysis of MLV contractility. The remaining rats were used for IHC and RNA collection from the mesentery tissue. All animals were housed in a facility accredited by the Association for the Assessment and Accreditation of Laboratory Animal Care and maintained in accordance with the policies defined by the Public Health Service Policy for the Humane Care and Use of Laboratory Animals, the United States Department of Agriculture's Animal Welfare Regulations and the Scott & White Animal Care and Use Committee.

Serum Analysis

Blood was collected in fasted (16hr) rats via the lateral saphenous veins at the start and end of the diet period. The saphenous vein was punctured using a 27gauge needle and blood was collected in a non-heparinized tube. Blood was allowed to clot for 1hour at room temperature and spun for ten minutes at 3,000g. Serum was then frozen and stored at -80^{o}C. Triglyceride and insulin concentrations were assessed using commercially available colorimetric kits, Bioassays® ETGA-200 and an insulin ELISA kit Linco® EZMRI-13k, respectively, following the manufacturers' protocols.

MLV Isolation

Rats were fasted for sixteen hours and were anesthetized with Innovar-Vet (0.3 ml kg-1 I.M.), which is a combination of a droperidol-fentanyl solution (droperidol 20 mg/ml, fentanyl 0.4 mg/ml), and diazepam (2.5 mg/kg IM). A midline excision was made and a loop of ileum was carefully exteriorized. Two to three MLV were carefully dissociated from the surrounding adipose tissue with care to prevent excess bleeding. Vessels were maintained in albumin-supplemented physiological saline solution (APSS, in mM: 145.0 NaCl, 4.7 KCl, 2 CaCl2, 1.17 MgSO4, 1.2 NaH2PO4, 5.0 glucose, 2.0 sodium pyruvate, 0.02 EDTA and 3.0 3-(N-morpholino) propanesulfonic acid (MOPS) and 1% w/v bovine serum albumin) at pH 7.4 at 38°C. MLVs were then cannulated onto matched pipettes in a CH-1 chamber® (Living Systems) and attached to separate pressure reservoirs. Only vessels that did not have apparent constriction sites due to damage were used. Vessels were then allowed to equilibrate at pressure 1cmH_2O for approximately thirty minutes. After the equilibration period each vessel was recorded for 5 minutes at pressures 1cm, 3cm, and 7cmH_2O. Vessels taken from the MetSyn rats and

their control counterparts were also stimulated with 1μM, and finally 10μM, Glib at each pressure after a fifteen-minute equilibration period. At the end of each experiment the bath solution was replaced with calcium-free APSS and maximal diameter at each pressure recorded.

Isolated Vessel Video Analysis

Lymphatic diameter were traced for each 5 min video capture with a vessel wall-tracking program developed and provided by Dr. Michael J. Davis (University of Missouri-Columbia) (58). Outer lymphatic vessel diameters were tracked 30 times per second, providing a tracing of diameter changes throughout the periods of systole and diastole. The following analogies to the cardiac pump parameters were derived: lymphatic tonic index, contraction amplitude, ejection fraction, contraction frequency, fraction pump flow, and systolic/diastolic diameters, as previously described. Statistical significance was determined through two-way analysis of variance with Fisher's post hoc analysis using the Statplus® (AnalystSoft) statistical software package. Data are represented as means ± standard error (SE) and significance represented independently at each figure.

Immunohistochemistry and RNA/Tissue Collection

Rats that were utilized for IHC were anesthetized as described above and then euthanized via thoracotomy. The mesenteric tissue from the duodenum to the cecum was collected. In the LPS-induced peritonitis model, the ileum was excised and pinned in a Sylgard-coated dish. Tissues were then fixed in methanol at -20°C for 1hr. Tissue collection for the MetSyn rats was performed similarly. Additionally, the cecum of each

MetSyn rats was weighed and measured. Remaining mesenteric tissues from MetSyn rats, from the ileum and jejunum, were also pinned out and fixed in RNALater ® overnight at 4°C for RNA isolation.

For IHC, fixed tissue was rinsed with PBS and the perivascular tissue was cut from the intestinal wall and root of the mesentery, such that two bundles were present in each section. These tissues were transferred to a clean dish and blocked with 5% goat serum in PBS for 2 hours at room temperature. The tissue was then stained overnight at 4°C with antibodies recognizing CD163 at 1:200 (AbD Serotec), CD206 at1:100 (Abcam), and MHCII at 1:200 (Santa Cruz) in combination. Tissues were then washed with PBS and stained with AlexaFlour® 488 or 647-conjugated goat secondary antibodies at 1:200 for the respective primary antibody host and isotype. Tissues were then mounted between two coverslips with Anti-fade® mounting solution to limit the restriction in tissue depth. Images were collected at 20x and 40x magnifications using a Leica scanning confocal microscope with lymphatic vessels centered in the field of view. One to three lymphatic vessels were "tracked" from the intestinal wall towards the root of the mesentery per staining combination. Cell counts from five separate 40x images and three separate 20x images were averaged per animal to get an accurate representation of tissue macrophage polarization and lymphatic vessel association.

Lymphatic Endothelial Cell Culture

Mesenteric lymphatic endothelial cells (mLECs) and mesenteric lymphatic muscle cells (mLMCs) were both obtained through mesenteric vessel explants. Cells were grown in EGM-2MV medium (Lonza) and used at passages 4-7. mLECs were

plated at a 60% confluence in a 12-well plate and allowed to grow to a 100% confluence. The mLECs were then serum starved with basal EGM media for 2 hours and exposed to either EGM-2MV supplemented with vehicle or LPS (20ng/ml) for 24 hours. These mLECs were then washed with ice-cold PBS and lysed in Trizol Reagent® (Life Sciences). RNA was collected as per the manufacturer's instructions. The mLMCs were plated at approximately 50% confluence and grown in Dulbecco's modified Eagle's medium (DMEM) with 10% fetal bovine serum (FBS). Upon reaching 80% confluence the mLMCs were serum starved for 2 hours in basal DMEM. The media was then replaced with DMEM supplemented with 2% serum and either PBS vehicle or LPS (20ng/ml) for 24 hours. Finally, the mLMCs were then washed with ice-cold PBS and RNA collected as described above.

RNA Collection and Quantitative Polymerase Chain Reaction (QPCR) Analysis

RNA was collected from the entire neurovascular bundle in both control and MetSyn rats. RNA was stabilized in RNALater at 4^{o}C overnight and then the neurovascular bundle was excised and homogenized in Trizol solution. The homogenate was then centrifuged for one minute at 1,000g and the lipid content removed to prevent interference in the RNA collection, as directed by the manufacturer. RNA from the tissues, mLECs, and mLMCs was then converted to cDNA using the Bio-Rad iScript cDNA Synthesis Kit® and using 1µg of RNA per reaction. Gene expression was analyzed using the ΔΔCt method with beta-actin serving as the housekeeping control. A list of genes and the primers used for this method are provided in Table 2.

Table 2: QPCR primer list of genes involved in activation of inflammation and macrophage polarization

Gene	Forward	Reverse
β-Actin	AAGTCCCTCACCCTCCCAAAAG	AAGCAATGCTGTCACCTTCCC
SM α-Actin	CATCAGGAAGGACCTCTATGC	CTGATCCACATCTGCTGGAAG
GAPDH	CAATGTGTCCGTCGTGGATCT	TGCTTCACCACCTTCTTGATGT
IL-6	TCCTACCCCAACTTCCAATGCTC	TTGGATGGTCTTGGTCCTTAGCC
CCL2	AGCATCCACGTGCTGTCTC	GATCATCTTGCCAGTGAATGAG
iNOS	CAGCCCTCAGAGTACAACGAT	CAGCAGGCACACGCAATGAT
MCSF	CCATCGAGACCCTCAGACAT	TGTGTGCCCAGCATAGAATC
GMCSF	GACCATGATAGCCAGCCACT	TTCCAGCAGTCAAAAGGGATA
CCL1	CTTAGCTTGGTCCTGGTTCTC	GAATCTTCTTCTGGCTGTACCT
TGFβ	CGTGGAAATCAATGGGATCAG	GGAAGGGTCGGTTCATGTCA
Lyve-1	AGGCTGAAGTTTAGGTGCACGAGA	GAGCCAACAGTGGCTTGCTTCTTT
Prox-1	TGTCCGACATCTCTCCTTATTCG	ACGGGTGTAAAAGAACATGAGCT
SM22	AGGCAGCTGAGGATTATGGA	CTGCCCAAAGCCATTACAGT

Results

LPS-Induced Peritonitis Severely Impairs MLV Pump Function

Mesenteric vessels isolated from LPS-injected rats had a significantly reduced diastolic diameter only at a pressure of 7cmH_2O (Figure 3). However, this was also associated with reduced vessel tone at pressures of 3cm and 7cmH_2O (Figure 3). Four of the seven lymphatic vessels isolated from LPS-injected rats exhibited no phasic contractions at any intramural pressure. The remaining three lymphatic vessels isolated from these animals displayed spontaneous lymphatic contractions but had abnormally low contraction frequency. This resulted in a dramatic and significant reduction in lymphatic frequency and lymph pump flow (Figure 4). In contrast, the control vessels had robust contractility and pressure sensitivity. The four non-contracting vessels were excluded from the analysis of the stroke volume, which was not significantly different from control MLV stroke volume. A summary of the contractile parameters for the LPS-injected rats is listed in Table 3.

Macrophage Polarization and Association with the MLVs

Mesenteric whole mounts were prepared from control and LPS-injected rats to examine the association of macrophages with the MLV and their polarization index. Mesenteric arcades were fixed and stained for the M2 markers CD206 (macrophage mannose receptor) and the scavenger receptor CD163. The mesenteric whole mounts were also stained for MHCII to identify M1 polarized macrophages. We took panoramic

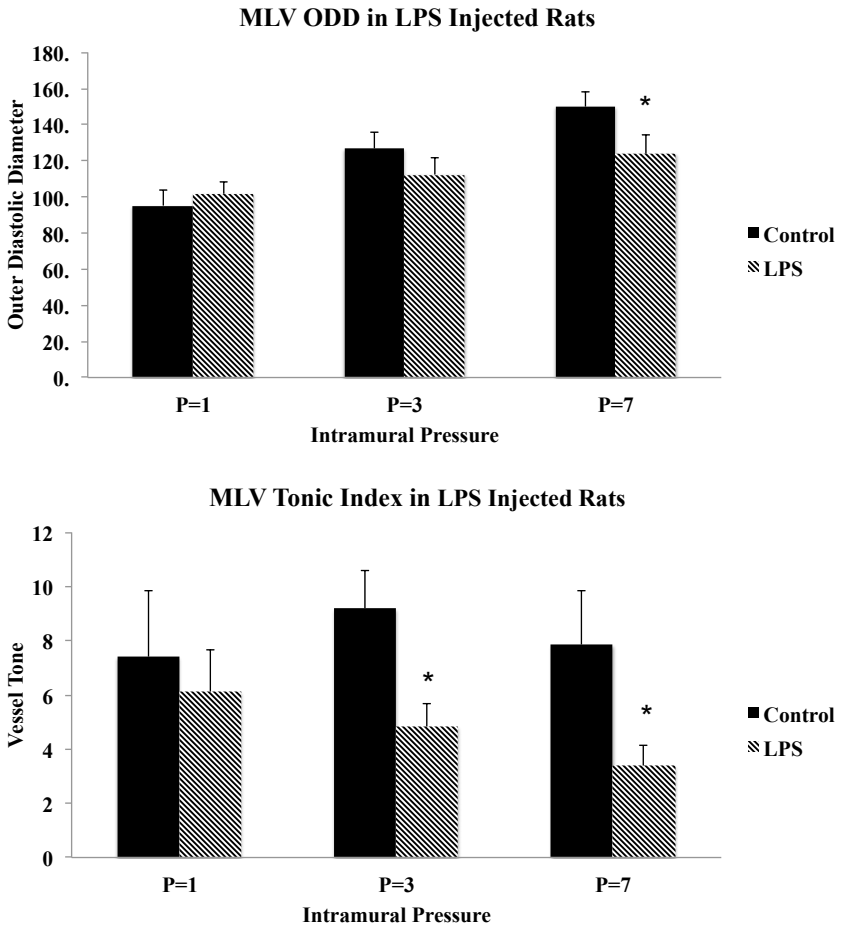

Figure 3. Outer diastolic diameter (ODD) and tonic index in MLVs isolated from control and LPS groups. MLVs isolated from LPS-injected rats had a significantly reduced diameter at a pressure of 7cmH_2O. Paradoxically, there was also a significant reduction in vessel tone at pressures of 3cm and 7cmH_2O. Data are presented as Mean ± standard error of the mean（SEM). N= 7 for each cohort. 2-way ANOVA * denotes significance at $p < 0.05$

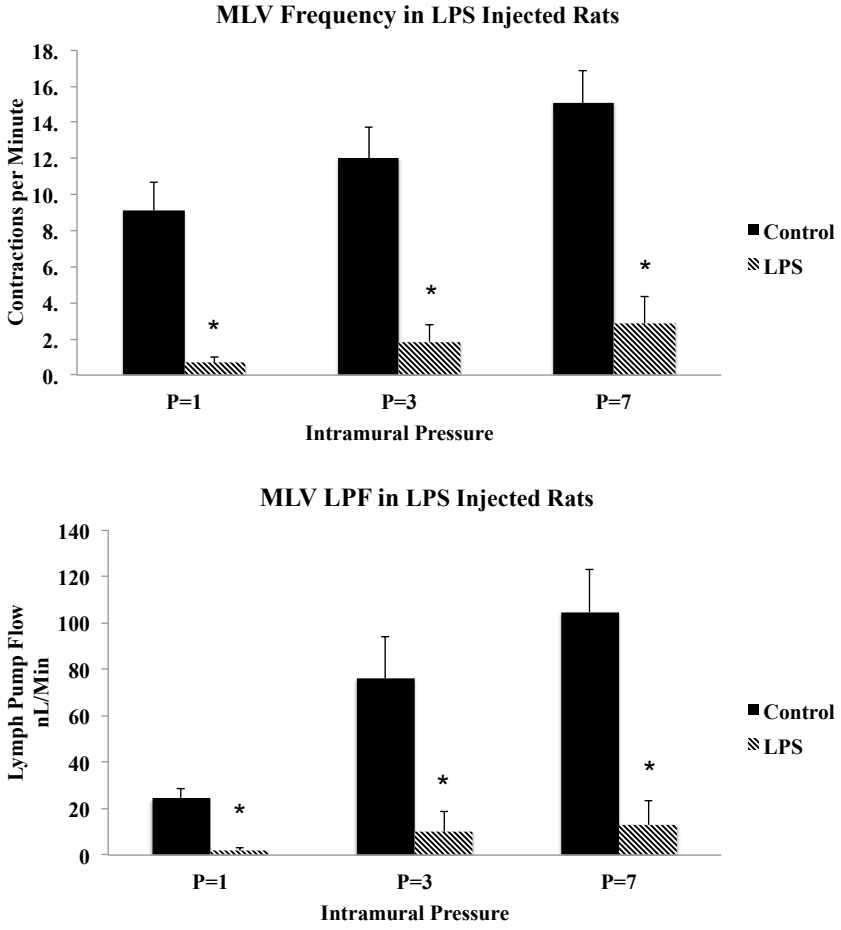

Figure 4. Contraction frequency and ejection fraction in LPS MLVs. MLVs isolated from LPS rats had a critical loss in spontaneous contractions that severely inhibited the lymph pump. Data are presented as Mean ± SEM. N= 7 for each cohort. 2-way ANOVA * denotes significance at $p < 0.05$

Table 3. Contractile parameters of MLV contractility of control and LPS groups

Mean ± SEM	Pressure (cmH_2O)	P=1	P=3	P=7
Outer Diastolic Diameter (uM)	Control MLVs	95.2 ± 8.5	127 ± 9.1	150 ± 8
	LPS MLVs	102 ± 6.8	112 ± 9.4	123.9 ± 10.5
Contraction Frequency per Minute	Control MLVs	9.13 ± 1.53	12 ± 1.72	15.1 ± 1.78
	LPS MLVs	0.69 ± 0.33	1.86 ± 0.94	2.86 ± 1.51
Stroke Volume (nL)	Control MLVs	3.34 ± 0.79	6.50 ± 1.15	7.11 ± 1.11
	LPS MLVs	3.07 ± 2.10	4.46 ± 2.76	3.77 ± 2.04
Lymph Pump Flow (nL/Min)	Control MLVs	24.3 ± 4.23	75.9 ± 18.4	105 ± 18.1
	LPS MLVs	1.76 ± 1.21	10.2 ± 8.33	13.1 ± 10.5
Tonic Index (% constriction)	Control MLVs	7.42 ± 2.44	9.18 ± 1.39	7.86 ± 1.99
	LPS MLVs	6.10 ± 1.54	4.83 ± 0.87	3.39 ± 0.76

Data are presented as Mean ± SEM for outer diastolic diameter, lymphatic contraction frequency, stroke volume, lymph pump flow, and tonic index.

images at 20x magnification in control rats to understand the macrophage tissue investiture on a large scale. We found that the perivascular adipose tissue was heavily invested with resident tissue macrophages that stained for both CD163 and CD206 (Figure 5). These cells were dispersed throughout the adipose tissue and spatially arranged in the clear mesenteric membrane that coats the tissue. We found that $CD163^{+}CD206^{+}$ macrophages also are found in direct contact with the lymphatic vessel itself (Figure 5). These cells commonly displayed the classical adipose tissue macrophage geometry as they were wedged between the hexagonal shaped perivascular adipocytes. However, this geometry was lost in the clear field mesenteric sheath or when they were associated with lymphatic vessels (Figure 5). $CD163^{-}CD206^{+}$ macrophages were present in low numbers with the vast majority of macrophages staining positive for both M2 markers. Macrophage cell density appeared highest near the MLV and counting at 40x magnification demonstrated a slight tropism toward the mesenteric collecting vessel. $MHCII^{+}$ cells displayed a strong tropism to the lymphatic vessel or other vascular structures (Figure 6). Double staining with CD206 revealed a dichotomy in staining profiles observed, with CD206+MHCII- and $MHCII^{+}CD206^{-}$ cells (Figure 6). $MHCII^{+}$ cells displayed an elongate morphology with multiple cellular projections and dendrites when found along the vessel. $MHCII^{+}$ cells in the peripheral tissue were generally smaller in size and had a circular phenotype. There was evidence for a small population of double positive $MHCII^{+}CD206^{+}$ cells whose morphology most closely matched the smaller $MHCII^{+}$ circular cells.

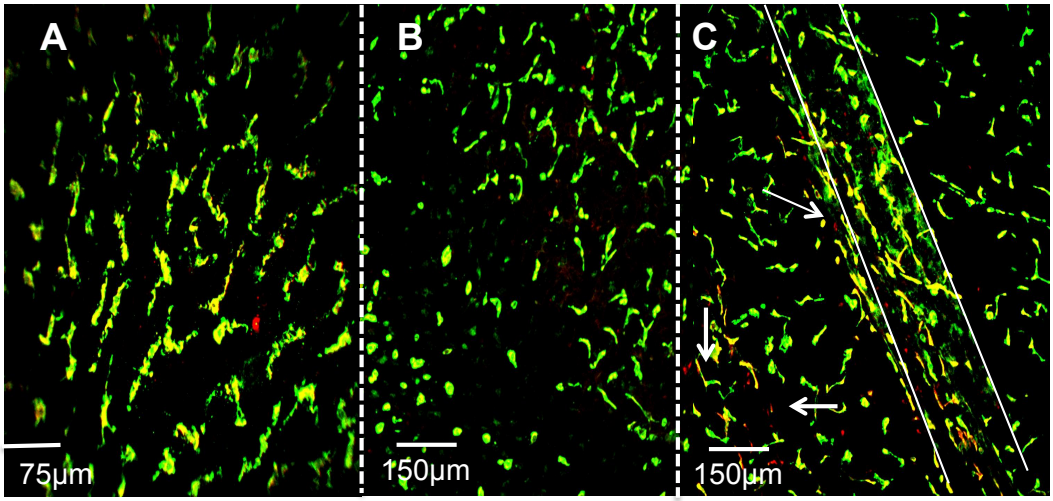

Figure 5. Panoramic view of immunofluorescence for M2 macrophages in a rat mesenteric whole mount prep. Macrophages were fixed in methanol and stained with CD206 (red) and CD163 (green). The majority of stained cells are $CD163^{+}CD206^{+}$ and are found within the clear-field tissue (A), the adjacent adipose (B), and the along the lymphatic vessel(C). There is also a small population of $CD163^{-}CD206^{+}$ cells that have a different morphology in that they are significantly smaller and ovoid (arrows). 20x magnification B-C, 40x magnification A.

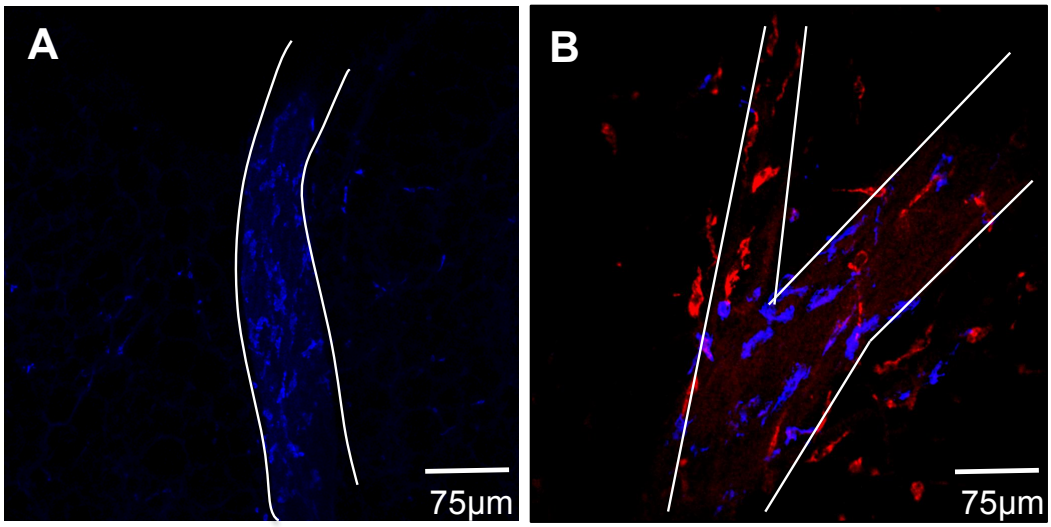

Figure 6. Immunofluorescence of M1 and M2 macrophage investiture in normal rat whole mount mesenteric tissue. Immunofluorescence identifies MHCII (Blue) and CD206 (Red) positive cells. (A) 20x magnification of control whole mount of normal rat mesentery demonstrates the investiture of $MHCII^{+}$ cells that display a tropism towards the lymphatic rather than within the tissue. (B) 40x magnification of mesenteric tissue stained for both MHCII (Blue) and CD206 (red). There is a dichotomy in staining profiles observed, with both $CD206^{+}MHCII^{-}$ and $CD206^{-}MHCII^{+}$ cells, but both cells can be found associated with the MLV. Straight white lines denote the lymphatic vessel borders.

LPS-Induced Peritonitis Increases Macrophage Accumulation and a M2 Phenotype

LPS injection caused a significant accumulation of macrophages in the mesenteric neurovascular bundle and peripheral tissue (Figure 7) and fibrotic appearance of the mesenteric sheath. These cells displayed a noticeable change in their morphology both within the perivascular tissue and the mesenteric sheath (Figure 7). Macrophages in the mesenteric sheath displayed a unique stellate morphology and were larger compared to their control counterparts. CD163 positive macrophages displayed an activated phenotype with multiple cellular extensions and spine-like dendrites within the tissue space. In contrast, the majority of mesenteric vessel-associated macrophages were ovoid in morphology suggesting they could be in the process of migrating. Macrophages were still predominantly double positive for both CD163 and CD206 (Figure 8) in the LPS-injected rats; however there was a significant increase in the presence of the $CD163^{-}$ $CD206^{+}$ polarization. The $CD163^{-}CD206^{+}$ phenotype displayed a strong tropism for the lymphatic collecting vessel (Figure 8). The $CD163^{-}CD206^{+}$ morphology was maintained as small ovoid cells with a prominent nuclear hole. The accumulation of macrophages in the tissue made the identification of lymphatic collecting vessels through autofluorescence difficult due to the large number of macrophages that were associated with the vessel. Each image stack was divided into 3 segments to allow proper three-dimensional counting. LPS injection increased the macrophage accumulation in the mesentery more than two-fold (Figure 9). The $CD163^{-}CD206^{+}$ phenotype displayed the largest fold change with a four-fold increase. Interestingly, there was no significant accumulation of $MHCII^{+}$ cells in the LPS-injected rats (Figure10).

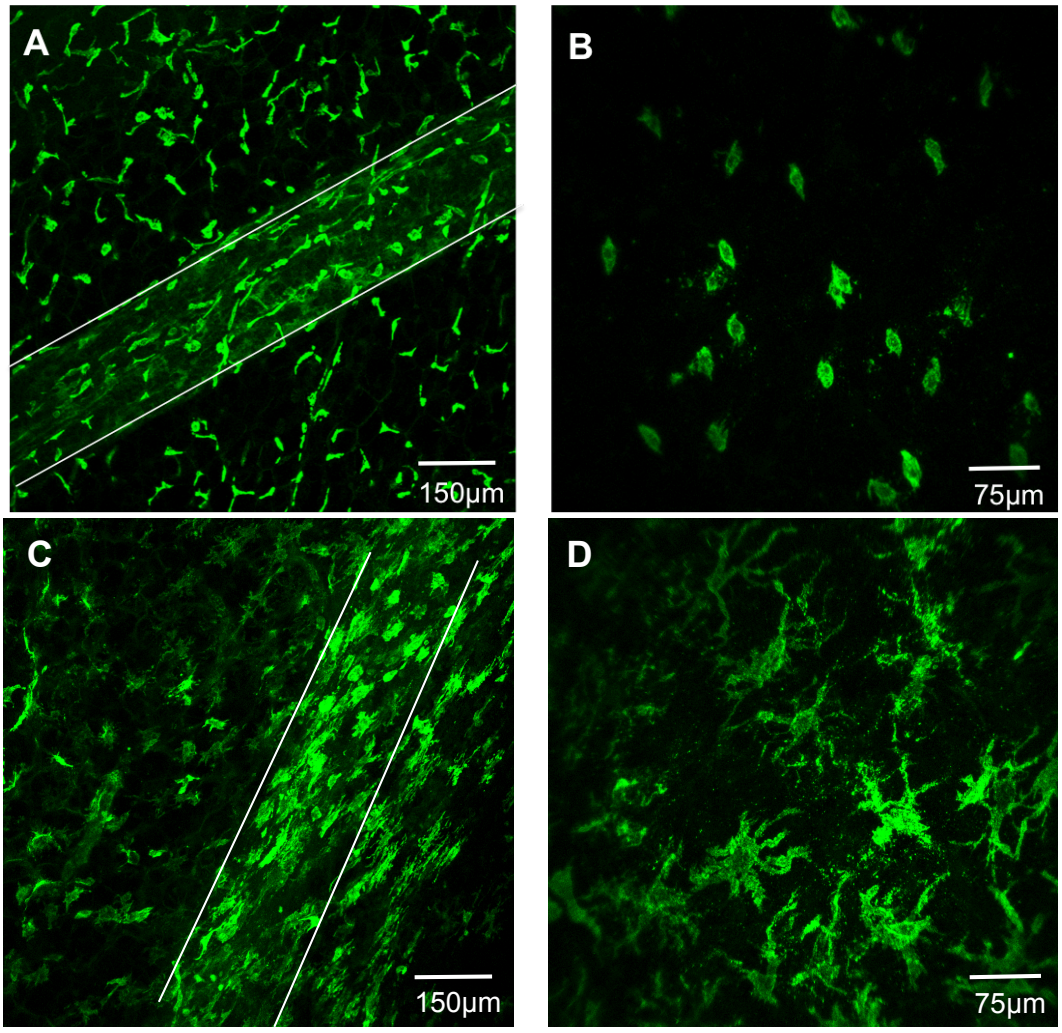

Figure 7. Macrophage accumulation and activation in the LPS rat mesentery. Mesenteric whole mounts taken from control (A and B) and LPS-injected (C and D) rats were stained with CD163 and scanned at 20x (A and C) and 40x (B and D). White lines denote the walls of a lymphatic collecting vessel.

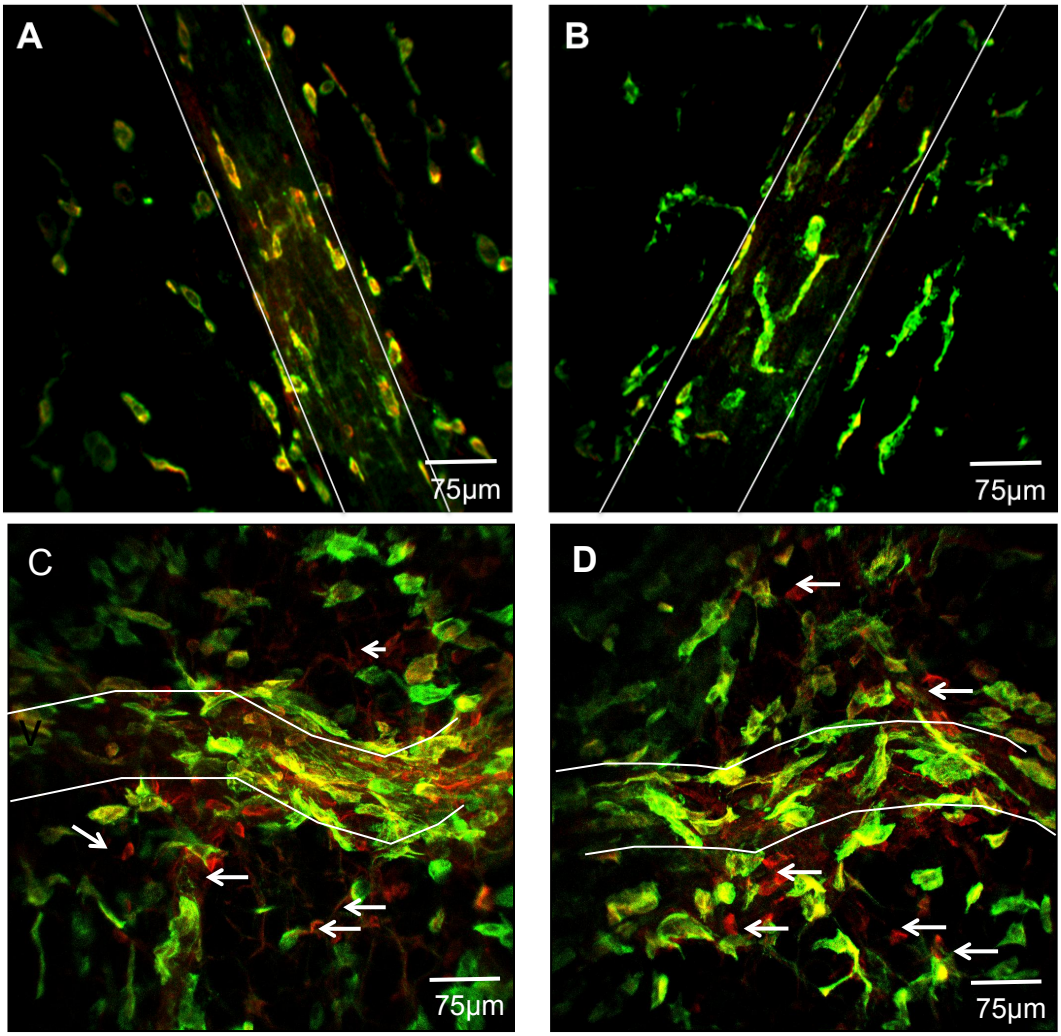

Figure 8. Evidence of M2 macrophage phenotypes in the LPS-injected rat mesentery. Mesenteric arcades from control (A and B) and LPS-injected (C and D) rats were stained for CD163 (green) and CD206 (red). Images of 40x magnification are shown. Arrows indicate the single positive $CD163^{-}CD206^{+}$ cells. MLV are outlined with white lines.

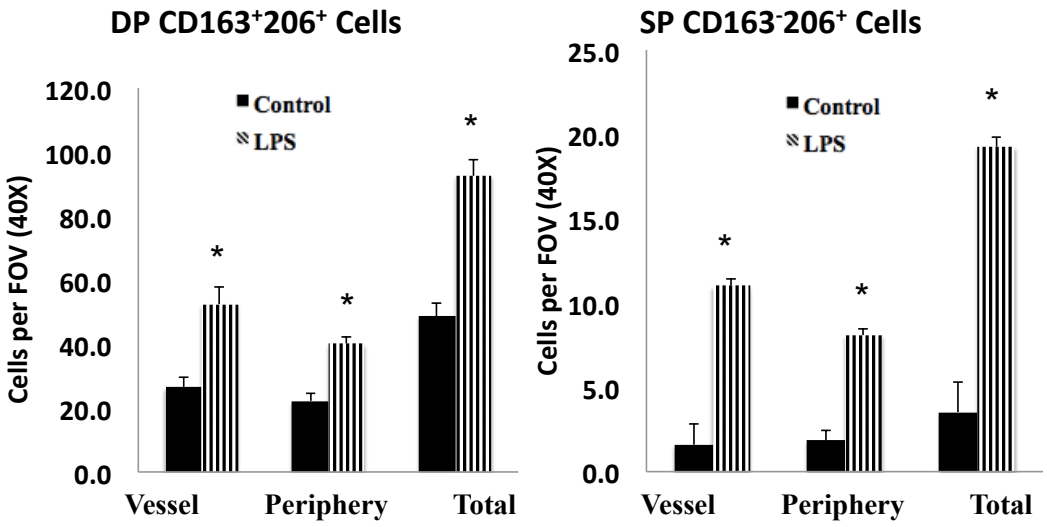

Figure 9. Quantification of the M2 macrophage phenotypes in control and LPS-injected rats. A minimum of five 40x image stacks were quantified and averaged per animal with 1μm slices and approximately 30-50 slices per stack focused around MLV. Cells that were in contact with the vessel were counted in association with the vessel and the remaining cells considered to be in the frame. Data are presented as Mean ± SEM. N= 4 for each cohort. 1-way ANOVA * denotes significance at $p < 0.05$

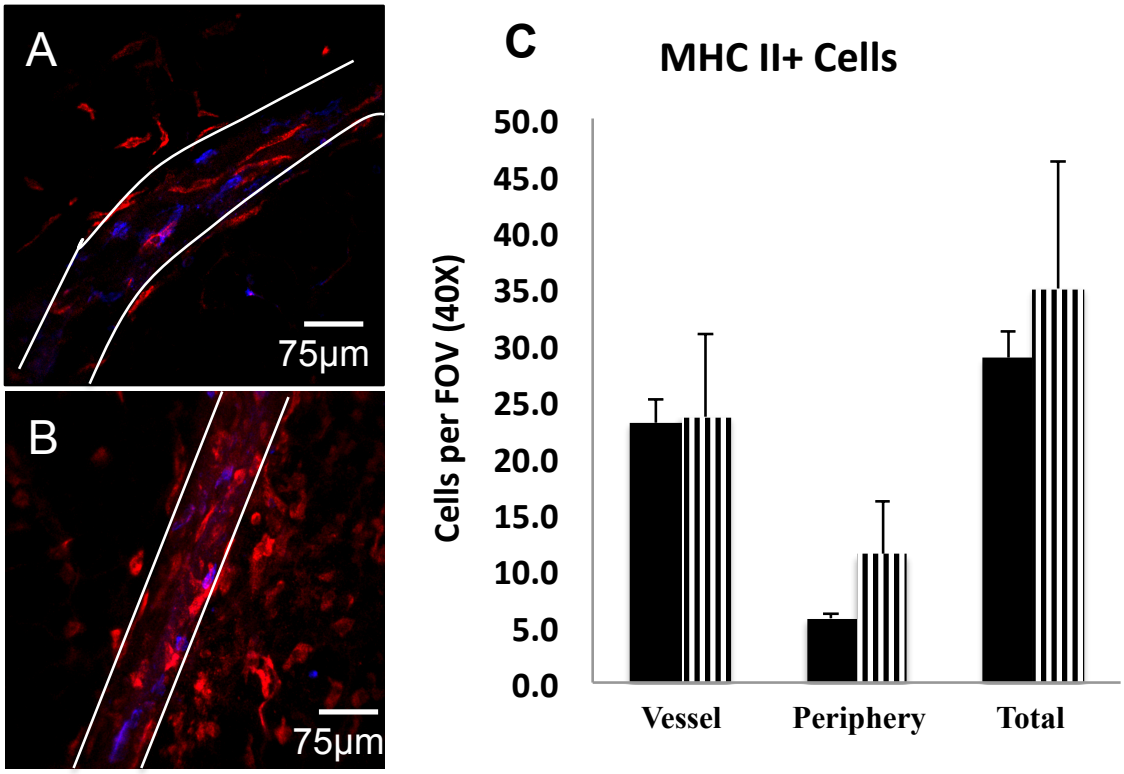

Figure 10. Lack of M1 polarized macrophages in the LPS-injected rat mesentery. Control (A) and LPS-treated rats (B) were stained for MHCII (blue) and CD206 (red). MLVs are outlined with white lines. (C) Summary data showing the number of $MHCII^{+}$ cells. Data are presented as Mean ± SEM. N= 4 for each cohort. 1-way ANOVA * denotes significance at $p < 0.05$

Gross Histological Alterations in the Cecum and Perivascular Adipose in MetSyn Rats

We observed that the cecum was abnormally small in the MetSyn rats and fasted cecum wet weight was roughly half that of controls when normalized to body weight (Figure 11 A-C). Mesenteric whole mount tissues that were fixed overnight at 4°C in RNALater provide further evidence for enlargement of the perivascular adipose tissue that encases the mesenteric neurovascular bundle (Figure 11D and 11E).

High-Fructose-Induced MetSyn Rats Exhibited Macrophages Skewed Toward M1 State

Immunofluorescence was also preformed on mesenteric arcades collected from MetSyn rats. Tissues were fixed and stained in the same manner as described for the LPS-injected rats. The dichotomy in staining for CD163/CD206 and MHCII staining was observed in control bundles; however the MetSyn tissues displayed a significant rise in the amount of $CD163^{+}MHCII^{+}$ cells (Figure 12). MetSyn mesenteric bundles had a modest but significant increase in the number macrophages (Figure 13) that was directly affected by the rise in $CD163^{+}MHCII^{+}$ double positive cells (Figure 13). There were no changes in the population of $CD163^{+}CD206^{+}$ cells nor was there an increase in the number of $CD163^{-}MHCII^{+}$ cells (Figure 13).

MLV Function is Not Restored with Therapeutic Levels of Glib in MetSyn Rats

MLVs were isolated from control and MetSyn rats and exposed to intramural pressures of 1, 3, and 7cmH_2O in APSS solution. Approximately half of the MetSyn MLVs demonstrated significantly reduced lymph pump flow as a function of a

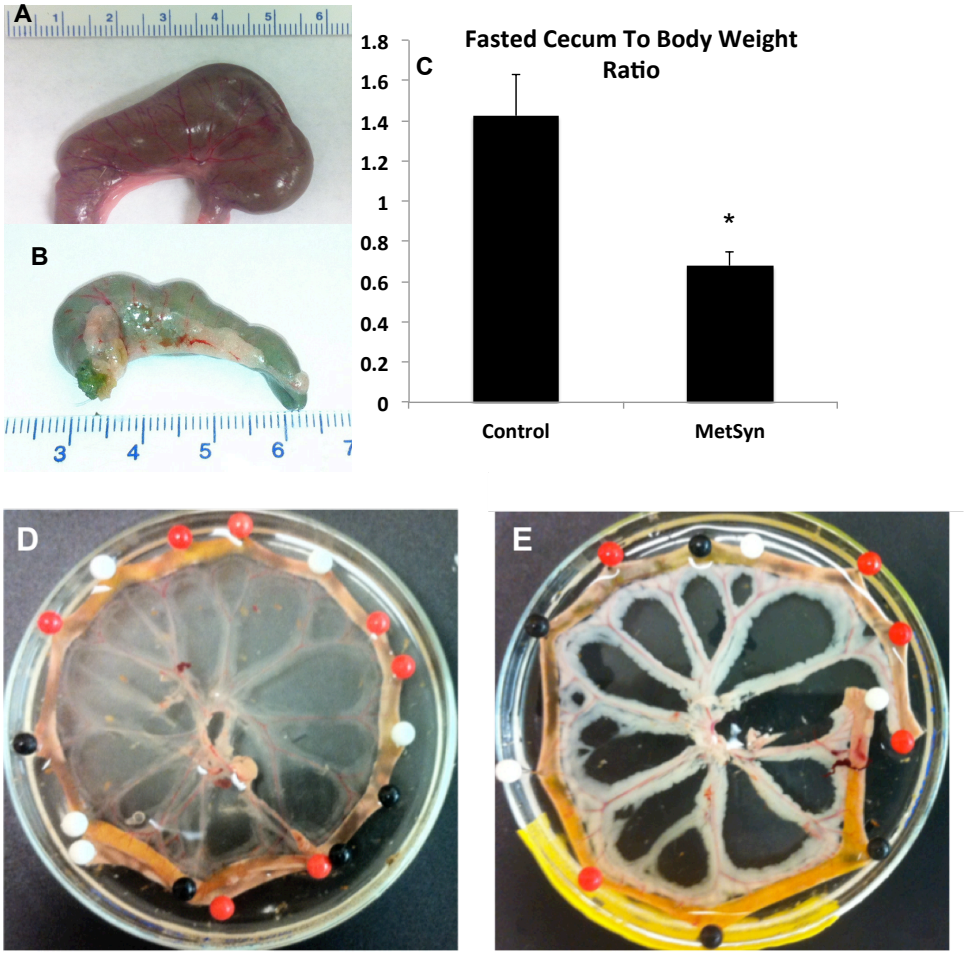

Figure 11. High fructose feeding-induced MetSyn results in gross histological changes in the cecum and mesenteric tissue. Cecum size in control (A) and MetSyn (B) rats is shown; (C) Cecum weight to body weight is shown for control and MetSyn rats. Mesenteric tissue bundles fixed in RNALater® overnight at 4^{o}C illuminates the increased adiposity in the perivascular depots of the mesenteric neurovascular bundles (D, Control; E, MetSyn). Data are presented as Mean ± SEM. N= 6 for each cohort. 1-way ANOVA * denotes significance at $p < 0.05$

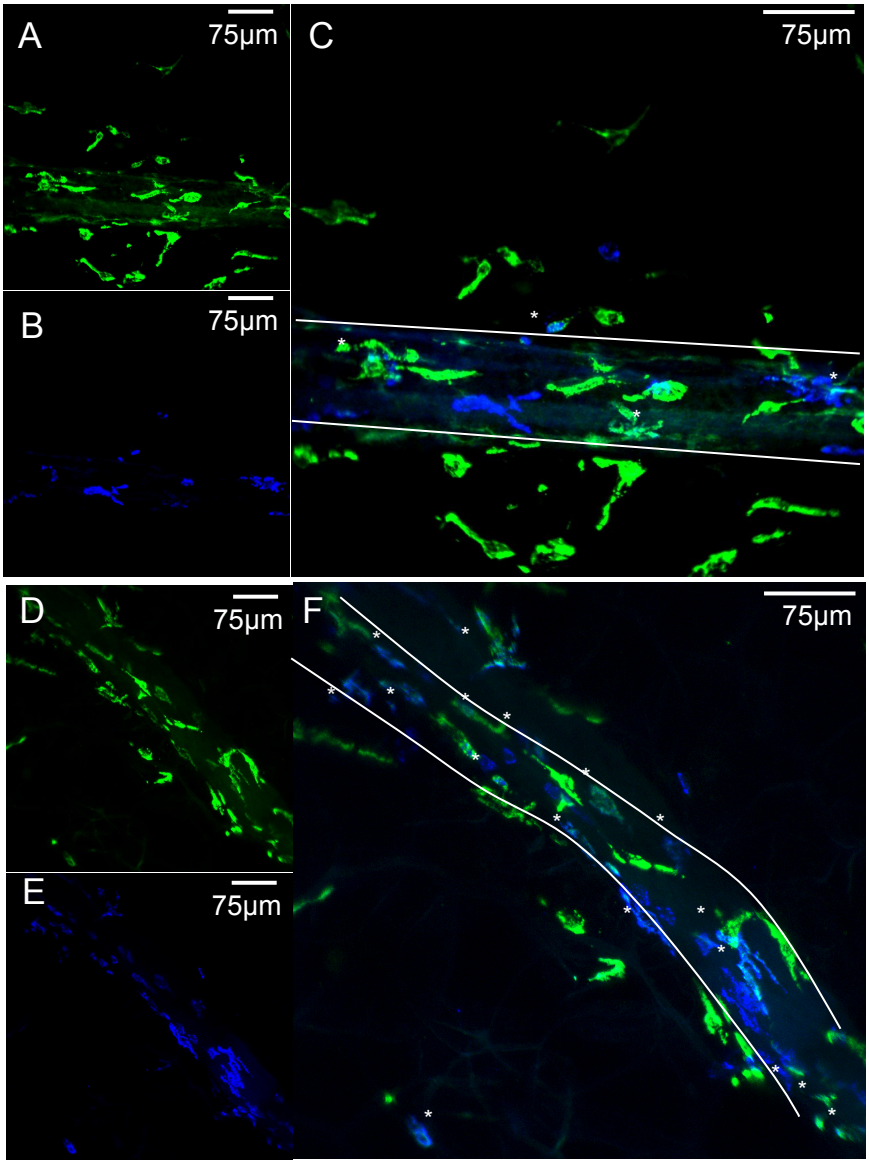

Figure 12. Macrophage profile in the neurovascular bundles of the mesentery in control and MetSyn rats. Representative image of a 40X field of view stained for CD163 (A,D green) and MHCII (B,E blue) to demonstrate single or dual staining (C, F merge). A, B, and C Control mesentery; D, E, and F MetSyn mesentery. White asterisks in C and F demonstrate $CD163^{+}MHCII^{+}$ cells. The lymphatic vessel is outlined with white lines.

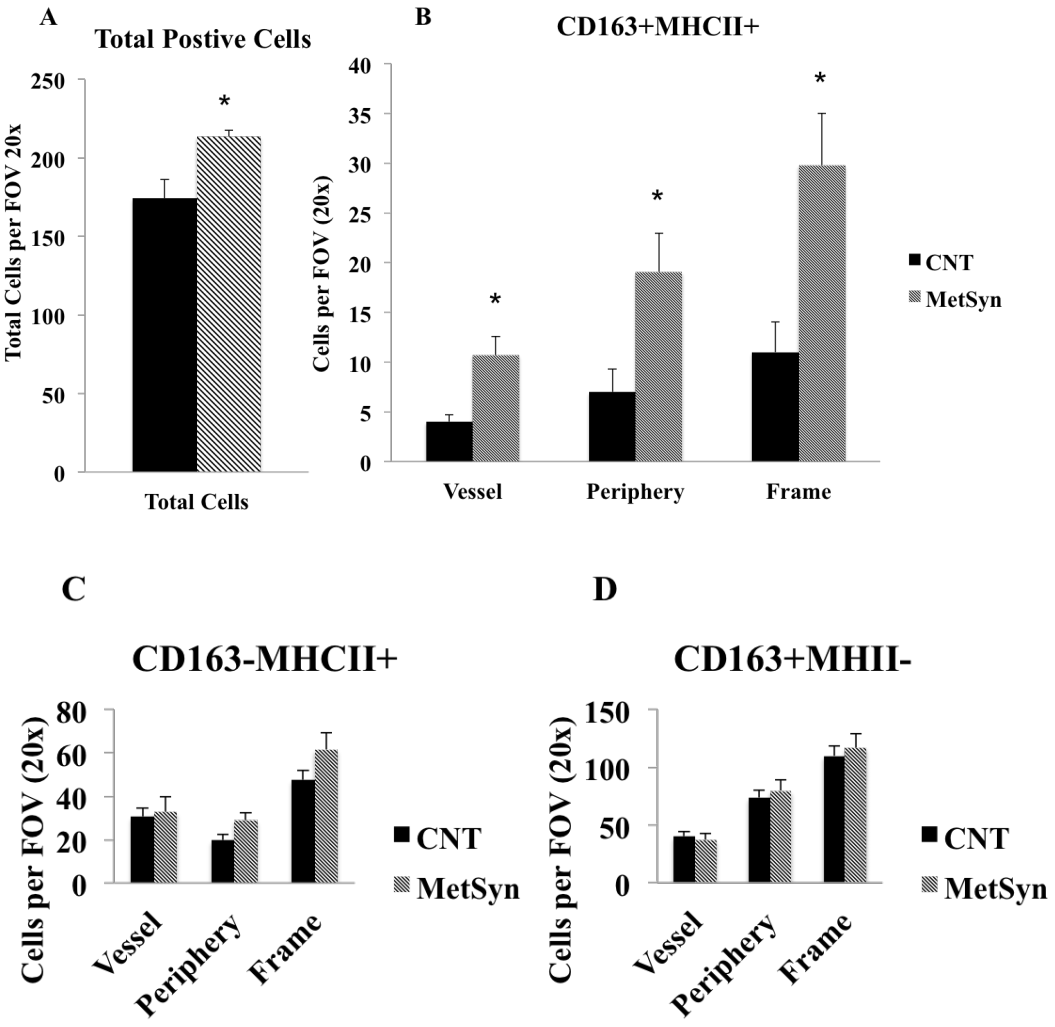

Figure 13. Summary data showing the number of single or double positive CD163, MHCII cells. The number of total positive cells (A), $CD163^{+}MHCII^{+}$ cells (B), $CD163^{-}MHC^{+}$ cells (C) and $CD163^{+}MHCII^{-}$ cells (D) are shown. Data are presented as Mean ± SEM. N= 6 for each cohort. 2-way ANOVA * denotes significance at $p < 0.05$

significantly lower phasic contraction frequency (Figure 14) and stroke volume (MSlo) (Figure 15). Additionally, the remaining vessels displayed abnormally high contraction frequencies (MShi) that were greater than control vessel frequency (Figure 14), but with a significantly reduced ejection fraction (Figure 15). Lymph pump flow in the MShi vessel population was not significantly different than in controls despite the altered contractility. Vessel diameters and tonic indexes were not significantly different in control, MSlo, or MShi groups (Figure 16). Control and MSlo vessels were also exposed to 1μM Glib (Glib) and 10μM Glib at each pressure to determine if Glib could restore lymph pump function through the inhibition of K_{ATP} channels. Glib at 1μM in MSlo vessels did not increase lymph pump flow despite an increase in phasic contraction frequency (Figure 17). Additionally, 1μM Glib did not significantly alter contraction frequency or lymph pump flow at pressures or 3 or 7cmH_2O (Figure 17). Ejection fraction, stroke volume, and vessel tone were all unchanged from basal values by the addition of 1μM Glib (Figure 18). To determine if the contraction frequency reduction was regulated by poor pacemaker function we maximally activated control and MSlo MLVs with 10μM Glib. Glib at 10μM dramatically increased contraction frequency in both control and MSlo MLVs. However, 10μM Glib significantly increased lymph pump flow (Figure 17) at only pressure 3cmH_2O in MSlo MLVs and did not significantly affect control lymph pump flow. Ejection fraction and stroke volume fell in control vessels, but not in MetSyn rats, at pressures of 3 and 7cmH_2O (Figure 18) in response to 10μM Glib. A summary of the contractile parameters is listed in Table 4.

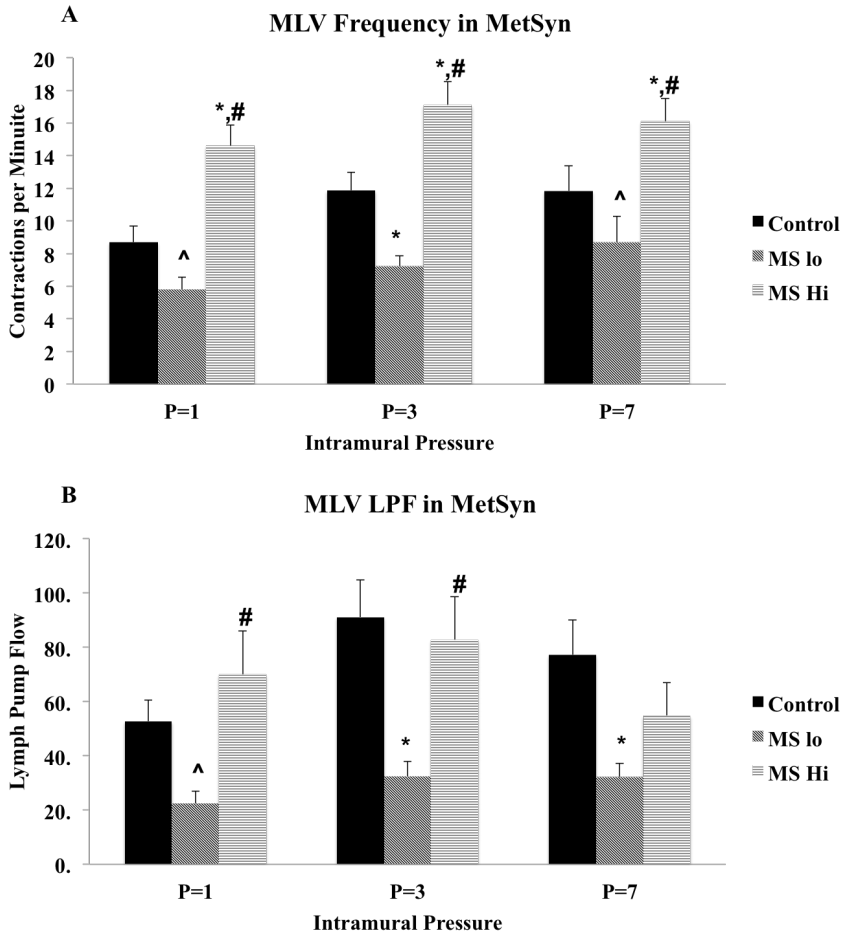

Figure 14. Impaired contractile frequency and lymph pump flow in the MetSyn MLV. MLVs isolated from MetSyn rats displayed two phenotypes and were separated into MSlo (<10 contractions per minute) and MShi (>10 contractions per minute) populations based on their contraction frequency at pressure 1cmH_2O. Data are presented as Mean ± SEM. n=10 control, 9MSlo, 11MShi. 2-way ANOVA and Fisher post-hoc. * denotes $p<0.05$; ^ denotes $p<0.1$ comparing MSlo or MShi versus control, # denotes $p<0.05$; " denotes $p<0.1$ comparing MSlo versus MShi.

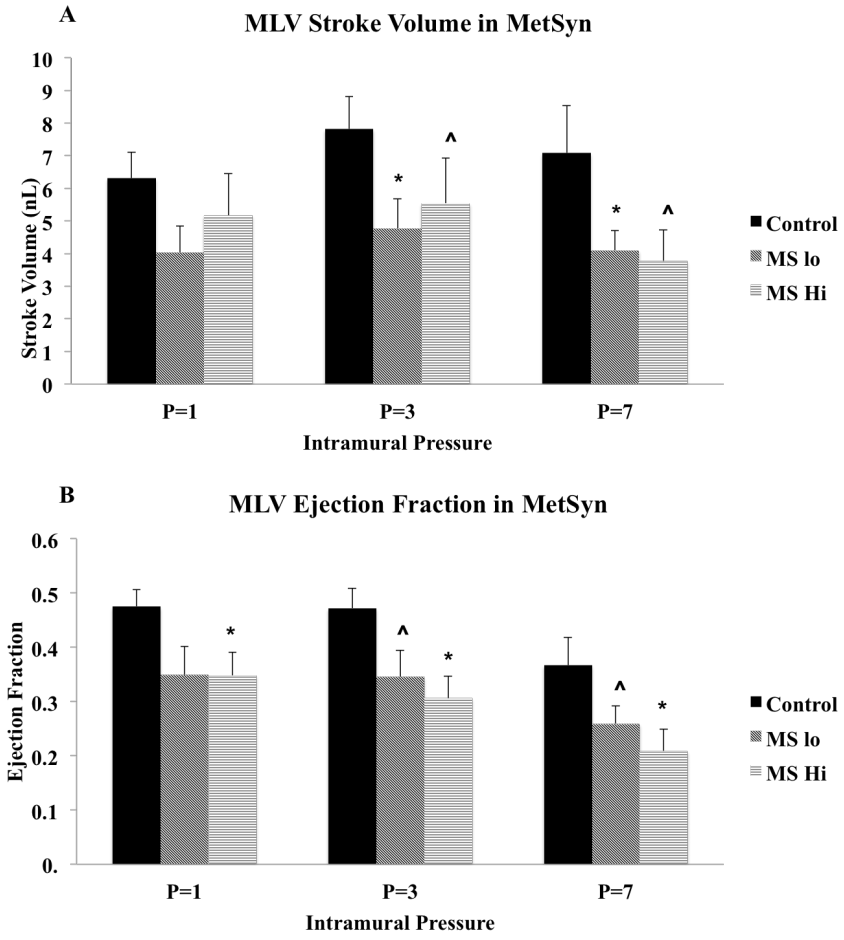

Figure 15. MLV from MetSyn rats have reduced stroke volume and ejection fraction. MLVs isolated from MetSyn rats displayed two phenotypes and were separated into MSlo (<10 contractions per minute) and MShi (>10 contractions per minute) populations based on their contraction frequency at pressure 1cmH_2O. Data are presented as Mean ± SEM. n= 10 control, 9MSlo, 11MShi. 2-way ANOVA and Fisher post-hoc. * denotes $p<0.05$; ^ denotes $p<0.1$ comparing MSlo or MShi versus control.

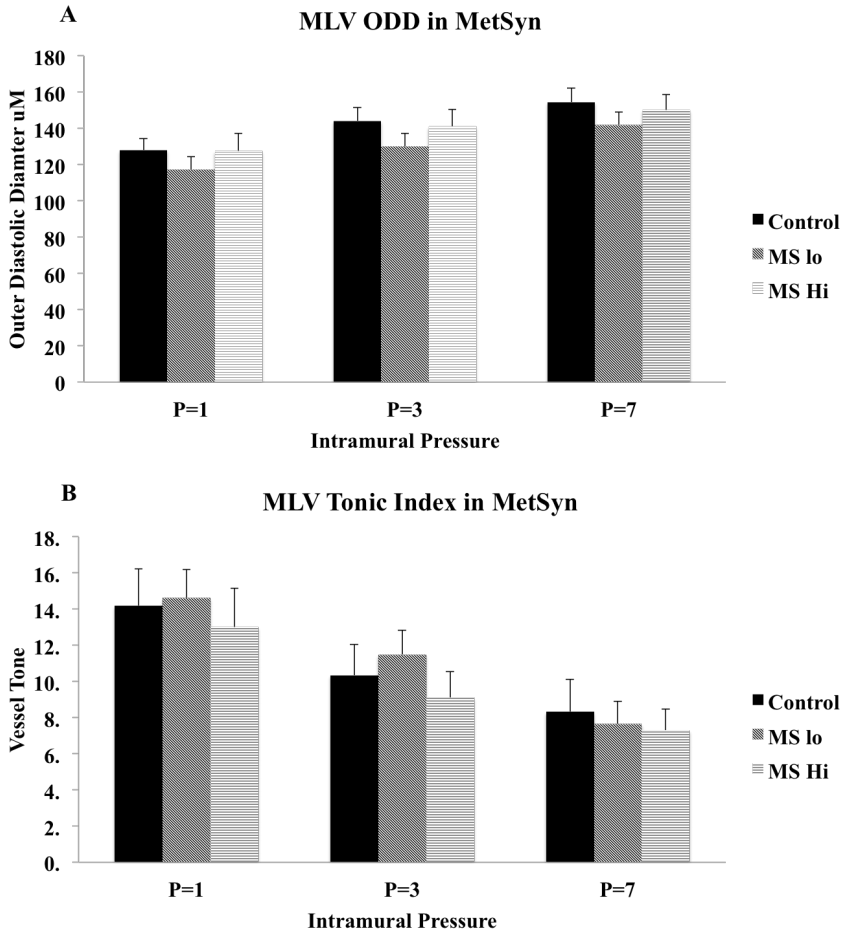

Figure 16. Vessel outer diastolic diameter and vessel tone are normal in the MLVs from MetSyn rats. MLVs isolated from MetSyn rats displayed two phenotypes and were separated into MSlo (<10 contractions per minute) and MShi (>10 contractions per minute) populations based on their contraction frequency at pressure 1cmH_2O. Outer diastolic diameter (ODD) and tonic index was determined. Data are presented as Mean ± SEM. n= 10 control, 9MSlo, 11MShi. 2-way ANOVA and Fisher post-hoc.

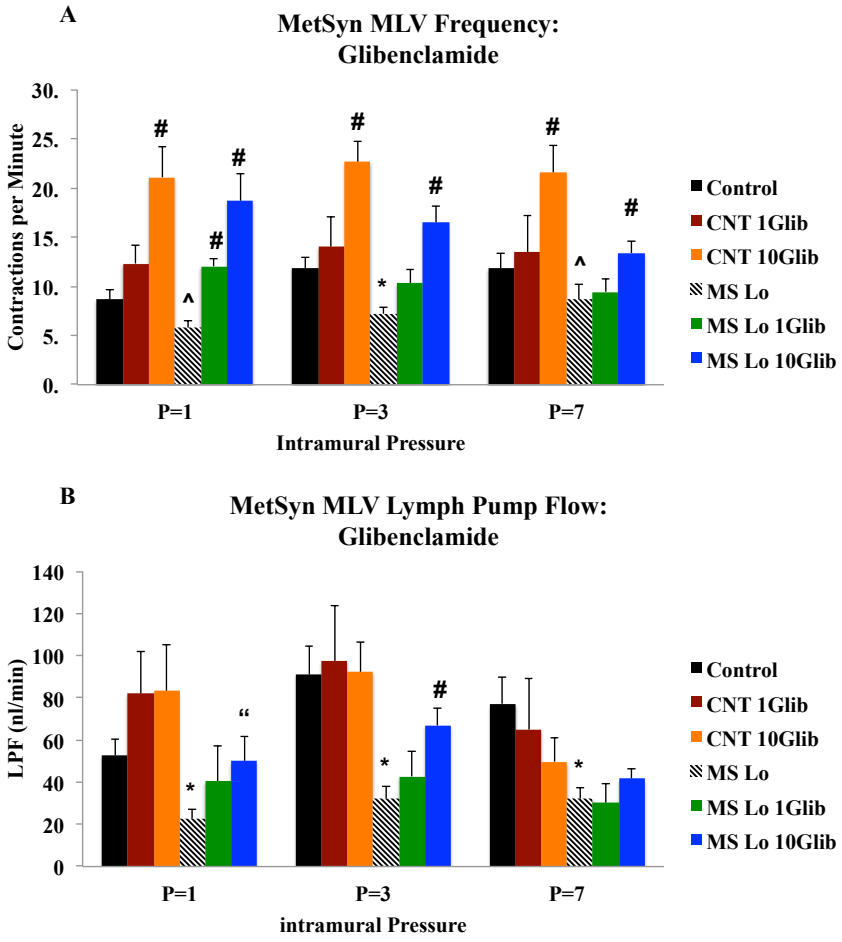

Figure 17. The effect of Glib on MLV contraction frequency and lymph pump flow in MetSyn MLVs. MLVs isolated from MetSyn rats that demonstrated a contraction frequency below 10 contractions per minute were characterized as MSlo. Data are presented as Mean ± SEM. n= 10 control and 9 MSlo. 2-way ANOVA and Fisher post-hoc. * denotes $p<0.05$; ^ denotes $p<0.1$ comparing MSlo versus control, # denotes $p<0.05$; " denotes $p<0.1$ comparing Glib versus APSS within each cohort.

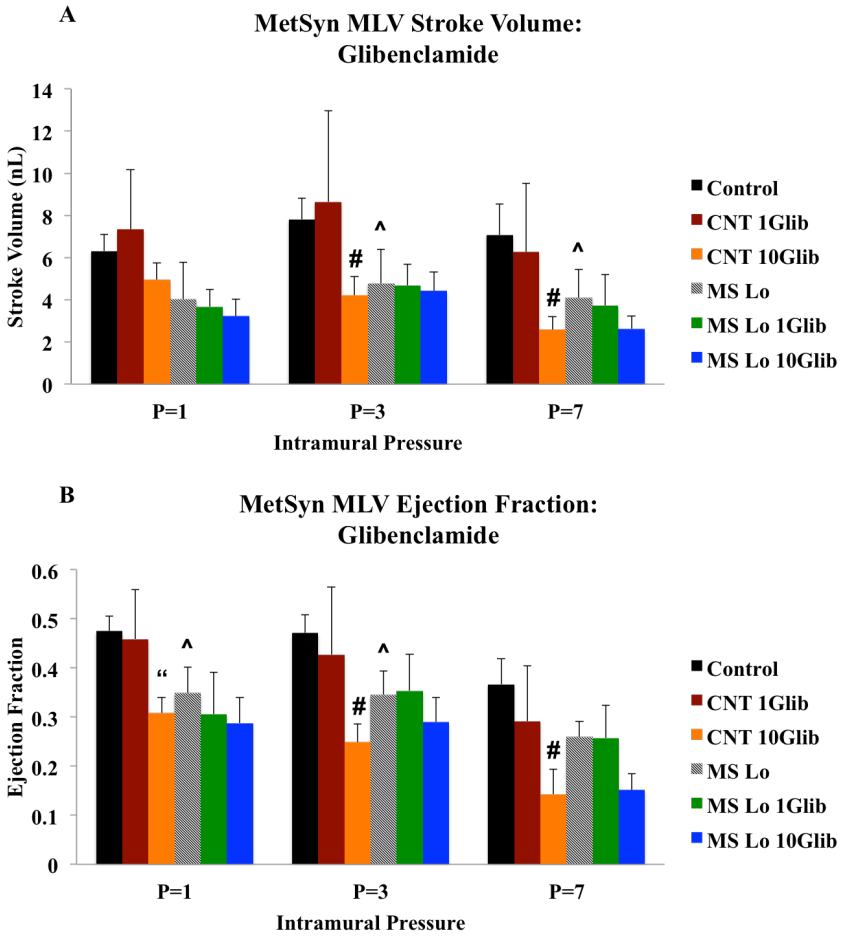

Figure 18. The effect of Glib on MLV stroke volume and ejection fraction in MetSyn. MLVs isolated from MetSyn rats that demonstrated a contraction frequency below 10 contractions per minute were characterized as MSlo. Data are presented as Mean ± SEM. n= 10 control and 9 MSlo for APSS pressure responses and n=4 for each cohort for Glib responses. 2-way ANOVA and Fisher post-hoc. * denotes $p<0.05$; ^ denotes $p<0.1$ comparing MSlo versus control, # denotes $p<0.05$; “ denotes $p<0.1$ comparing Glib versus APSS within each cohort.

Table 4. Contractility parameters from the control and MetSyn MLVs

Mean ± SEM	Pressure (cm H2O)	P=1	P=3	P=7	P=1 1Glib	P=3 1Glib	P=7 1Glib	P=1 10 Glib	P=3 10 Glib	P=7 10Glib
Outer Diastolic Diam. (uM)	Control	128 ± 6.50	144 ± 7.4	154 ± 7.9	139 ± 16.8	154 ± 19.0	163 ± 20.0	133 ± 12.9	150.6 ± 12.5	158 ± 12.2
	Mslo	117 ± 7.2	130 ±7.2	142 ±7.9	111 ± 13.7	123 ± 12.5	130 ± 12.2	119 ± 0.8	139 ± 2.4	148 ± 3.0
	Mshi	127.5 ±9.8	141± 9.5	150 ± 8.5	nd	nd	nd	nd	nd	nd
Contraction Frequency per Minute	Control	8.7 ± 1.0	11.9 ± 1.1	11.9 ± 1.5	12.3 ± 1	14.0 ± 3.1	13.5 ± 3.7	21.1 ± 3.0	22.6 ± 2.1	21.6 ± 2.8
	Mslo	5.8 ± 0.7	7.2 ± 0.7	8.7 ± 1.6	12.1 ± 0.8	10.4 ± 1.4	8.7 ± 1.3	18.4 ± 2.7	16.7 ± 1.7	14.7 ±1.2
	Mshi	14.6 ± 1.3	17.1 ± 1.4	16.1 ± 1.4	nd	nd	nd	nd	nd	nd
Stroke Volume (nL)	Control	6.31 ± 0.8	7.8 ± 0.99	7.08 ± 1.47	7.3 ± 2.8	8.6 ± 4.3	6.3 ± 3.2	4.9 ± 0.8	4.2 ± 1.0	2.6 ± 1.5
	Mslo	4.02 ± 0.81	4.77 ± 0.90	4.10 ± 0.61	3.7 ± 1.7	4.7 ± 1.6	3.7 ± 1.3	3.2 ± 0.8	4.4 ± 0.9	2.6 ± 0.6
	Mshi	5.17 ± 1.28	5.55 ± 1.38	3.78 ± 0.96	nd	nd	nd	nd	nd	nd
Lymph Pump Flow (nL/Min)	Control	52.7 ± 7.8	91.4 ± 13.7	77.2 ± 12.8	82.0 ± 19.8	97.5 ± 13.7	65.1 ± 24.4	83.2 ± 21.8	92.4 ± 14.0	49.8 ± 11.6
	Mslo	22.4 ± 4.5	32.5 ± 5.3	32.1 ± 5.0	40.3 ± 16.8	42.8 ± 11.8	30.4 ± 8.6	50.1 ± 11.4	67.0 ± 8.1	41.6 ± 4.8
	Mshi	70.0 ±16.1	82.8 ± 15.8	54.8 ±12.1	nd	nd	nd	nd	nd	nd
Tonic Index (% constriction)	Control	14.2 ± 2.1	10.3 ± 1.7	8.3 ± 1.8	8.7 ± 2.9	7.4 ± 1.9	5.2 ± 1.7	10.9 ± 2.9	7.6 ± 0.9	6.0 ± 1.8
	Mslo	14.6 ± 1.6	11.5 ± 1.33	7.6 ± 1.3	11.5 ± 3.3	7.3 ± 1.1	5.6 ± 1.0	16.5 ± 2.7	8.9 ± 0.6	5.5 ± 0.2
	Mshi	13.0 ± 2.1	9.1 ± 1.5	7.3 ± 1.2	nd	nd	nd	nd	nd	nd

Data are presented as Mean ± SEM for outer diastolic diameter, lymphatic contraction frequency, stroke volume, lymph pump flow, and tonic index. n=10 control, 9MSlo, 11MShi for pressures of 1, 3, and 7cmH_2O. n= 4 for control and MSlo vessels stimulated with Glib.

Macrophage Recruitment and Polarization Factors and iNOS Expression

RNA was also collected from the mesenteric bundles of MetSyn and control rats. Levels of MCP-1 and iNOS mRNA were both significantly elevated in the mesenteric tissue of MetSyn animals (Figure 19). We cultured mLECs and mLMCs and stimulated them with 20ng/ml of LPS for a 24-hour period. Inflammatory gene expression and macrophage maturation markers were assessed using QPCR and the ΔΔCt method, with β-actin (βAct) and smooth muscle α-actin (SMA) used as housekeeping controls. LPS-treated mLECs expressed significantly elevated levels of glyceraldehyde 3-phosphate dehydrogenase (GAPDH), MCSF, IL-6, Prox-1, and TNFα when compared to vehicle-stimulated mLECs (Figure 20). The mLECs dramatically increased the expression of GMCSF, iNOS, monocyte chemoattractant protein 1 (CCL2), and chemokine ligand 1 (CCL1), as abundance of these RNAs increased greater than 10 fold in response to LPS (Figure 20). The mLMCs also up-regulated genes associated with tissue inflammation, including GAPDH, MCSF, GMCSF, TGFβ, and transgelin (SM22) (Figure 21). CCL2, IL-6, and iNOS expression were highly activated in mLMC cultures in response to LPS stimulation (Figure 21). The threshold values of each gene tested are listed in Table 5.

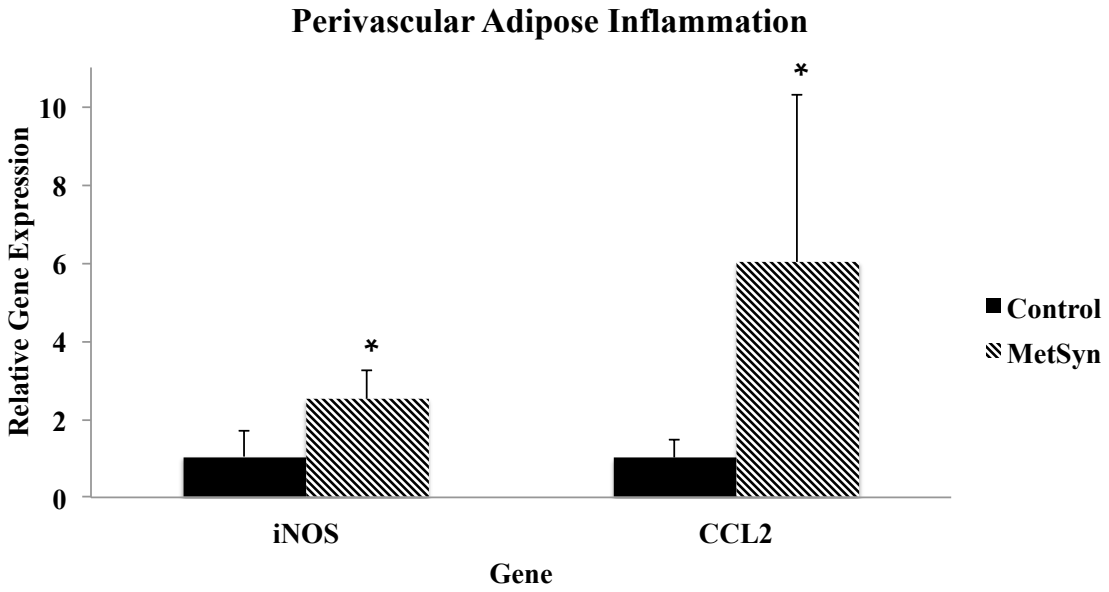

Figure 19. Mesenteric neurovascular bundles have elevated expression of CCL2 and iNOS. Mesenteric neurovascular bundles were fixed overnight in RNALater® at 4^{o}C and RNA extracted. Relative gene expression was calculated as described in the Methods section. MetSyn neurovascular bundles had higher expression of both iNOS (2.5 fold) and CCL2 (6 fold) as compared to control tissues. Data are presented as Mean ± SEM. N=6; * denotes significance at $p<0.05$

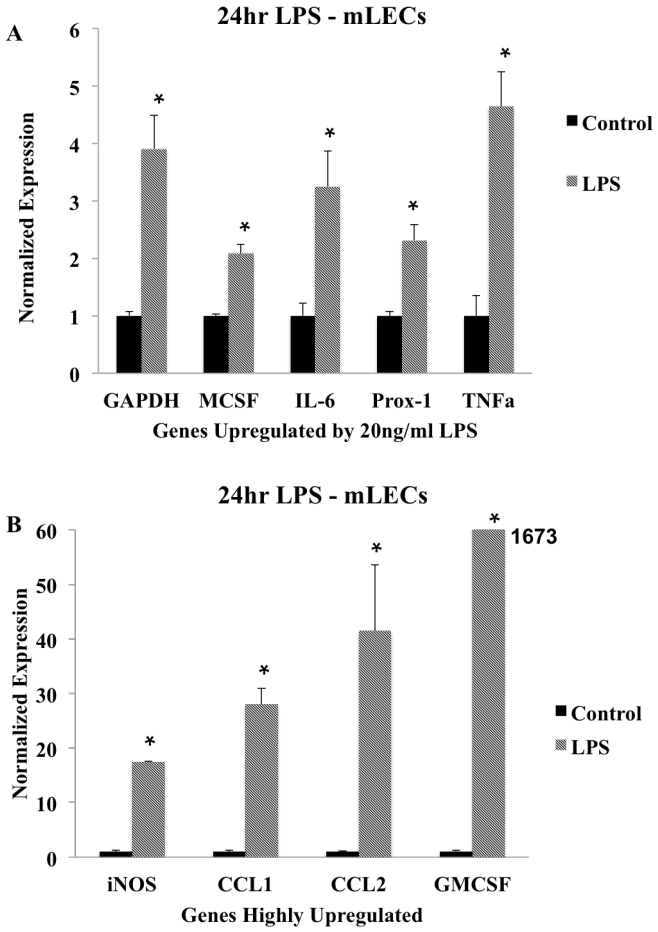

Figure 20. LECs increase expression of inflammatory genes and macrophage maturation genes in response to LPS. LECs were treated either with PBS (vehicle, control) or 20ng/ml LPS for 24 hours. RNA was collected and subjected to real time PCR using specific primer sets. Normalized expression was determined as described in the Methods section. (A) LECs increased expression of GAPDH, MCSF, IL-6, Prox-1, and TNFα in response to LPS stimulation. (B) LECs demonstrated a dramatic increase in the expression of iNOS, CCL1, CCL2, and GMCSF (1673 fold higher) in the LPS-treated group as compared to control group. Data are presented as Mean ± SEM. N=3; * denotes significance at $p<0.05$

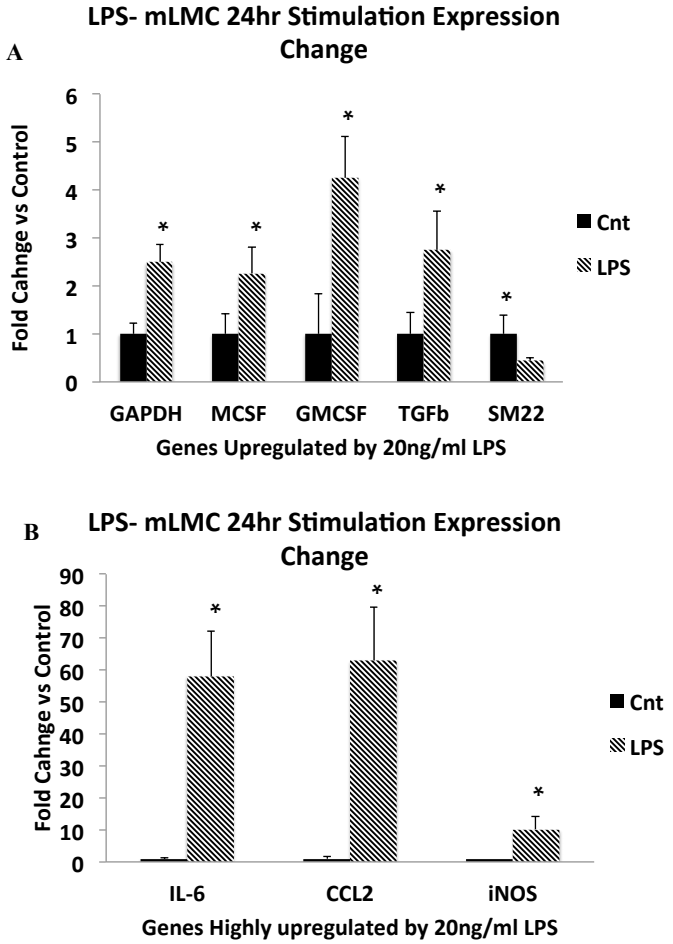

Figure 21. mLMC increase expression of inflammatory genes and macrophage maturation genes in response to LPS. The mLMCs were treated either with PBS (vehicle, control) or 20ng/ml LPS for 24 hours. RNA was collected and subjected to real time PCR using specific primer sets. (A) mLMC-treated with LPS showed a significant increase in the expression of GAPDH, MCSF, GMCSF, TGF-beta, and SM22 as compared to the control cells. (B) IL-6, CCL2, and iNOS expression was highly increased in response to LPS stimulation. Data are presented as Mean ± SEM. N=3; * denotes significance at $p<0.05$

Table 5. Gene threshold cycle values for both mLECs and mLMCs after stimulation with LPS.

Gene	mLEC-Vehicle	mLEC-LPS	mLMC-Vehicle	mLMC-LPS
Beta Actin	15.7	15.6	DNC	DNC
Smooth Muscle Actin	DNC	DNC	16.6	17.1
GAPDH	20.6	18.5	18.5	17.6
IL-6	28.7	26.9	24.1	18.7
CCL2	21.5	16.1	24.4	18.6
iNOS	27.9	23.5	25.3	22
MCSF	22.7	21.5	20.9	20.2
GMCSF	30.5	19.7	28.3	26.4
CCL1	27.1	22.1	20.9	20.2
TGFb	DNC	DNC	23.6	22.6
Lyve-1	22	23.5	DNC	DNC
Prox-1	21.8	20.5	DNC	DNC
SM22	DNC	DNC	18.8	20.4

The threshold cycle values from the QPCR of treated mLECs and mLMCs. Cells were exposed to vehicle control (PBS) or 20ng/ml of LPS for 24hrs. RNA (1µg) was converted to cDNA and QPCR was used to determine the relative expression of genes that regulate tissue inflammation and macrophage recruitment and polarization.

Discussion

The presented data have demonstrated that both acute (LPS-injection) and chronic (MetSyn) inflammatory conditions impair the intrinsic pump characteristics of the lymphatic vessel. In addition, an increase in macrophage accumulation and altered macrophage polarization in the surrounding tissue and in contact with mesenteric collecting lymphatic vessels are seen in both of these models. Furthermore this study has provided evidence for a direct role for the lymphatic tissue in shaping macrophage homeostasis and polarization through the expression of macrophage chemoattractant and maturation factors. These functional characteristics of lymphatics may contribute to resident tissue macrophage homeostasis under physiological and pathophysiological conditions (Figure 22) such as MetSyn or infection and may contribute to the increased risk for lymphedema in MetSyn.

Our data provides the first characterization of the macrophage polarization and spatial association with MLVs in both the LPS-induced peritonitis and MetSyn. The recruitment and association of macrophages with lymphatic tissues have been previously documented with LPS-induced inflammation in a mouse model, although macrophage polarization has not been addressed in these studies (164, 187, 191). A mouse model of LPS-induced peritonitis demonstrated a role for $CD11b^{+}$ myeloid cells in lymphatic dysfunction and poor fluid clearance in the diaphragm (164). These macrophages are a source of the pro-lymphangiogenic factors vascular endothelial growth factor C and D (VEGFC, VEGFD) that regulate endothelial sprouting and proliferation. These

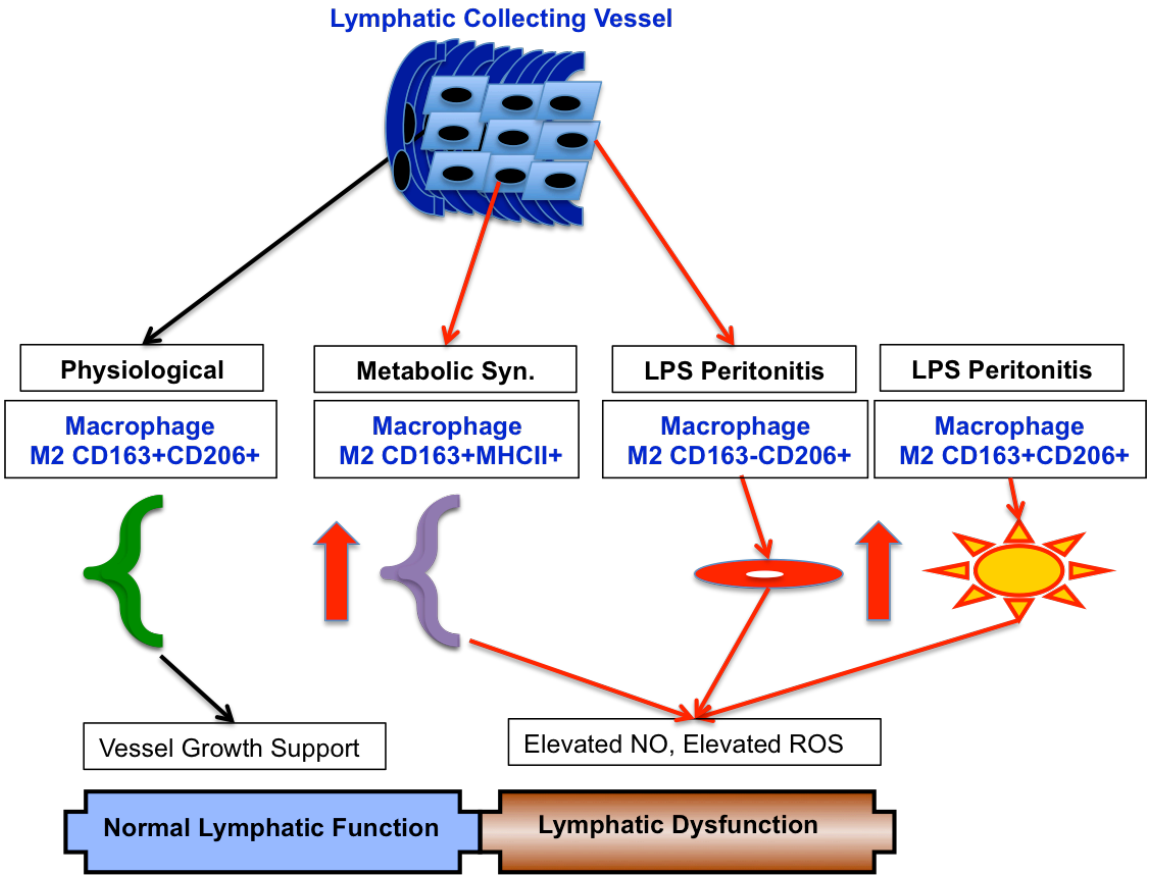

Figure 22. Schematic of the crosstalk between lymphatic collecting vessels and macrophage populations in the different disease models. MetSyn increases $CD163^{+}MCHII^{+}$ M1 skewing of the macrophage population. LPS-induced peritonitis also increases the accumulation of $CD163^{-}CD206^{+}$ and $CD163^{+}CD206^{+}$ cells.

investigators demonstrated a role for $CD11b^+$ cells as initiators of fibrosis and lymphangiogenesis (164). Additionally, functional parameters of lymphatic contractility were not measured in the collecting vessels that drain the tissue. Macrophage influx into the lymphatic space utilizes both expansion of monocyte-derived cells and expansion of resident tissue macrophages. LPS-activated $CD11b^+$ macrophages can also activate a lymphatic endothelial cell progenitor phenotype and contribute to the inflammation-driven lymphangiogenesis (120). We did not address the role of lymphangiogenesis in the LPS-induced inflammation or MetSyn models and focused our efforts on describing the contractility changes that are required for proper lymphatic function. However, LECs can express the macrophage mannose receptor (CD206) (142, 202). It is a distinct possibility that the morphology of the $CD163^-CD206^+$ cells is indicative of LECs or macrophage-derived lymphatic endothelial cell precursors. However, the $CD163^-$ $CD206^+$ cells were brightly positive for CD206 and observed in the tissue without association with the lymphatic vessel. The M2b polarization is induced in response to TLR agonist and immune complexes. M2b macrophages are characterized as a quasi-inflammatory phenotype that produces both IL-10 and TNFα, while expressing a high level of iNOS and CCL1 (218, 220). CD206 expression is associated with the TGFβ and IL-4 and STAT6 signaling axis that has been described in other models of peritoneal inflammation. TGFβ can stimulate the M2b phenotype(311) and is critical to the resolution of peritonitis (327). M2b macrophages have been previously described in the peritoneum of murine burn models, demonstrating a critical role for CCL1 in the regulation and proliferation of the M2b phenotype (11, 165). Our results (Figures 20 and

21) show that both mLMCs and LECs express high levels of CCL1 and GMCSF in response to LPS stimulation, suggesting a potential mechanism whereby lymphatic vessels contribute to the stromal environment for macrophage proliferation and activation. This has relevant implications in tissue inflammation as macrophages reside along, and in the vicinity of, lymphatic vessels under physiological and pathophysiological conditions. Macrophage proliferation and polarization have been recently linked to exposure level of either MCSF or GMCSF to induce a M2 or M1 response, respectively (75, 174). The majority of macrophages in the control mesenteric tissue resembled an M2a phenotype, characterized by double staining for $CD163^{+}CD206^{+}$, consistent with reports for adipose tissue macrophages. The $CD163^{+}CD206^{+}$ phenotype expanded significantly in the LPS-injected model and was closely associated with lymphatic tissues. This is likely a chemoattractant response to CCL2 and our data supports previous reports of CCL2 up-regulation upon TLR activation (245).

LPS has been historically used to activate an M1 phenotype in macrophage in the in vitro systems. The M1 phenotype is also induced by GMCSF exposure and is characterized by increased expression of MHCII, increased co-stimulatory molecule expression, and inflammatory cytokine production (91, 174). We did not observe a significant increase in the expression or presence of MHCII positive cells in response to LPS despite the dramatic expansion of macrophages. Previous reports have suggested a role of glucocorticoid production in the maintenance of the M2 polarization and expression of CD163 in the peritoneal macrophages (265). Additionally, daily LPS

administrations can result in endotoxin tolerance that results in down regulation of TLR4 and increases anti-inflammatory gene expression such as IL-10 and TGFβ (234, 358) and may suggest a role of peritoneal M2b macrophages. In the mouse, iNOS expression strongly correlates with the either the M1 or M2b polarization (195, 200, 219). Extensive studies with rat macrophages have yet to be been done to confirm this paradigm, and the iNOS expression in human macrophages is not clear (241, 268, 269). Furthermore rat peritoneal macrophages have high levels of NO production that is also strain-dependent and may not be limited to specific polarizations(186, 221). Investigations into the expression of iNOS in the rat macrophage populations will be critical to determining further roles for macrophage polarization function and coordination of lymphatic function.

MLVs from LPS-injected rats had severely impaired lymphatic contractility. Phasic contraction frequency was absent in half the vessels studied and reduced function was described in the remaining three vessels that maintained phasic contractions. The inhibition in contraction frequency and decreased tonic index fit very well with the current understanding of overproduction of NO, a potent inhibitor of lymphatic contractility (323). It is likely that the $CD163^{+}CD206^{+}$ and/or the $CD163^{-}CD206^{+}$ cells express iNOS despite displaying evidence for a M2 phenotype and were responsible for the lymphatic dysfunction in our isobaric preps (186, 221). Others have demonstrated a role for iNOS-expressing $CD11b^{+}$ $Gr1^{+}$ monocytes in the suppression of mouse popliteal lymphatic contractility in response to oxazolone-driven inflammation (187). However, this study was performed using intra-vital microscopy of a lymphatic vessel *in vivo* and

would be subject to vasoactive substances or cells carried in the lymph and potentially different tissue pressures. In our studies, we isolated lymphatic vessels from the tissue and flushed any cells or lymph prior to experimentation allowing us to set specific and consistent pressure stimuli. This, in turn, allowed for a critical assessment of the intrinsic contractility and lymph pump function by a single lymphangion and its embedded resident macrophage population. Previous work in our lab has demonstrated that macrophages are embedded in the vessel and are present on isolated lymphatic vessel preps (unpublished data). Regional activation of inflammation and altered macrophage polarization may play a significant role in the determination of lymphedema risk in unilateral cases.

We have also provided evidence for the lymphatic dysfunction in the MetSyn state. Lymph pump flow inhibition has been described in other models of chronic inflammation. TNBS-induced ileitis caused significant inhibition of MLV pump in guinea pigs that was partially restored by a NOS inhibitor and the K_{ATP} channel blocker Glib (204, 340). A rat model of TNBS-induced colitis also demonstrated impairment of MLV contractility and poor lymph flow due to regional inflammation in the small intestine (unpublished results). We have previously reported that MLV have poor lymphatic function in a high fructose fed rat model of MetSyn (357). Other investigators have replicated these results in genetic and diet-induced models of obesity and the MetSyn state in the mouse(25, 262, 330). Lymphatic dysfunction in MetSyn is consistently due to a reduction in phasic contraction frequency that significantly lowers lymph pump flow. A similar dysfunction in MetSyn MLVs is reported in this study with

the addition of a new MLV contractile response that has not been previously described. We observed that approximately half of the MLVs isolated from MetSyn rats displayed an abnormally high basal contraction frequency (MShi >10beats/minute at 1cmH_2O) that was significantly higher than control vessels. However, indices of contraction strength both were significantly reduced, resulting in no net change in the lymph pumping ability. Thus we report that the MetSyn has two patterns of lymphatic dysfunction: 1) a low contraction frequency and potentially low ejection fraction, and 2) a high contraction frequency and sharply reduced contraction strength. Despite a similar reduction in contraction frequency, MetSyn vessels displayed a different phenotype from LPS-injected contractility responses that were also marked by low tone, suggesting an overproduction of NO. In contrast, oxazolone-induced inflammation in the mouse induced a similar dichotomy in popliteal lymphatic contractility, demonstrating both high frequency and low frequency behavior (187). Both NO and ROS have significant effects on lymphatic vessel contractility (204, 355, 356). Regional inflammation and the regulation of both NO and reactive oxygen species may explain the origin of these different contractile patterns. We also assessed the ability of the anti-diabetic drug Glib to increase the lymph pump flow in MSlo rats due to its lower risk of edema compared to other anti-diabetic drugs. Glib acts on K_{ATP} channels to increase membrane potential and increase membrane depolarization frequency. Serum levels for patients on Glib spike to as high as 1μM in the serum and we utilized that as our therapeutic concentration. We found that 1μM Glib had little effect on MLV contractility in either control or MSlo vessels and thus may not have any therapeutic benefit in regards to

lymphatic function. Glib (10μM) was able to restore lymphatic contractility in a guinea pig model of ileitis (204, 321). We found that 10μM Glib significantly increased contraction frequency at each pressure in both control and MSlo rats. Despite the increase in frequency, lymph pump flow was not significantly increased due to a reduction in stroke volume in control vessels. High dose Glib increased lymph pump flow in the MSlo MLVs only at a pressure of 3cmH_2O. This, in part, may be explained by the loss of pressure sensitivity by pacemaker cells in MetSyn rats in response to Glib. Control vessels increased their contraction frequency in response to pressure and this pressure sensitive regulation was also observed in response to glibenclamide stimulation (100, 318). In contrast to MSlo vessels that lost pressure sensitivity under both 1μM and 10μM Glib, indicating lymphatic pacemaker impairment in MSlo vessels and contributes to the lymphatic dysfunction in MetSyn.

The macrophage accumulation and polarization is also altered in the mesenteric tissue of MetSyn rats. In contrast to the LPS model, we found only a modest increase in macrophage accumulation that was specifically due to the increased accumulation of $CD163^+MHCII^+$ cells. We believe this fits well with previous reports of adipose tissue macrophage polarization toward an M1 state (195). We also found elevated expression of CCL2 and iNOS in the mesentery of MetSyn rats. Dietary endotoxin is a significant contributor to the inflammation in the adipose tissue and liver, and is a key driver in the pathogenesis of MetSyn (35, 36). Dietary endotoxin is directly linked to chylomicron production and the MLVs are the transport route for chylomicrons produced in the intestine (105). It is possible that mesenteric vessels can sense luminal dietary

endotoxins, such as LPS, and regulate macrophage polarization and homeostasis through the production of various cytokines, as previously stated. Previous studies have demonstrated that the lymphatic endothelium expresses TLRs and is sensitive to most TLR agonists (155, 245). Infection of LECs with cytomegalovirus also increases the production of GMCSF (90). Our data showing an increase in the production of MCSF and GMCSF in LECs in response to LPS suggest a novel role for the lymphatic endothelium in the regulation of the resident macrophage homeostasis.

In conclusion, the results presented in this study have provided new evidence linking alterations in macrophage activation and polarization with direct and controlled measures of lymphatic vessel contractility under acute and chronic inflammatory conditions. Data have also demonstrated a stromal function for mLECs and mLMCs in the regulation of macrophage homeostasis through the production of MCSF, GMCSF, and CCL1. Lymphatic dysfunction was apparent despite a lack of gross obesity in MetSyn group. An increase in perivascular adipose expansion has been observed in MetSyn animals that are associated with macrophage polarization skewed to a M1 phenotype. Whereas in the LPS-treated group there was no obvious change in the perivascular adipose and the lymphatic impairment is associated with an M2 polarization. Hence, the data presented here establish that the macrophages present in the mesentery tissue and/or on the walls of lymphatics are potent regulators of lymphatic vessel contractility under acute and chronic conditions of inflammation.

CHAPTER III

ENDOTHELIAL NOS DEFICIENCY MEDIATES THE LOSS OF FLOW-MEDIATED INHIBITION IN THORACIC DUCTS OF A HIGH FRUCTOSE FED RAT MODEL OF METABOLIC SYNDROME

Overview

Endothelial dysfunction is a hallmark of insulin resistance and the metabolic syndrome (MetSyn). We have previously demonstrated that stretch-mediated mesenteric lymphatic contractile parameters are impaired in MetSyn rats. Since thoracic duct lymphatics are more sensitive to flow response, we hypothesized that compromised thoracic duct endothelial function in the MetSyn animal will impact the shear sensitive thoracic duct function. To test our hypothesis, we used high fructose diet induced MetSyn rats and determined the changes in stretch- and flow-dependent mechanisms in their thoracic ducts using isobaric measurements. While thoracic ducts from rats with MetSyn did not show any significant changes in pressure-dependent isobaric measurements, the vessels displayed a lack of flow-mediated inhibition of contraction frequency and significantly altered shear sensitivity in vessel tone. Thoracic ducts from rats with MetSyn responded to the exogenous NO donor SNAP with reduced contraction frequency and reduced vessel tone suggesting a functional response to NO. Control rats treated with the NOS blocker LNAME had reduced flow sensitivity and closely resembled thoracic ducts from MetSyn rats. LNAME treatment of MetSyn thoracic ducts exacerbated the reduced flow-mediated inhibition. The ROS-scavenging agent TEMPOL

did not restore flow-mediated inhibition of contractions in MetSyn thoracic ducts. Western blots of thoracic ducts revealed a 50% reduction in the expression of eNOS in MetSyn group when compared to normal thoracic ducts. Thus our data provide the first evidence that MetSyn conditions diminish eNOS expression in thoracic duct endothelium, thereby affecting the flow-mediated functional characteristics of thoracic duct in MetSyn animals.

Introduction

The incidence of metabolic syndrome (MetSyn) has steadily risen, accompanying the rise of obesity (114). The MetSyn increases the risk of cardiovascular disease and type II diabetes mellitus (TIIDM). Approximately 85% of the patients with TIIDM also fall under the MetSyn spectrum (153). Diagnosis of the spectrum relies on the patient fulfilling 3 or more of the 5 criteria: systolic blood pressure >135mmHg, high waist circumference (>40in male, >35in female), hypertriglyceridemia (>150mg/dl), hyperglycemia (>100mg/dl fasting glucose), and low high-density lipoprotein (<40mg/dl male, <35mg/dl female) (115). The MetSyn is also described as chronic yet is a sub-clinical inflammatory state with elevated production of reactive oxygen species (ROS) and mitochondrial dysfunction. Elevations in ROS production by hyperglycemia and insulin resistance factor heavily into the observed hypertensive state, which is characterized by reduced NO bioavailability (16, 39, 161, 178, 278).

Obesity is the most significant driver of the MetSyn state and is also linked to the development of diabetes and hypertension (194). Obesity has been described as a mild

edematous state and is a significant risk factor in the development of lymphedema following a mastectomy or other surgical cancer therapies (2, 67, 126, 166, 244). Lymphedema is a chronic and progressive disease, resulting from dysfunction of the lymphatic system that can arise due to genetic abnormalities (primary) or due to vessel damage or dysfunction (secondary) (254, 256). Morbidly obese patients are at high risk for developing spontaneous lymphedema, suggesting a role for lymphatic failure in obesity and MetSyn (12, 85, 87, 193, 208). However the regulatory mechanisms of lymphatic contractility under pathophysiological conditions, including MetSyn, have not been studied.

Lymphatic function is critical to the uptake of macromolecules from the interstitial space and the maintenance of tissue fluid homeostasis. Lymph is carried through the lymphatic system through at least one node as it is returned to the blood supply at the juncture of the thoracic duct and the subclavian vein. Lymph must be transported against a net pressure gradient and the intrinsic lymphatic contractility and the presence of uni-directional valves is critical for this function (17, 352). Muscularized lymphatic vessels exhibit regular phasic contractions and tonic contractions to provide the necessary pressure stimulus to drive lymph flow (212). The lymphatic tissue is a unique muscle phenotype that has both contractile proteins found in cardiac and classical smooth muscle (226, 228). The lymphatic contraction cycle is described in a similar manner to the cardiac cycle and is regulated by both pressure and shear-dependent mechanisms (100, 101). Though specific pacemaker cells are not yet identified in

lymphatics, pacemaker activity drives lymphatic muscle depolarizations and calcium spikes which precede phasic contractions.

Pacemaker activity is sensitive to stretch and frequency is positively correlated to increasing pressure (100, 318). Lymphatic vessels, particularly the thoracic duct, are also regulated by sheer stress-induced NO production by the lymphatic endothelium (100). NO regulates lymphatic muscle relaxation through the activation of guanylate cyclase and increased cGMP levels (103). The actions of both PKG and PKA mediate the vasodilatory effects of NO stimulation (315). In response to imposed flow, or exogenous NO donors, thoracic duct frequency sharply falls and vessel tone decreases (100). Blockade with a NOS inhibitor abolishes this flow-mediated inhibition of thoracic duct contractility. To maintain proper fluid homeostasis, the lymphatic system must be able to relax when lymph formation and pressure gradients favor passive flow. Flow-mediated inhibition reduces phasic contractility and reduces vessel tone thereby reducing resistance to flow.

The high fructose fed rat model of MetSyn has also been demonstrated to have significant endothelial dysfunction in the blood vasculature (312). This has been linked to blunted vasodilatory responses due to the loss of tetrahydrobiopterin (BH4) (6, 279). BH4 is a critical co-factor for the production of NO and is sensitive to the redox stress of the cell (280). Elevated levels of ROS have been described in the high fructose fed rat model due to a significant increase in NADPH oxidase activity (66, 82, 303). Insulin is a key regulator of expression of eNOS and can increase NO production through phosphorylation at serine 1117 (338). Elevations in inflammatory cytokines can also

inhibit expression of eNOS and reduce NO production (16, 122) and the lymphatic vessels are exposed to much higher cytokine concentrations than blood endothelial cells (211). Hence in this study we have raised a question whether eNOS and/or ROS-mediated NO mechanism(s) are impaired in the lymphatic endothelium, consequently affecting lymphatic function in MetSyn animals.

We have previously reported that MLV exhibit diminished contractile activity in a high fructose model of MetSyn (357). Since the lymphatic thoracic duct is sensitive to the sheer-induced production of NO for proper contractility regulation, we have hypothesized that perturbation in thoracic duct endothelial cell activity in MetSyn animals will affect the flow-dependent NO mechanisms, thereby impairing the thoracic duct lymphatic function. We have utilized a high fructose fed rat model of MetSyn to address the role for NO in the regulation of thoracic ducts.

Materials and Methods

Animal Handling

A total of forty-eight male Sprague Dawley rats were used in this study. Twenty-three rats were given a high fructose feed (HFF) diet (60% fructose, ID.89247 Harlan Teklad®, 66% caloric content from fructose) for seven weeks to induce the MetSyn, while the remaining twenty-five animals were given standard rodent chow. Water and feed were available ad libitum except during pre-experiment (sixteen hour) fasting. Blood was collected in fasted (sixteen hour) rats via the lateral saphenous veins at the start and end of the seven-week diet period. The lower leg was shaved clean and the

lateral saphenous vein was punctured using a 27-gauge needle and blood was collected in a non-heparinized tube. Blood was allowed to clot for 1hr at room temperature and spun for ten minutes at 3,000g. Serum was then frozen and stored at -80°C. MetSyn was confirmed through evaluating triglyceride and insulin concentrations, assessed via commercially available kits (colorimetric kit Bioassays® ETGA-200, and an insulin ELISA kit Linco® EZMRI-13k, respectively). All animals were housed in a facility accredited by the Association for the Assessment and Accreditation of Laboratory Animal Care and maintained in accordance with the policies defined by the Public Health Service Policy for the Humane Care and Use of Laboratory Animals, the United States Department of Agriculture's Animal Welfare Regulations and the Scott & White Animal Care and Use Committee.

Rats fasted sixteen hours were anesthetized with Innovar-Vet (0.3 ml/kg I.M.), which is a combination of a droperidol-fentanyl solution (droperidol 20 mg/ml, fentanyl 0.4 mg/ml), and diazepam (2.5 mg/kg IM). Once an anesthetic plane was reached, an incision was made through the chest ventral wall and the lymphatic thoracic duct was isolated and cut into two 1-cm segments. One segment was snap frozen in liquid nitrogen and stored at -80°C for protein collection. The remaining thoracic duct segment was maintained in albumin supplemented physiological saline solution (APSS, in mM: 145.0 NaCl, 4.7 KCl, 2 CaCl2, 1.17 MgSO4, 1.2 NaH2PO4, 5.0 glucose, 2.0 sodium pyruvate, 0.02 EDTA and 3.0 3-(N-morpholino) propanesulfonic acid (MOPS) and 1% w/v bovine serum albumin) at pH 7.4 at 38°C. This thoracic duct segment was then cannulated onto carefully matched pipettes in a CH-1 chamber® (Living Systems) and

attached to independently adjustable pressure reservoirs. The thoracic duct was given thirty minutes to stabilize at an intramural pressure of 1cm H_20 and spontaneous contractions were consistent. Experimental “n" values are as listed. Each thoracic duct was exposed to pressures of 1cm, 3cm, and 5cmH_20 and 5-minute video recordings and diameter tracings were made at each intramural pressure. Nine control thoracic ducts and seven MetSyn thoracic ducts were exposed to 100μM SNAP at pressures of 1cm, 3cm, and 5cmH_20. Sixteen control thoracic ducts and thirteen MetSyn thoracic ducts were set to a pressure of 3cmH_20 and exposed to imposed flows by raising input and lowering output reservoirs such that transmural pressure was maintained at 3cm H_20 (example; 5cm input-2.5cm output is equivalent to F=1). These thoracic ducts were then returned to a pressure of 1cm H_20 and were treated with either 1mM TEMPOL or 100μM LNAME and the pressure and flow responses repeated. Six control and six MetSyn thoracic ducts were exposed to 1mM TEMPOL for a twenty-minute equilibration and their responses to each pressure and flow recorded. Ten control and seven MetSyn thoracic ducts were incubated in 100μM LNAME for twenty minutes and their responses to each pressure and flow recorded. Each experiment concluded with a twenty-minute equilibration in calcium-free APSS and maximal diameters at each pressure were determined for vessel tone calculation. Due to inherent variation between animals and vessels responses, tonic indexes were normalized to their level at a pressure of 3cmH_20 prior to imposed flow.

Isolated Vessel Video Analysis and Statistics

Lymphatic diameter traces were made for each 5-min video with a vessel wall-tracking program developed and provided by Dr. Michael Davis (53). Outer lymphatic

vessel diameters were tracked thirty times per second providing a trace of diameter changes throughout periods of systole and diastole. The following analogies to the cardiac pump parameters were derived: lymphatic tonic index, contraction amplitude, ejection fraction, contraction frequency, fraction pump flow, and systolic/diastolic diameters, as previously described (17). Lymphatic contractility is inhibited by flow as the vessel no longer needs to actively "pump" if pressure gradients favor positive flow. Contractions decrease average vessel diameter as a function of their frequency and ejection fraction and thus vessel resistance to flow will increase on the order of (1/ radius^4), according to Poiseuille's equation of resistance, as vessel length and viscosity are unchanged. To approximate the increase in vessel resistance, we took the total average diameter of the thoracic duct over that 5-min period and compared it to the average diastolic diameter (assumes a state of no contractions and no average radius change). The difference in true average diameter and diastolic diameter was halved to obtain the average radius change due to contractions and compared using 2-way analysis of variance (ANOVA) and reported as a mean radius change (in microns). As diastolic diameters were used, this calculation is independent of vessel tone and is dependent on frequency and the change in diameter during contraction.

Statistics and Reporting

Statistical significance was determined through 2-way ANOVA with Fisher's post hoc analysis using the Statplus® (Analyst soft) statistical software package. Data are represented as means ± standard error of the means (SEM) and significance represented independently at each figure.

Protein Isolation and Western Blotting

Snap frozen thoracic duct sections were thawed in 60μL of chilled 2x NuPage® sample buffer with protease inhibitor cocktail, phosphatase inhibitor cocktail, and 1x NuPage® reducing agent. Thoracic ducts were then sonicated for three minutes in a water bath sonicator and iced for five minutes. This process was repeated three times and then each sample was refrozen at -80°C. Samples were then thawed on ice and spun down at 1,000g to remove insoluble material and heated for ten minutes at 70°C, as per the manufacturer's instructions. Thoracic duct samples were loaded in alternating fashion (n=6) in a 4-20% NuPage gel. Gels were run at 150v and then transferred to 0.45-micron nitrocellulose overnight. Nitrocellulose membranes were stained with Ponceau S to ensure proper protein transfer and integrity. The blot was cut to allow simultaneous probing of eNOS and beta actin (βACT) and blocked in 5% milk for three hours. Mouse anti-rat βACT (Santa Cruz) and mouse anti- rat eNOS (BD Bioscience) were utilized at 1:5,000 and 1:1,000 dilutions, respectively, overnight at 4°C. Blots were rinsed with Tris-buffered saline (TBS, pH 7.4) and probed with goat anti-mouse antibody conjugated with horseradish peroxidase at 1:10,000 and 1:2,000 dilutions, respectively, for three hours at room temperature. Blots were imaged using SuperSignal West Dura Chemiluminescent Substrate® (Pierce) on an ImageQuant LAS-4000® (GE) System with linear scale adjustment to minimize background noise. Signal intensity was quantified using Image J and values normalized to βACT. The eNOS /βACT ratios were assessed with 1-way ANOVA for statistical significance.

Results

Pressure- and Flow-Dependent Responses in MetSyn: Loss of Flow-Mediated Inhibition

Thoracic ducts were isolated from each cohort and exposed to pressures of 1cm, 3cm, and 5cm. There was no significant difference in diastolic diameter of thoracic ducts from the normal and MetSyn group. However, there was a large variability of thoracic duct diameters within both control and MetSyn cohorts with values ranging from 1100 microns in diameter down to 650 microns. Such a large range in diameters will have significant effect on the magnitudes of stroke volume and lymph pump flow. As such, we have focused solely on the normalized contractility parameters, ejection fraction and fractional pump flow, to reduce the variability in volume-based metrics.

There was a significant increase in lymphatic contraction frequency in the MetSyn thoracic ducts observed at a pressure of 5cmH_2O (Figure 23). MetSyn thoracic ducts also displayed a significantly lower ejection fraction at pressures of 3cm and 5cmH_2O (Figure 23). Fractional pump flow values were not significantly affected at any pressure in the thoracic duct vessels in MetSyn group since the elevated frequency negated the decrease in ejection fraction (Figure 24). In addition MetSyn thoracic duct lymphatics did not exhibit a significant difference in tone at any pressure when compared to control vessels (Figure 24).

The contraction frequency decreased sharply in control thoracic ducts in response to imposed flow as expected. In contrast, the imposed flow inhibition of contractility was blunted in the MetSyn thoracic ducts (Figure 25). The imposed flow inhibition of

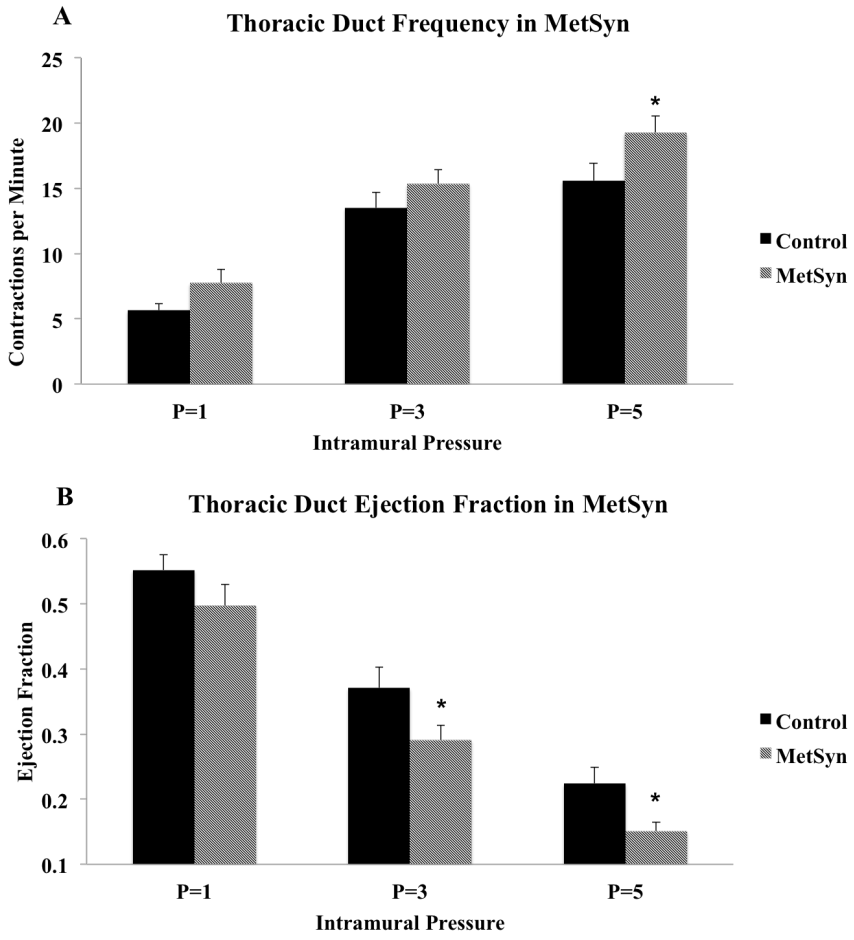

Figure 23. Changes in contraction frequency and ejection fraction in thoracic ducts of rats with MetSyn. (A) Thoracic duct contractions per minute were counted in each pressure as described in the Methods section; (B) ejection fraction was calculated as described in the Methods section at each pressure. Data are presented as Mean ± SEM. N=23 MetSyn, 20 Control. 2-way ANOVA * denotes significance at $p < 0.05$ comparing MetSyn to control values at the same pressure

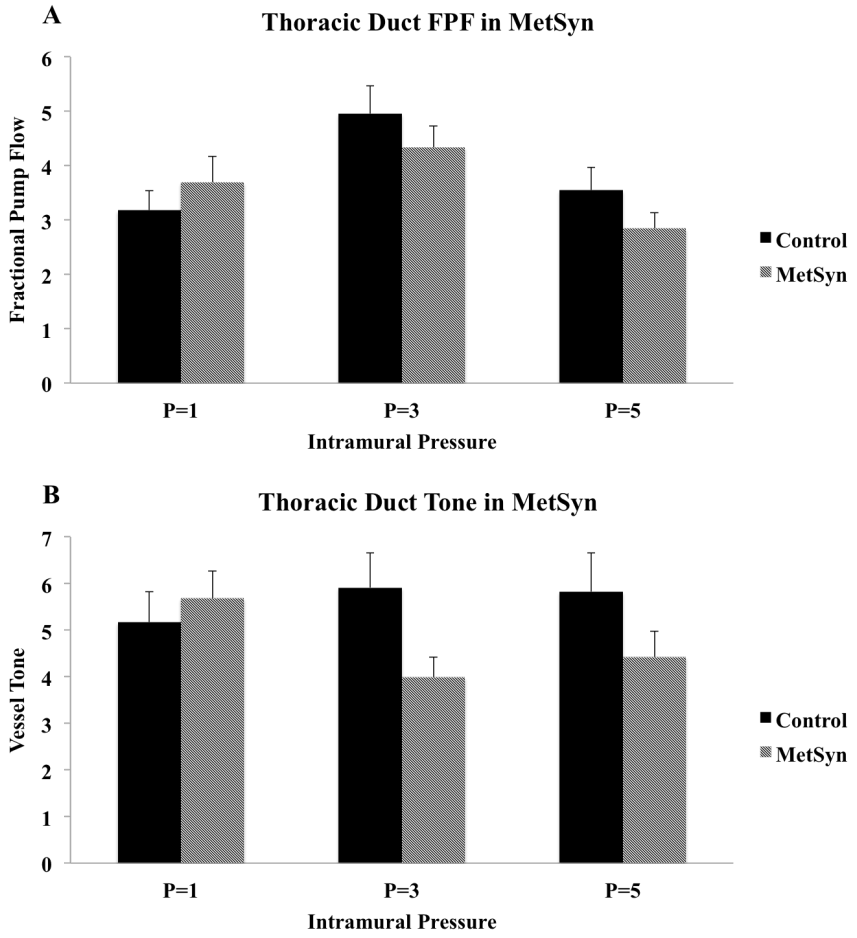

Figure 24. Changes in fractional pump flow and tonic index in thoracic ducts of rats with MetSyn. (A) Fractional pump flow and (B) vessel tone was calculated as described in the Methods section. Data are presented as Mean ± SEM. N=23 MetSyn, 20 Control. 2-way ANOVA * denotes significance at $p < 0.05$ comparing MetSyn to control values at the same pressure

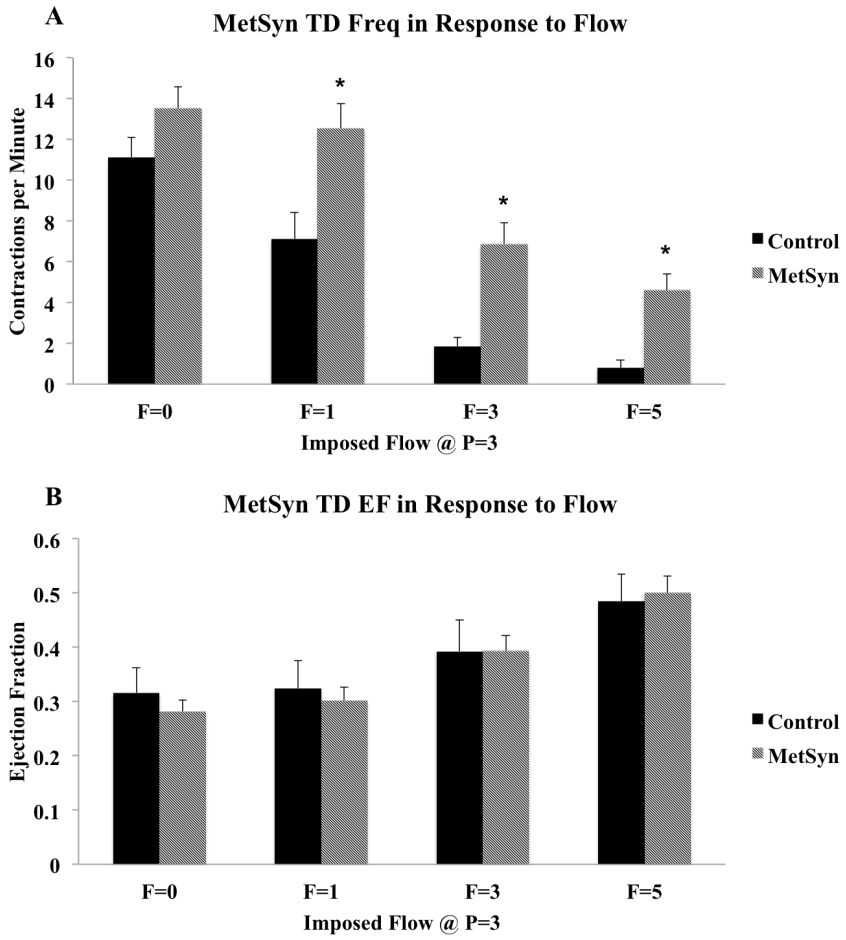

Figure 25. Loss of flow-mediated inhibition of contractility in the thoracic ducts of rats with MetSyn. Thoracic duct vessels intramural pressure was maintained at 3cmH_2O. Vessel contraction (A) and ejection fraction (B) was counted and calculated as described in the Methods section, at different imposed flow conditions. Data are presented as Mean ± SEM. N=13 MetSyn, 16 Control. 2-way ANOVA * denotes significance at $p < 0.05$ comparing MetSyn to control values at the same pressure

contractility was blunted in the MetSyn thoracic ducts as contraction frequency was significantly higher than controls at each flow. Thoracic duct ejection fraction was not significantly different between control and MetSyn thoracic ducts, however ejection fractions rose with increasing flow gradients (Figure 25). The increased contraction frequency significantly increased the MetSyn thoracic duct resistance to flow at 3cm and 5cmH_20 (Figure 26). MetSyn thoracic ducts had significantly higher normalized tone at flow of 5cmH_20 and had a significantly different flow*tone response (Figure 27). Linear regression analysis of normalized tone revealed a significant difference in the interaction between flow and thoracic duct tone. Control tone decreased ($y = -0.02x$) with imposed flow while MetSyn thoracic ducts demonstrated a slight constriction ($y = 0.05x$) in response to imposed flow (Figure 27).

Lymphatic Thoracic Ducts from MetSyn Rats are Responsive to NO

Since thoracic ducts from MetSyn rats displayed a blunted flow-mediated inhibition, we determined their sensitivity with exogenous NO. Vessels were exposed to the NO SNAP at 100μM to assess lymphatic muscle response to NO at each pressure. Exposure to 100μM SNAP significantly reduced lymphatic contraction frequency in both control and MetSyn vessels (Figure 28). In agreement with our findings during imposed flow, ejection fraction was not significantly reduced in control thoracic ducts after exposure to 100μM SNAP. However, we found that ejection fraction was significantly reduced at a pressure of 3cmH_20 in MetSyn thoracic ducts exposed to 100μM SNAP. Additionally, 100μM SNAP significantly reduced vessel tone in control thoracic ducts at each experimental pressure. In contrast, MetSyn tone was significantly

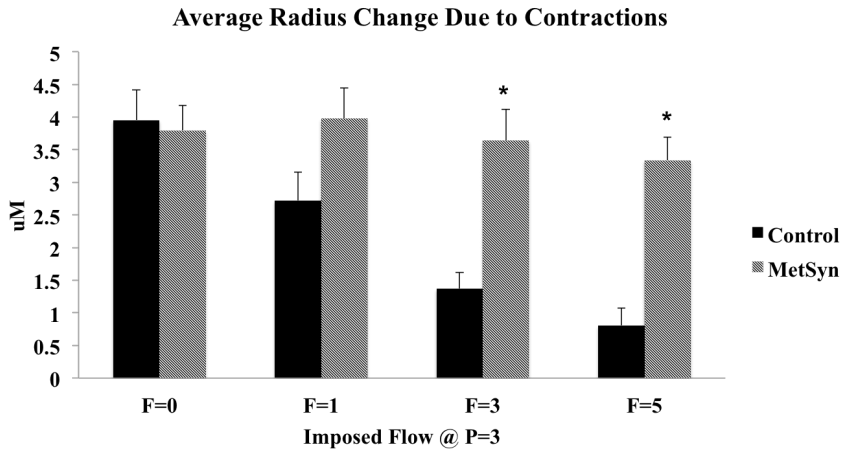

Figure 26. Loss of flow-mediated inhibition in MetSyn thoracic ducts increases vessel resistance to flow as a function of average vessel radius. The vessel resistance was calculated as described in the Methods section. Data are presented as Mean ± SEM. N=13 MetSyn, 16 Control. 2-way ANOVA * denotes significance at $p < 0.05$ comparing MetSyn to control values at the same pressure

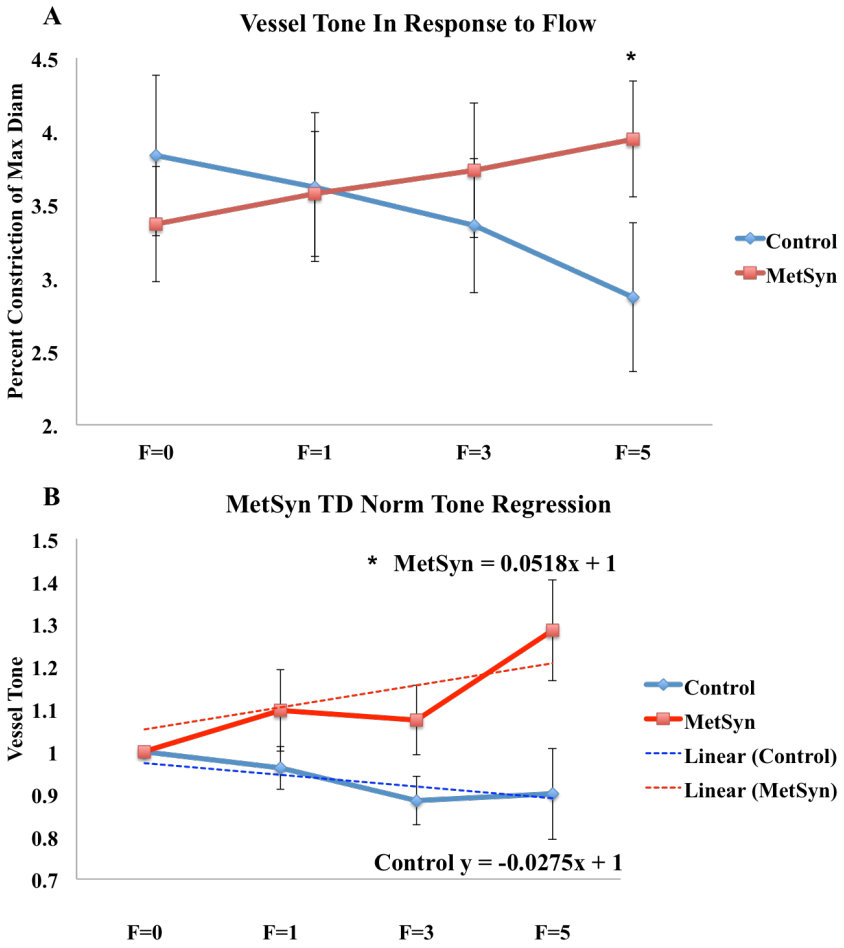

Figure 27. Loss of flow-mediated inhibition of vessel tone in MetSyn thoracic ducts. Vessel tone in response to flow (A) and the liner regression of imposed flow and tone (B) was calculated as described in the Methods section. Data are presented as Mean ± SEM. N=13 MetSyn, 16 Control. 2-way ANOVA * denotes significance at $p < 0.05$ comparing MetSyn to control

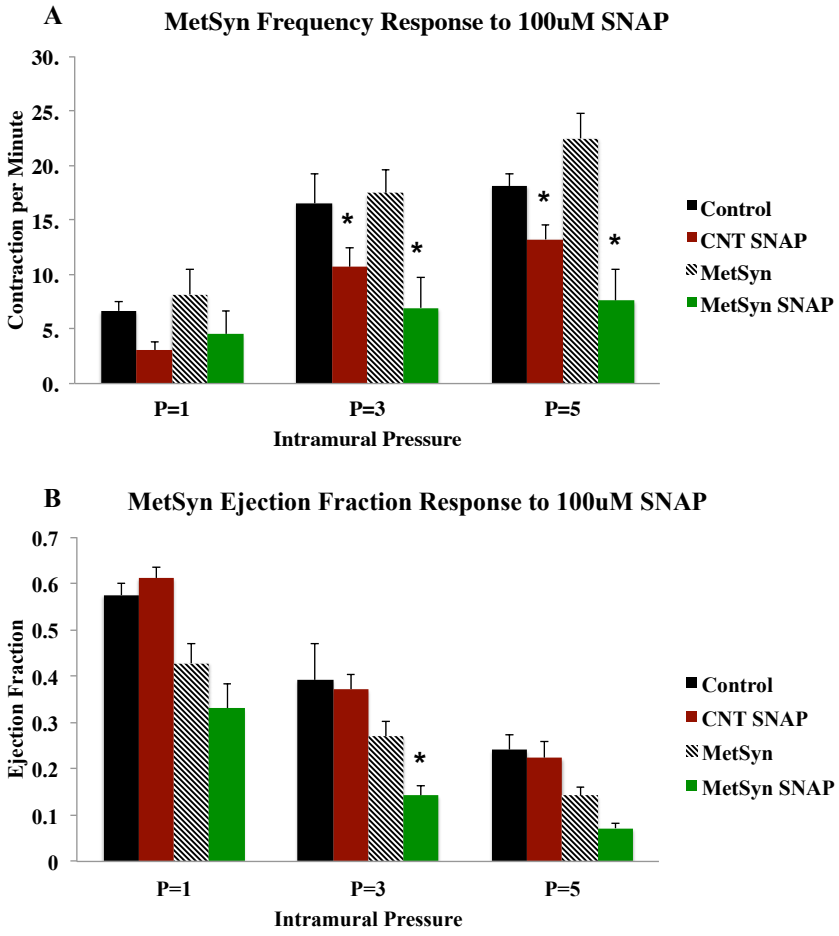

Figure 28. Contraction frequency and ejection fraction in thoracic ducts in response to 100uM SNAP. (A) contraction frequency was counted as contractions per minute for each pressure; (B) ejection fraction was calculated as described in the Methods section. Data are presented as Mean ± SEM. N=7 MetSyn, 9 Control. 2-way ANOVA * denotes significance at $p < 0.05$, ^ denotes significance at $0.05 < p < 0.1$ comparing within the cohort

lowered by SNAP only at a pressure of 1cm but was not statistically different at pressures of 3cm or 5cmH_20 (Figure 29). However, the cohort of MetSyn thoracic ducts treated with SNAP exhibited significantly lower tone basally compared to control vessel tone at pressures of 3cm and 5cmH_20, and this may have masked the SNAP response (Figure 29). *TEMPOL Did Not Restore Flow-Mediated Inhibition*

ROS are known to reduce NO bioavailability and ROS have been implicated in endothelial dysfunction. We used 1mM TEMPOL to block the effect of ROS, in order to assess the role of NO bioavailability in the MetSyn thoracic ducts at each pressure and flow. Contraction frequency and ejection fraction were not affected by 1mM TEMPOL in both control and MetSyn vessels under any experimental pressure or flow condition (Figure 30).

Control Thoracic Ducts Gain MetSyn Phenotype by Exposure to LNAME

NO is a potent regulator of lymphatic contractility and the thoracic duct is specifically sensitive to flow-mediated NO production. We wanted to determine the role of NO production in MetSyn thoracic duct contractility regulation in response to both pressure and imposed flow conditions. LNAME (100μM) significantly increased contraction frequency in control thoracic ducts at a pressure of 5cmH_2O and trended higher ($0.05 < p < 0.1$) at pressures of 1cm and 3cmH_2O (Figure 31). Interestingly, 100μM LNAME also significantly increased contraction frequency of MetSyn vessels at each pressure. However, ejection fraction of control and MetSyn vessels was unaffected by LNAME except for a reduction observed in control vessels at a pressure of 1cmH_2O (Figure 31). While vessel tone was increased in response to LNAME in control vessels

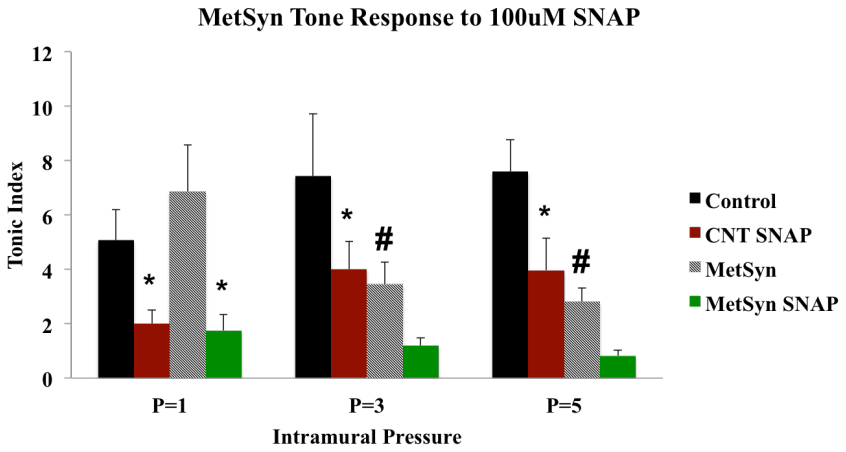

Figure 29. Exogenous NO reduces vessel tone in both control and MetSyn thoracic duct. Vessel tone was calculated as described in the Methods section. Data are presented as Mean ± SEM. N=7 MetSyn, 9 Control. 2-way ANOVA * denotes significance at $p < 0.05$, ^ denotes significance at $0.05 < p < 0.1$ comparing within the cohort, # denotes significance at $p < 0.05$, “ denotes significance at $0.05 < p < 0.1$ comparing across cohorts

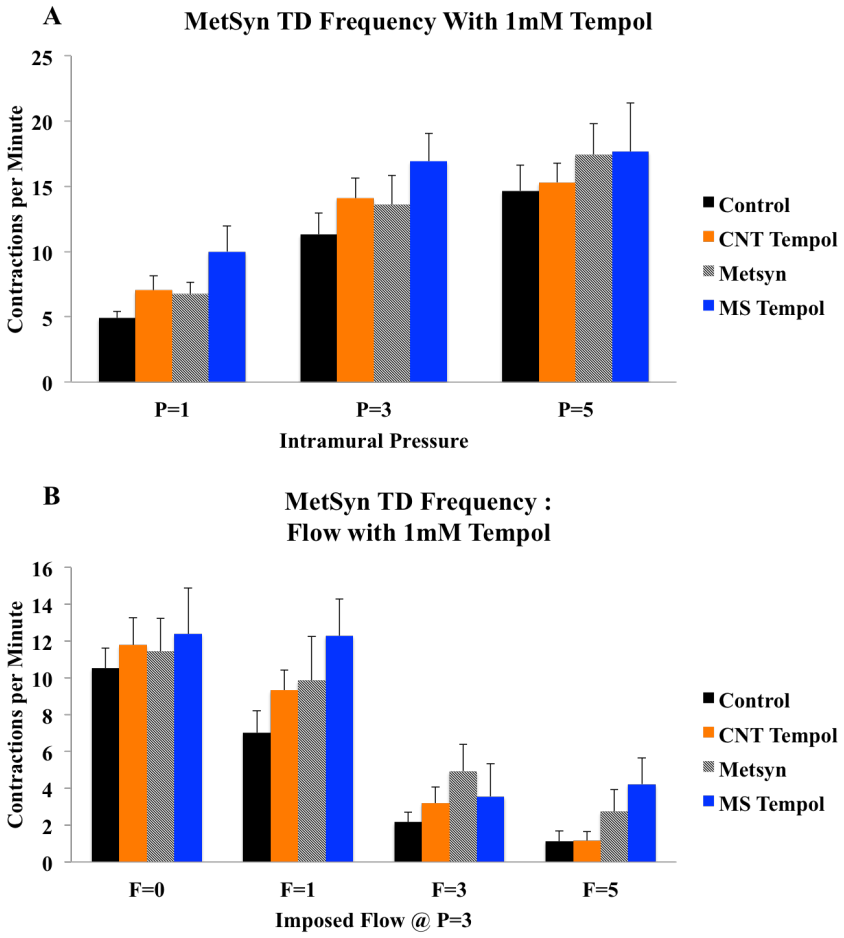

Figure 30. Inhibition of ROS did not restore flow-mediated inhibition in MetSyn thoracic duct. Thoracic ducts (TD) vessel contractile frequency in the presence of 1mM TEMPOL was measured at each pressure (A) and under different flow conditions (B). Data are presented as Mean ± SEM. N=6 MetSyn, 6 Control. 2-way ANOVA * denotes significance at $p < 0.05$, ^ denotes significance at $0.05 < p < 0.1$ comparing within the cohort

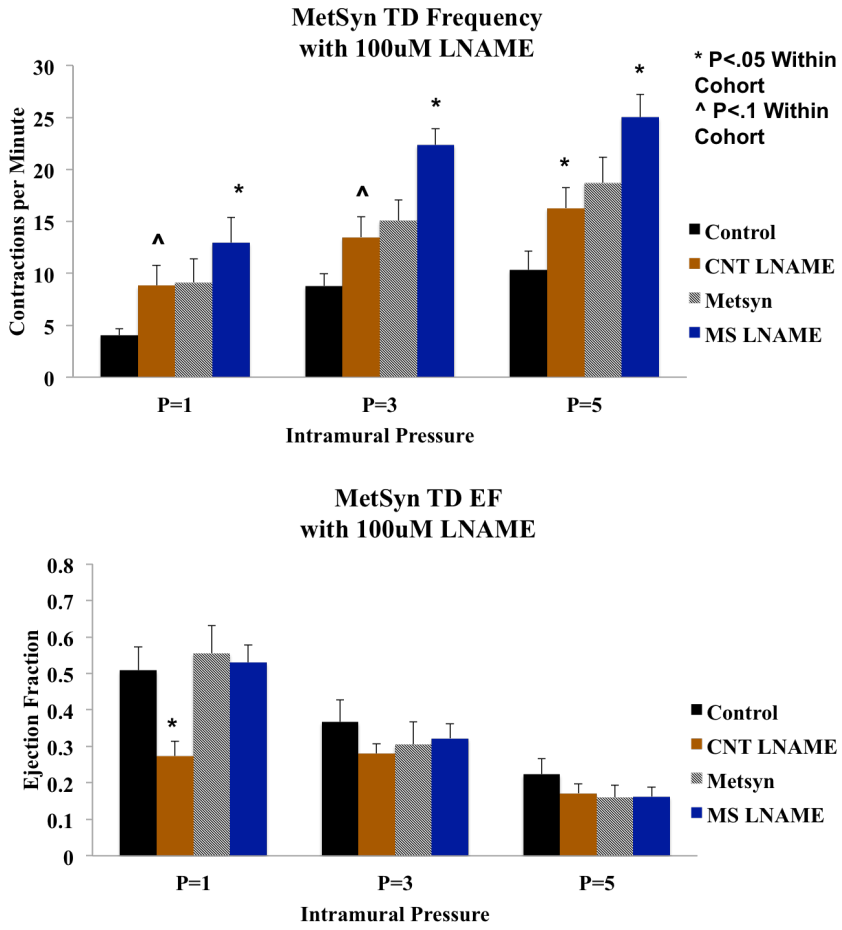

Figure 31. Changes in contraction frequency and ejection fraction of control and MetSyn thoracic ducts in the presence of LNAME. Thoracic ducts (TD) were equilibrated for twenty minutes in 100μM LNAME and their responses to pressure were recorded and analyzed for contraction frequency (Top Panel) and ejection fraction (Bottom Panel). Data are presented as Mean ± SEM. N=7 MetSyn (MS), 10 Control (CNT). 2-way ANOVA * denotes significance at $p < 0.05$, ^ denotes significance at $0.05 < p < 0.1$ comparing within the cohort

at pressures of 3cm and 5cmH_2O, LNAME had no significant effect on vessel tone in MetSyn thoracic ducts (Figure 32). As described earlier, control frequency decreases with imposed flow and this reduction is blunted in MetSyn vessels. MetSyn thoracic ducts had significantly higher contraction frequency at flows 1cm, 3cm, and trended higher at 5cmH_2O flow ($p<0.1$; Figure 33). LNAME significantly increased contraction frequency in control vessels at flows of 1cm and 3cmH_2O. Control thoracic ducts treated with LNAME were not statistically different than the contraction frequency response in MetSyn thoracic ducts. As expected, LNAME exacerbated the loss of flow-mediated inhibition phenotype observed in MetSyn thoracic ducts. LNAME significantly increased contraction frequency in MetSyn thoracic duct at each imposed flow. In agreement with our SNAP response, LNAME did not affect ejection fraction in either control or MetSyn thoracic ducts (Figure 33). The rise in contraction frequency by LNAME increased vessel resistance to flow as demonstrated by the higher change in radius as a result of spontaneous contractions (Figure 34). LNAME also increased normalized tone in control thoracic ducts at flows of 1cm and 3cmH_2O, whereas, there was no significant effect observed in MetSyn thoracic ducts (Figure 34). Table 6 summarizes the contraction parameters from each treatment cohort and their combined responses.

ENOS Insufficiency in the Thoracic Ducts Isolated from MetSyn Rats

Thoracic ducts were snap frozen in liquid nitrogen and stored at -80C. Protein was harvested under denaturing conditions and utilized for western blots. Protein from six control and six MetSyn thoracic ducts was loaded in alternating fashion and probed

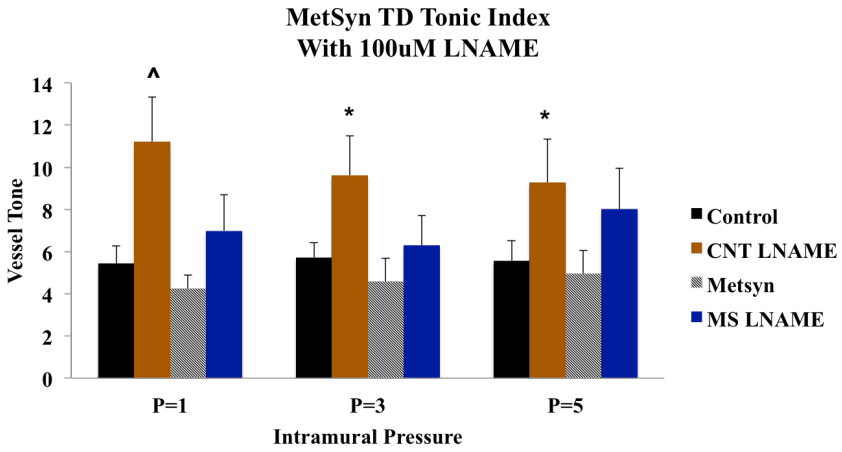

Figure 32. Changes in vessel tone in the control and MetSyn thoracic ducts in the presence of LNAME. Thoracic ducts (TD) were equilibrated with 100μM LNAME for twenty minutes and their functional responses to pressure and flow were determined. Vessel tone was calculated as described in the Methods section. Data are presented as Mean ± SEM. N=7 MetSyn (MS), 10 Control (CNT). 2-way ANOVA * denotes significance at $p < 0.05$, ^ denotes significance at $0.05 < p < 0.1$ comparing within the cohort

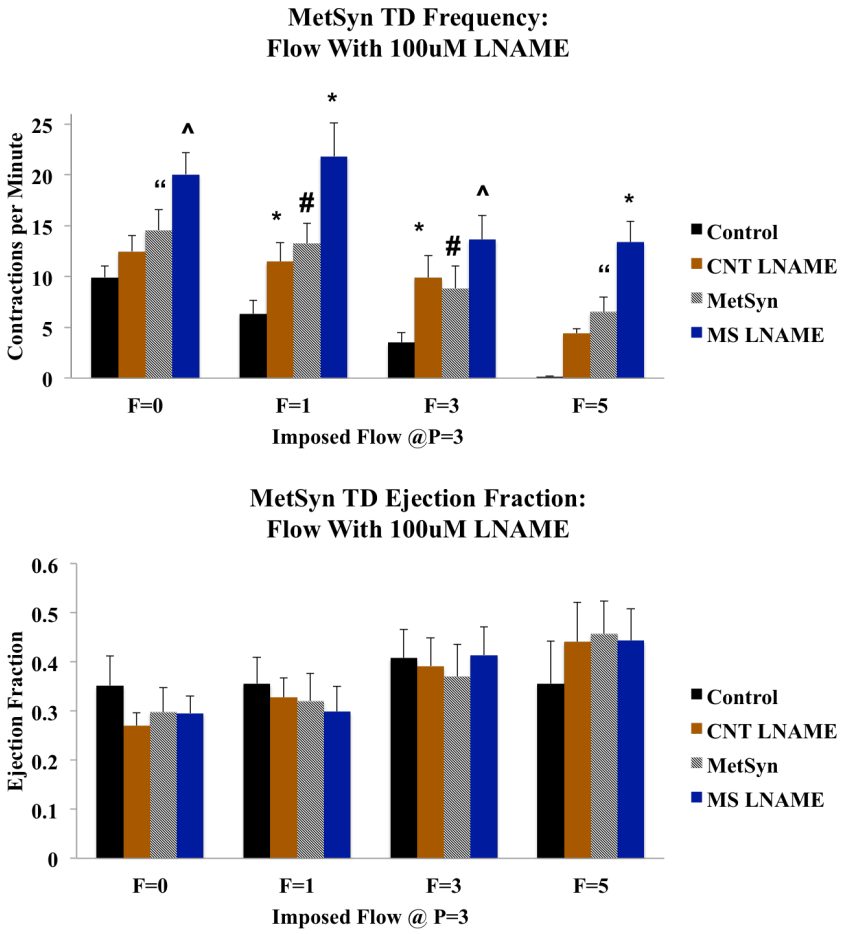

Figure 33. Changes in contraction frequency and ejection fraction in both control and MetSyn thoracic ducts in the presence of LNAME. Thoracic ducts (TD) were equilibrated with 100μM LNAME for twenty minutes and their functional responses to pressure and flow were reassessed as described in the Methods section. Data are presented as Mean ± SEM. N=7 MetSyn (MS), 10 Control (CNT). 2-way ANOVA * denotes significance at $p < 0.05$, ^ denotes significance at $0.05 < p < 0.1$ comparing within the cohort, # denotes significance at $p < 0.05$, “ denotes significance at $0.05 < p < 0.1$ comparing across cohorts

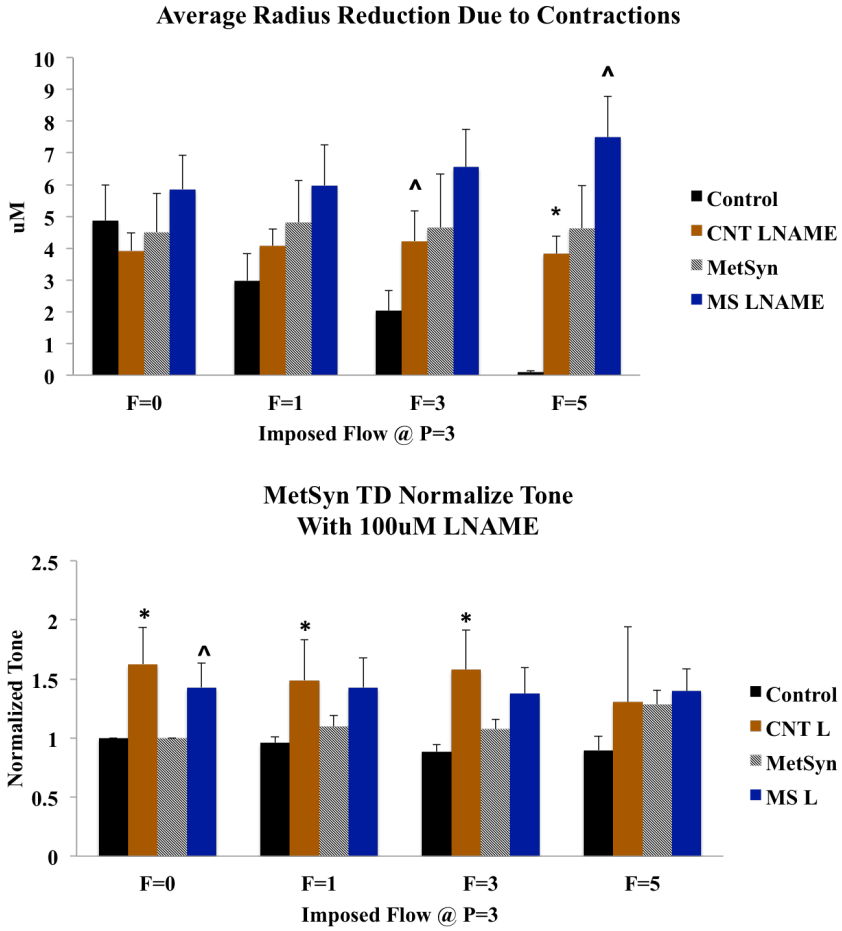

Figure 34. Changes in vessel resistance and tone under different flow conditions in control and MetSyn groups in the presence of LNAME (L). Vessel resistance (Top panel) and tone (bottom panel) was calculated as described in the Methods section. Data are presented as Mean ± SEM. N=7 MetSyn (MS), 10 Control (CNT). 2-way ANOVA * denotes significance at $p < 0.05$, ^ denotes significance at $0.05 < p < 0.1$ comparing within the cohort

Table 6. Summary of contractile parameters for MetSyn and control thoracic ducts

Mean ± SEM	Cohort	P=1	P=3	P=5	F=0	F=1	F=3	F=5
Outer Diastolic Diameter	Control	749 ± 30.2	790 ± 29.2	809 ± 28.8	785 = 28.7	787 ± 28.8	807 ± 28.9	780 ± 29.
	MetSyn	776 ± 24.9	822 ± 25.7	831 ± 25.8	838 ± 29.5	836 ± 29.3	836 ± 29.1	833.4 ± 28.7
Frequency	Combined Control	5.66 ± 0.52	13.5 ± 1.18	15.6 ± 1.3	11.1 ± 0.98	7.11 ± 1.31	1.85 ± 0.46	0.80 ± 0.39
	Control SNAP	3.07 ± 0.75	10.6 ± 1.79	13.2 ± 1.38	nd	nd	nd	nd
	Control TEMPOL	7.03 ± 0.52	14.1 ± 1.54	15.3 ± 1.95	11.8 ± 1.46	9.3 ± 1.11	3.2 ± 0.88	1.17 ± 0.05
	Control LNAME	8.8 ± 1.96	13.5 ± 1.13	16.3 ± 1.98	12.5 ± 1.61	11.5 ± 1.88	9.89 ± 2.16	4.4 ± 0.46
	Combined MetSyn	7.76 ± 1.02	15.4 ± 1.1	19.3 ± 1.3	13.5 ± 1.05	12.5 ± 1.22	6.88 ± 1.03	4.61 ± 0.81
	MetSyn SNAP	4.54 ± 2.07	6.94 ± 2.80	7.63 ± 2.91	nd	nd	nd	nd
	MetSyn TEMPOL	10.0 ± 1.96	16.9 ± 2.1	17.7 ± 3.7	12.4 ± 2.48	12.3 ± 1.99	3.6 ± 1.76	4.2 ± 1.41
	MetSyn LNAME	12.9 ± 2.41	22.4 ± 1.57	25.0 ± 2.18	20.1 ± 2.11	21.8 ± 3.30	13.7 ± 2.34	13.4 ± 2.03
Ejection Fraction	Combined Control	0.55 ± 0.02	0.37 ± 0.03	0.22 ± 0.02	0.32 ± 0.05	0.32 ± 0.05	0.39 ± 0.06	0.48 ± 0.05
	Control SNAP	0.61 ± 0.02	0.37 ± 0.03	0.22 ± 0.03	nd	nd	nd	nd
	Control TEMPOL	0.53 ± 0.05	0.40 ± 0.03	0.27 ± 0.02	0.39 ± 0.05	0.43 ± 0.05	0.51 ± 0.04	0.48 ± 0.06
	Control LNAME	0.27 ± 0.04	0.28 ± 0.03	0.17 ± 0.03	0.02	0.33 ± 0.04	0.39 ± 0.06	0.44 ± 0.08
	Combined MetSyn	0.50 ± 0.03	0.29 ± 0.02	0.15 ± 0.01	0.28 ± 0.02	0.30 ± 0.03	0.39 ± 0.03	0.5 ± 0.03
	MetSyn SNAP	0.33 ± 0.05	0.14 ± 0.02	0.07 ± 0.01	nd	nd	nd	nd
	MetSyn TEMPOL	0.49 ± 0.07	0.29 ± 0.06	0.16 ± 0.05	0.03 ± 0.05	0.29 ± 0.06	0.41 ± 0.05	0.52 ± 0.04
	MetSyn LNAME	0.53 ± 0.05	0.32 ± 0.04	0.16 ± 0.03	0.30 ± 0.03	0.30 ± 0.05	0.41 ± 0.06	0.44 ± 0.07
Tonic index	Combined Control	5.17 ± 0.66	5.91 ± 0.74	5.82 ± 0.08	3.83 ± 0.55	3.62 ± 0.51	3.36 ± 0.46	3.34 ± 0.90
	Control SNAP	2.00 ± 0.50	4.00 ± 1.04	3.97 ± 1.19	nd	nd	nd	nd
	Control TEMPOL	4.24 ± 0.69	4.10 ± 0.96	3.64 ± 0.95	4.04 ± 0.82	3.85 ± 0.75	3.41 ± 0.62	3.13 ± 0.69
	Control LNAME	11.2 ± 0.83	9.62 ± 1.87	9.27 ± 2.07	3.23 ± 0.37	3.29 ±0.41	3.11 ±0.54	1.92 ± 0.37
	Combined MetSyn	5.68 ± 0.59	3.98 ± 0.43	4.42 ± 0.55	3.37 ± 0.39	3.57 ± 0.43	3.59 ± 0.46	3.87 ± 0.38
	MetSyn SNAP	6.85 ± 0.8	1.18 ± 0.29	0.82 ± 0.21	nd	nd	nd	nd
	MetSyn TEMPOL	5.06 ± 0.72	4.19 ± 1.08	4.69 + 1.07	3.27 ± 0.83	2.38 ± 0.62	2.29 + 0.52	2.97 ± 0.52
	MetSyn LNAME	6.99 ± 1.35	6.30 ± 1.45	8.02 ± 1.57	5.74 ± 0.68	5.67 ± 0.71	5.05 ± 0.71	5.33 ± 0.66

Data are presented as means ± SEM for outer diastolic diameter, lymphatic contraction frequency, ejection fraction, and tonic index. Due to inherit variability in contraction, each treatment (SNAP, TEMPOL, LNAME) was compared with the APSS values for those specific vessels in determining functional response.

for eNOS and βAct. One MetSyn sample was excluded from quantitative analysis due to an aberrant βAct signal. We normalized eNOS signal intensity to βAct and found a consistent and significant reduction in eNOS expression in the MetSyn thoracic ducts (Figure 35).

Discussion

The results presented in this study demonstrate the first evidence that lymphatic ducts isolated from rats with MetSyn exhibit a blunted flow-mediated inhibition of contractility that significantly impaired their conduit contractility regulation. However, MetSyn thoracic ducts were sensitive to both exogenous NO supplied by SNAP and NOS inhibition when treated with LNAME. This demonstrates that the NO sensitivity and regulation in the lymphatic muscle cells and pacemaker cells is functional and suggests an inadequate production of NO by the endothelial cells. Control vessels also demonstrated a blunted flow-mediated inhibition of contractility when treated with LNAME. Scavenging of ROS with TEMPOL did not restore flow-mediated inhibition nor did it affect lymphatic vessel contractility. Western blots revealed a significant loss of eNOS expression by the MetSyn thoracic duct and may account for the blunted flow-mediated dysfunction. These observations have been summarized into the working model for lymphatic thoracic duct dysfunction in MetSyn (Figure 36).

Our results provide further evidence for the role of NO production in response to sheer stress as a critical regulator of lymphatic contractility. Imposed flow causes a sharp

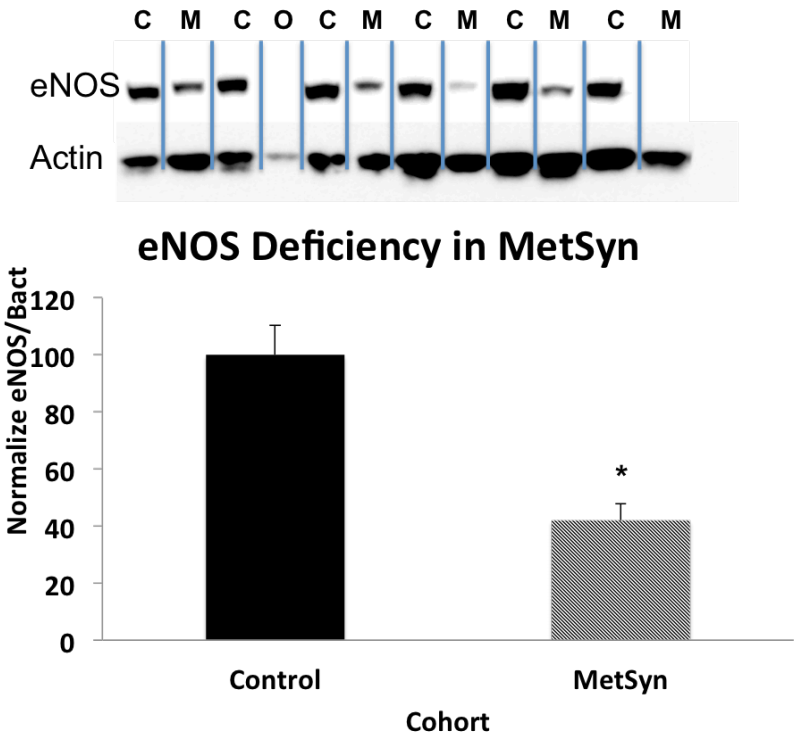

Figure 35. Reduced expression of eNOS in thoracic ducts isolated from MetSyn rats. Protein was collected from thoracic ducts isolated from control and MetSyn rats and used for western blots to assess eNOS expression. Beta actin (βAct) was used as a loading control. Top Panel: a representative western bot; C-control sample, M-MetSyn sample, O-omitted sample in the analysis due to low amount of protein loading. Bottom Panel: Quantitative analysis of eNOS expression. The eNOS/ βAct ratios were normalized to control values. The values obtained from 3 different blots were used for the analysis. Data are presented as Mean ± SEM. N=5 MetSyn, 6 Control. 2-way ANOVA * denotes significance at $p < 0.05$

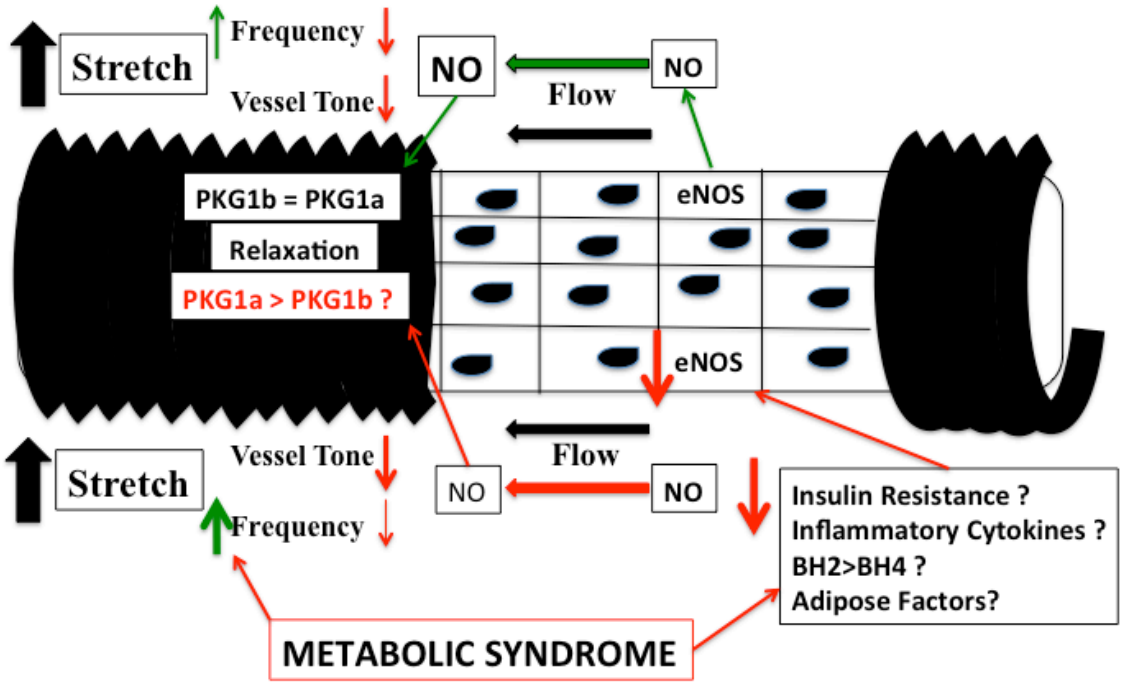

Figure 36. Working model of thoracic duct dysfunction in the metabolic syndrome. Loss of flow-mediated inhibition appears to be partly mediated through reduced eNOS expression. Loss of insulin signaling, inflammatory cytokines, and oxidative stress can each contribute to lowered eNOS expression. Despite the loss in eNOS signaling, MetSyn thoracic ducts appear to be highly sensitive to NO. Lymphatic thoracic ducts express a high level of PKG1b that is less sensitive to elevated cGMP than PKG1a. An adaptive response could include increased expression of PKG1a in the MetSyn thoracic ducts. Other unknown factors are also at play as lymphatic vessel dysfunction is exacerbated by NOS inhibition with LNAME. Control vessels take on a MetSyn phenotype characterized by blunted flow-mediated inhibition of contraction frequency when treated with LNAME, but contraction frequency in MetSyn thoracic ducts is still significantly higher, suggesting a gain of function that increases pacemaker cell depolarization.

reduction in contraction frequency in control thoracic ducts and this response was blunted in the MetSyn. Others have demonstrated a critical for NO in the shear-induced relaxation of the lymphatic pump and vessel tone (102, 317, 322). NO stimulates guanylate cyclase and increases cGMP levels that result in both activation of PKA and PKG that hyperpolarize the lymphatic muscle (103, 315). Poor endothelial dysfunction has been consistently reported in the blood vasculature in both rodent models and human studies (21, 34, 46, 194, 294, 303, 347). Thoracic ducts isolated from MetSyn rats displayed blunted flow-mediated inhibition, as contraction frequency was significantly higher than control thoracic ducts. Under most conditions, the lymphatic contractility is required for proper lymphatic transport of fluid and macromolecules from the interstitial space. However, if conditions favor passive flow, these phasic contractions increase vessel resistance to flow as a function of decreased vessel diameter. The sustained contractility in the MetSyn thoracic ducts significantly increases vessel resistance to flow by reducing average vessels diameter. The post-prandial lymphagogic effect is one such event where lymph flow increases four to six fold over fasting levels as dietary fat is packaged into chylomicrons and transported through the lymphatic system (28, 182, 284, 301). Poor dilation and inhibition of contractility will increase the resistance to lymph flow, driven in part by increased filtration of intestinal capillaries and the peristaltic action of the intestine. We have previously reported impairment in the MLV contractility in an identical high fructose fed rat model of MetSyn (357). In that study rat MLV dysfunction was correlated with low contraction frequency and similar results were described in mouse models of MetSyn (25, 262, 330, 357). In contrast, MetSyn

thoracic ducts have an elevated contraction frequency and this is likely due to poor NO bioavailability.

Under isobaric conditions the spontaneous contractions in the thoracic duct are sufficient to propel fluid and increase NO production in a self-regulatory manner (104). Inhibition of eNOS under non-flow conditions increased contraction frequency and our data supports this finding. However, MetSyn thoracic ducts also increased their contraction frequency in response to LNAME. This could be an adaptive mechanism in response to the poor functioning smaller pressure-sensitive lymphatic (357) collecting vessels, as previously reported (357). Another explanation would be that, in addition to losing NO production, there is likely an elevated contractile stimulus that results in hyperactivity of the pacemaker cells. Additional studies are warranted to support this notion.

Flow-mediated inhibition was originally described as a sharp reduction in contraction frequency, reduced vessel tone, and reduced ejection fraction (102). Interestingly, we observed a positive correlation between ejection fraction and imposed flow. Previous reports have suggested that ejection fraction decreases over time in response to flow through NO production (102). In our study, control rat thoracic duct ejection fractions were not consistently changed by either SNAP or LNAME. A significant reduction in ejection fraction was noted with 100μM LNAME at an intramural pressure of 1cmH_2O. We surmise that the reduction of ejection fraction in response to LNAME is likely due to the doubling of contraction frequency and reduction

in calcium store uptake, since calcium-induced calcium release from the sarcoplasmic reticulum is critical for contraction amplitude and ejection fraction (319).

Animal age and weight are both potentially responsible for the differences observed in the thoracic duct ejection fraction in response to flow between our study and previous reports (100-102). A previous study has identified elevated ROS production in the mesenteric vessels of aged animals, which have lymphatic contractility impairments as well. We did not see an acute effect of the ROS scavenging molecule TEMPOL, although it was a very acute application and likely insufficient to alter the cellular proteins that are sensitive to chronic oxidative stress. Additionally, elevated ROS production is linked to reduced contraction frequency (298, 353, 356) and we have reported an elevated contractile frequency in the thoracic ducts of MetSyn rats. Superoxide readily combines with NO to create peroxynitrite and it is possible that the elevated production of ROS is insufficient to reduce lymphatic thoracic duct contractility as evidenced by an appreciable role of endogenous NO production. Additionally, the short time frame of TEMPOL exposure may be insufficient to restore thoracic duct levels of BH4, which is a critical regulator of eNOS activity (29, 39, 178).

We have demonstrated a significant reduction in the expression eNOS that supports our findings of reduced flow-mediated inhibition response. Endothelial dysfunction is multifaceted and loss of eNOS expression is just one aspect of this phenomenon. Phosphorylation of eNOS at serine 1177, the availability of L-arginine substrate for key enzymes, the presence of critical cofactors such as BH4, and the oxidative stress of the cell all feed into endothelial dysfunction (92). Reduced eNOS

expression is commonly observed in models of obesity and diabetes, and can partly be explained through insulin resistance and the chronic inflammatory state. As lymph drains the interstitial fluid, it hosts a concentrated milieu of inflammatory cytokines as compared to the blood (211). Inflammatory cytokines (131, 135-137) and elevated fatty acids reduce insulin sensitivity (292) and promote endothelial dysfunction (109, 122, 274). Studies in the blood vasculature have linked endothelial dysfunction with insulin resistance, and therapies that increase insulin resistance often restore endothelial function (21, 34, 161, 232). The role of insulin on lymphatic endothelial function is not well described despite its presence in common cell culture media formulations used for lymphatic endothelial cell cultures. In the blood vasculature, insulin increases eNOS expression and activates eNOS through phosphorylation (70, 92, 217). Rosiglitazone belongs to the thiazolidinedione class of drugs that increase insulin sensitivity and, as a consequence, endothelial function, through activation of PPARγ. However, thiazolidinedione treatment has also been linked with weight gain, fluid retention, mild edema, and increased risk of cardiovascular pulmonary edema, suggesting that it may have off target consequences on lymphatic function (169). Interestingly, ZDF rats were previously described to have poor lymphatic clearance of tissue macromolecules and blood vascular dysfunction (45). In that study, treatment with rosiglitazone restored capillary function but did not restore lymphatic function (45).

Additionally, the adipose tissue has recently been described as a potent producer of vasodilators that are reduced in models of adipose tissue inflammation (110, 210, 240). Lymphatic tissues have a unique association with adipose tissue that has yet to be

fully described and often adipocytes can't be completely dissociated from the thoracic duct during isolation without damaging the vessel. While the high fructose fed MetSyn model does not display overt obesity, we have previously reported perivascular adipose accumulation in this model (357) and the prototypical adipose depots are chronically inflamed (276). However, we did not observe an increase in vessel tone in the MetSyn thoracic ducts. The effects of the adipose-derived relaxing factors and stimulating factors on lymphatic contractility have not been explored in regards to the duality of lymphatic contractility.

Loss of NO through abrogation of eNOS expression does not completely explain thoracic duct dysfunction in the MetSyn rats. Control thoracic ducts treated with LNAME displayed similar frequencies as MetSyn thoracic ducts without LNAME. However, LNAME-treated MetSyn thoracic ducts demonstrated further increased contraction frequency under both pressure and imposed flow. In addition, MetSyn thoracic ducts displayed a very unique constriction in response to flow, but MetSyn thoracic duct tone was not significantly affected by LNAME in contrast to the significant increase in tone in control thoracic ducts. This suggests that endogenous production of NO and increased NO sensitivity in the MetSyn thoracic duct are able to mask a gain of function that increases pacemaker activation and uncouples endogenous NO production from vessel tone. It is likely that multiple pathways drive the thoracic duct dysfunction, including hypersensitivity to NO, reduced NO production by the endothelium, and increased activation of the pacemaker cell(s). Many questions arise in response to the observations here. Is the reduced eNOS expression due to insulin resistance or elevated

inflammatory cytokine loads? How do insulin and glucose concentrations regulate lymphatic endothelial eNOS and redox potential? Is there an elevated fatty acid flux into the lymphatics that reduces insulin sensitivity? *In vitro* analysis using tissue specific lymphatic cells holds promise for clarification of these issues. Additionally, other mechanisms of lymphatic contractility regulation must be explored and more studies are needed to fully describe lymphatic endothelial dysfunction in the MetSyn.

CHAPTER IV

DISCUSSION: SUMMARY AND CONCLUSIONS

Implications

The MetSyn is a serious disease that underscores a significant risk for cardiovascular disease due to the presence of multiple metabolic impairments. The syndrome has risen in association with both type II diabetes and obesity as a result of poor diet and a sedentary lifestyle and afflicts over 34% of the population (237). Exercise and proper nutrition is the strongest therapy and preventative measure for MetSyn, which has reached into the hundreds of millions for estimated annual medical care costs (89). Obesity is the strongest driver of the MetSyn phenotype in humans and up to 85% of type II diabetic individuals are diagnosed with the MetSyn (153). The morbidity of these interrelated diseases has drawn significant focus on the drivers of pathologies. Great strides have been made in uncovering the roles of adipose dysfunction, insulin resistance, and endothelial dysfunction that directly affect the risk of cardiovascular disease and mortality in these patients. However, lymphatic function is often overlooked in these disease states, despite it role in maintenance of tissue fluid and macromolecule homeostasis and immunosurveillance.

Obesity is often characterized as a mild edematous state and has been historically known as a critical risk factor for the development of lymphedema following cancer surgeries and nodal biopsies (2, 126, 166, 324). There has also been evidence of poor macromolecule clearance from the adipose tissue in obesity and diabetes (9). Obese

humans often exhibit increased skin infections, surgical site infections, and delayed immune responses (139). Similar observations have been reported in obese rodent models and there is a known impairment in both the innate and adaptive cellular compartments (65, 185, 195, 287, 295). In this study, we have demonstrated that activation of macrophages, which are important mediators of tissue homeostasis and inflammation, is associated with impaired lymphatic contractility of the MetSyn animals in the mesenteric bed. Each of these observations suggests a connection between the MetSyn and lymphatic dysfunction. This connection has recently crystallized with the observation of development of spontaneous lymphedema in the morbidly obese population (12, 41, 81, 87, 193, 208, 214). Up to 80% of the morbidly obese patients can expect to develop massive localized lymphedema (MLL) at some point in their life. This form of lymphedema is associated with severe accumulation of interstitial fluid that progresses into a large fibrotic mass that resembles a sarcoma (41, 81, 111). MLL impairs the patient's ability to exercise and severely reduces their quality of life. Resolution from surgical procedures to remove the associated mass of fatty and fibrotic tissue that develops in MLL is temporary and the lymphedema will return if the underlying metabolic dysfunction is not addressed (85). Additionally, human type II diabetes patients were found to have aberrant lymphangiogenesis in the skin and a highly inflammatory expression profile (118). Elevated lymphangiogenesis and inflammation has been described in rodent models of colitis that are associated with poor lymph function (3, 47). Interestingly, genetic models that have poor lymphatic vessel formation develop spontaneous obesity in adulthood (123, 125). Lymphedema is a chronic and

progressive disease that causes persistent quality of life issues and is a major health concern with the rising incidence of MetSyn.

The lymphatic system serves critical functions in the maintenance of tissue and fluid homeostasis while also directing immune responses. Contrary to popular opinion, the lymphatic system is not a passive conduit from which lymph "drains" from the tissue and it requires the coordinative action of phasic contractions and uni-directional valves to drive lymph flow (352). In contrast to the heart, the lymphatic system is not a circuitous system and mammals lack the lymphatic hearts found in lower organisms. Instead, the lymphatic vessels themselves are able to drive lymph against a pressure gradient through both phasic and tonic contractions of muscularized collecting lymphatic vessels (352). The action of extrinsic forces such as tissue compression, inspiration, or muscle contractions in addition to the intrinsic pumping of the lymphatic system drive lymph from the periphery centripetally back to the blood circulation at the junction of the subclavian vein and the thoracic duct.

The smallest functional contracting unit of the lymphatic system is called the lymphangion and it defines the contracting vessels both upstream and downstream of a uni-directional valve (212). The contractility of the lymphangion is regulated by physical stimuli such as stretch and flow (100), but contractility is under control of both inflammatory and neural interactions (318, 320). The phasic contractility of the lymphatic system bears similarity to that of the heart and similar contractile parameters, while also displaying tonic constrictions that are typical of smooth muscle in the blood vasculature. Lymphatic muscle expresses elements of both the classic smooth muscle

contractile machinery and cardiac muscle proteins but the mechanisms regulating the two pathways are still unclear (226, 228). Phasic contractions drive the necessary pressure gradients to propel fluid downstream and this is critical to lymphatic function (17). For proper lymph transport, lymphatic vessels must also be able to regulate conduit function, when conditions favor passive lymph flow, through the regulation of tonic contractions. The data presented in this dissertation have provided consistent and broad evidence to support the hypothesis that lymphatic function is impaired in the MetSyn and have described novel mechanisms modulating MLV and lymphatic thoracic duct dysfunction in a rodent model of MetSyn.

Inhibition of the lymphatic pump under inflammatory conditions has been previously described in multiple disease states (152, 340) and loosely associated with myeloid cell activation (120, 164, 187). However, the majority of these studies rely on lymphatic clearance of dyes or tracers from the interstitial space to describe lymphatic dysfunction (164). Liao et al. have utilized intravital microscopy to visualize lymphatic contractility *in vivo* in response to oxalozone-induced inflammation and in response to activated monocytes (187). These studies provide a great display of lymphatic function in disease states but are limited by the influence of multiple confounding factors, such as the effect of extrinsic forces driving lymph, uncontrolled tissue pressures that are often affected by injection of the dye upstream of the imaging field, unknown contractile regulation by cells and contents within the lymph, and the identity of the local inflammatory cells in the vicinity of the vessel.

We have utilized an isolated lymphatic vessel preparation that controls transmural pressure and focuses on the specific contractility of a single lymphangion. This provides the necessary understanding of the lymphatic contraction regulation independent of tissue factors or forces. Our previous study was the first such example of lymphatic dysfunction in the MetSyn state (357) and similar observations have now been made in mouse models of MetSyn (25, 262, 330). Interestingly, we have observed similar contractility impairment as described in the work published by Liao et al. in that two different phenotypes of lymphatic contractility were displayed in inflamed vessels (187). We observed a MetSyn MLV phenotype characterized by low frequency and low ejection fraction, which suggests an overproduction of NO by the resident macrophage population (187), and it was the dominant phenotype in our previous study (357). In addition, we have also described a high frequency low ejection fraction phenotype in the MLV of rats with MetSyn, and both of these contractile patterns have been observed previously (187). This suggests that there is likely a separate mechanism by which activated macrophages or monocytes can regulate lymphatic function into a low or high contractility phenotype.

The role of NO in the regulation and inhibition of lymphatic contractility has been well described (26, 27, 102, 104, 264, 267, 281, 315, 323). Substance P (SP) is known to cause a significant increase in contraction frequency and reduction in ejection fraction in addition to a modest tone change at low doses (7, 55). Macrophages and eosinophils are both sources of SP in the periphery and its production may underlie the hyper-contractility phenotype. SP is also involved in the inflammation and pathogenesis

of obesity and its production by innate immune cells could play a role in the alterations of lymphatic contractility (97, 113, 156).

This dissertation has provided critical evidence to suggest that the macrophage populations that reside within the wall of the collecting lymphatic vessels must be discussed in regards to the contractility of the lymphatic vessels under disease and physiological states. We provide evidence of isolated MLV contractility impairment in both chronic (MetSyn) and acute (LPS-induced peritonitis) inflammatory states. In each situation we found an alteration in the macrophage population that resides within the tissue and along the collecting lymphatic vessel. Specifically, we have identified two major macrophage polarizations that are associated with lymphatic collecting vessel dysfunction. The LPS-induced peritonitis model includes massive macrophage accumulation in the mesenteric neurovascular bundles and the perivascular adipose tissue. We found that lymphatic vessels demonstrated extreme densities of macrophages in association with the MLV that suggests a basal chemoattractant index. This could be due to innate production of chemoattractant proteins, such as chemokine (C-C motif) ligand 2(CCL2) (155, 245, 263), or "leak" from the lymph (48), which is a concentrated source of cytokines and chemokines (211). Our data demonstrate a role for M2 macrophages, characterized as $CD163^{+}CD206^{+}$, in the maintenance of the normal mesenteric tissue function. Chronic injections of LPS into the peritoneum increased this macrophage pool two fold and they exhibited morphological characteristics of activation, e.g., appearance of dendrites and spines. However, LPS also induced a significant increase in the presence of $CD163^{-}CD206^{+}$ cells that displayed a different

morphology. It is likely these $CD163^{-}CD206^{+}$ cells represent the quasi-inflammatory M2b macrophage phenotype that is induced by TLR activation and immune complexes (11, 165, 200, 218, 219). Both of these cells types were significantly elevated in the mesenteric perivascular tissue and in association with the MLV. MLVs isolated from the LPS-injected rats had critically reduced lymph pump function. Four of seven vessels used in the study lacked any phasic contractions at any pressure and the remaining three exhibited poor contractility. It is likely that excess NO production by these macrophages is the critical element in the mediating this dysfunction.

We have also provided new evidence to support the hypothesis that the lymphatic vessel provides a stromal environment for resident macrophages through production of the MCSF and GMCSF. These two molecules are critical to monocyte/macrophage maturation and polarization. Loss of MCSF signaling significantly reduces the number of macrophages and the MCSF/GMCSF ratio is critical to the polarization of the M1 and M2 phenotype. Cultured mLMCS and mLECs both expressed high levels of MCSF and GMSCF in the presence of LPS. We also found a large increase in the production of CCL2 and CCL1 in the LPS-stimulated mLECs. CCL2 is critical to monocyte recruitment and is a classic marker of tissue inflammation. Interestingly, CCL1 has been described as a potent activator of the M2b macrophage phenotype and critical for maintenance of that polarization state (11). CCL1 production by the lymphatic muscle and endothelium may regulate the $CD163^{-}CD206^{+}$ M2b macrophages identified in the LPS-induced peritonitis model. mLECs were unique in that GMCSF expression was almost non-existent in the basal state despite high MCSF expression. However, GMCSF

exhibited a massive increase in response to LPS and could act as an inflammatory switch.

GMCSF is commonly used to induce the M1 macrophage polarization with in vitro systems. We found a significant skewing of the adipose tissue macrophages to an M1 polarization in the MetSyn rats as evidenced by a significant increase of $CD163^{+}MHCII^{+}$ cells. This fits well with the current paradigm of a M1 shift in the adipose tissue in conditions of obesity and MetSyn (195). The dysfunction of the intrinsic lymphatic pump likely contributes to the mild edematous state that accompanies obesity, the increased risk of skin infections, and the lymphedema observed in the morbidly obese population. Macrophage activation and polarization will have critical effects on lymphatic collecting vessel function. Suppression of the lymphatic pump will result in edema, however this association may have been selected as a mechanism to prevent dissemination of infection through the lymphatic system (187, 254, 255). Increased dietary endotoxin is a driver of the MetSyn phenotype and inflammation. Conditions for excess dietary endotoxin absorption (35, 72, 79, 105, 116, 328) have been described and present a possible scenario for the alterations in lymphatic vessel function and macrophage polarization observed in the MetSyn rats (35, 79).

For proper lymphatic function, vessels must also be able to regulate their function as a conduit system when conditions favor passive flow. The lymphatic system displays keen sheer sensitivity that is mediated primarily by NO. Endothelial dysfunction is a hallmark of the MetSyn and contributes to the hypertension associated with the disease state (21, 46, 274, 294, 305). Endothelial dysfunction refers to the

inability of endothelial cells to produce the appropriate level of vasodilatory agents particularly NO. Poor NO bioavailability is responsible for the hypertension observed in many obese and diabetic rodent models.

The lymphatic thoracic duct is the largest lymphatic vessel in the body and sheer stress in response to flow is a critical regulator of its contractility (101). Flow-mediated inhibition of contractility has been well documented in the lymphatic thoracic duct (100). However, the presence of endothelial dysfunction and the flow-mediated inhibition of contractility response in the lymphatic vasculature have been ignored in MetSyn research, despite the evidence for poor lymph function. We utilized a high fructose fed rat model of MetSyn and demonstrated a significant reduction in the flow-mediated inhibition of contractility. Thoracic ducts from MetSyn rats also appeared to have elevated NO sensitivity despite the poor response to flow. This suggested a reduced bioavailability of NO in the MetSyn thoracic duct. Western blots for eNOS demonstrated a sharp reduction (60%) in eNOS expression in MetSyn thoracic ducts. This supported our finding of blunted flow-mediated inhibition of contractility and suggests that increased lymphatic resistance to flow may also contribute to the lymphatic dysfunction described in obese and MetSyn patients.

There have been a significant number of studies that have described the expression and activation of eNOS in the blood vasculature in relation to insulin resistance and obesity (39, 70, 92, 178). Similar mechanisms have yet to be described for the lymphatic endothelium and many questions remain to fully explain the lymphatic thoracic duct impairment in MetSyn rats. Intriguingly, treatment of normal thoracic

ducts with LNAME induces a flow-mediated inhibition of contractility response similar to that observed in the MetSyn thoracic duct. However, MetSyn thoracic ducts had an even greater exacerbation of poor flow-mediated inhibition of contractility when treated with LNAME. This suggests that the MetSyn lymphatic thoracic duct phenotype is unlikely to be due to just eNOS expression abrogation. There have been recent studies that have observed a significant role of adipose-derived relaxation factors that are reduced in adipose dysfunction (110). Additionally, the adipose tissue is also a source of contraction stimulating factors in obesity, yet their role on the lymphatics is unknown (210, 240). We hypothesize that reduced NO production, increased NO sensitivity, and activation of the thoracic duct pacemaker cells combine to drive the MetSyn thoracic duct phenotype.

Limitations

The mouse myeloid system has been critically described and cell populations distinguished by specific combinations of proteins markers. The expression of these markers and specificity for similar cell types in the human and rat have been questioned. Additionally, advances in the production or reliable and specific antibodies against rat proteins is lacking compared to antibodies to the same proteins in humans and mice. This has hampered the ability to clearly identify immune cell populations and especially macrophage polarizations, which fall on a spectrum of activation in the tissue rather than specific polarizations (219). We utilized immunohistochemistry to identify rat macrophages using antibodies that have been well validated in the rat. Current studies in

the rat commonly utilize the expression of MHCII, CD163, and CD206 in the identification of rat macrophages and use in the identification of M1 and M2 “skewness” (334, 335). However, extensive characterization of specific macrophage phenotypes requires a more detailed understanding of rat macrophage heterogeneity and identification of potential specific markers. In addition to the reliability of specific antibodies and known markers, the mouse model also has the advantage of genetic manipulation that can allow perturbations of gene expression or entire cell populations. Use of intra-vital microscopy of fluorescently labeled macrophage populations will also increase our understanding of dynamic macrophage behavior and flux along the lymphatic vessels.

We chose to use the rat model due to its similarity in the lymphatic contractility as human lymphatic vessels to appropriately assess the role of inflammation, macrophage phenotype, and lymphatic contractility. The mouse has only a few lymphatic beds that display consistent and functional lymphatic contractility and may not lend itself to being as strong a model for the lymphatic impairment in MetSyn. However, mouse models provide powerful tools that may provide key insight into the role of different macrophage populations and interaction with the lymphatic vasculature. The strength of this work lies in the direct control and isolation of a specific lymphangion through isobaric preparations. This provides unique evidence for dysfunction of the lymphatic pump and an argument for the inclusion of macrophages in the regulation of lymphatic collecting vessel function. In situ observations of lymphatic functions will also provide significant information detailing lymphatic contractility

dysfunction in the tissue and how this relates to the maintenance of tissue homeostasis by macromolecule clearance. Additionally, differences in observation between both isobaric and *in situ* studies will provide evidence for the role of the lymphatic microenvironment and lymph contents in the paracrine regulation of lymphatic function.

There is also a significant lag in the research on endothelial dysfunction and the role of insulin in the lymphatic endothelial cell regulation and specifically in species and tissue-specific endothelial cell cultures. Gender- and tissue-specific cell culture lines of different regional lymphatic tissues are needed to further and completely characterize the lymphatic endothelial response to insulin. Additionally, characterization of the lymph composition, including glucose, fatty acids, insulin, and inflammatory cytokines, will be crucial to delineating the mechanisms by which eNOS expression is reduced in MetSyn thoracic ducts. There is a significant overlap in the symptoms of the MetSyn and lymphatic dysfunction and more research needs to be targeted to this connection for proper health care of a growing population at risk for lymphedema.

REFERENCES

1. **Abate N**. Obesity and cardiovascular disease: Pathogenetic role of the metabolic syndrome and therapeutic implications. *Journal of Diabetes and its Complications* 14: 154-174, 2000.

2. **Ahmed RL, Schmitz KH, Prizment AE, and Folsom AR**. Risk factors for lymphedema in breast cancer survivors, the Iowa Women's Health Study. *Breast Cancer Res Treat* 2011.

3. **Alexander JS, Chaitanya GV, Grisham MB, and Boktor M**. Emerging roles of lymphatics in inflammatory bowel disease. *Ann N Y Acad Sci* 1207 Suppl 1: E75-85, 2010.

4. **Ali AT, Hochfeld WE, Myburgh R, and Pepper MS**. Adipocyte and adipogenesis. *European Journal of Cell Biology* 92: 229-236, 2013.

5. **Alizadeh Dehnavi R, Beishuizen ED, van de Ree MA, Le Cessie S, Huisman MV, Kluft C, Princen HM, and Tamsma JT**. The impact of metabolic syndrome and CRP on vascular phenotype in type 2 diabetes mellitus. *European Journal of Internal Medicine* 19: 115-121, 2008.

6. **Alp NJ, Mussa S, Khoo J, Cai S, Guzik T, Jefferson A, Goh N, Rockett KA, and Channon KM**. Tetrahydrobiopterin-dependent preservation of nitric oxide-mediated endothelial function in diabetes by targeted transgenic GTP-cyclohydrolase I overexpression. *J Clin Invest* 112: 725-735, 2003.

7. **Amerini S, Ziche M, Greiner ST, and Zawieja DC**. Effects of substance P on mesenteric lymphatic contractility in the rat. *Lymphat Res Biol* 2: 2-10, 2004.

8. **Archer SL, Huang JM, Hampl V, Nelson DP, Shultz PJ, and Weir EK**. Nitric oxide and cGMP cause vasorelaxation by activation of a charybdotoxin-sensitive K channel by cGMP-dependent protein kinase. *Proc Natl Acad Sci U S A* 91: 7583-7587, 1994.

9. **Arngrim N, Simonsen L, Holst JJ, and Bulow J**. Reduced adipose tissue lymphatic drainage of macromolecules in obese subjects: a possible link between obesity and local tissue inflammation? *Int J Obes (Lond)* 37: 748-750, 2013.

10. **Arterburn DE, Maciejewski ML, and Tsevat J**. Impact of morbid obesity on medical expenditures in adults. *Int J Obes (Lond)* 29: 334-339, 2005.

11. **Asai A, Nakamura K, Kobayashi M, Herndon DN, and Suzuki F**. CCL1 released from M2b macrophages is essentially required for the maintenance of their properties. *Journal of Leukocyte Biology* 92: 859-867, 2012.

12. **Asch S, James WD, and Castelo-Soccio L**. Massive localized lymphedema: an emerging dermatologic complication of obesity. *J Am Acad Dermatol* 59: S109-110, 2008.

13. **Aschen S, Zampell JC, Elhadad S, Weitman E, De Brot M, and Mehrara BJ**. Regulation of adipogenesis by lymphatic fluid stasis: part II. Expression of adipose differentiation genes. *Plastic and Reconstructive Surgery* 129: 838-847, 2012.

14. **Atchison DJ, and Johnston MG**. Role of extra- and intracellular Ca2+ in the lymphatic myogenic response. *Am J Physiol* 272: R326-333, 1997.

15. **Azzout-Marniche D, Becard D, Guichard C, Foretz M, Ferre P, and Foufelle F**. Insulin effects on sterol regulatory-element-binding protein-1c (SREBP-1c) transcriptional activity in rat hepatocytes. *The Biochemical Journal* 350 Pt 2: 389-393, 2000.

16. **Barbato JE, Zuckerbraun BS, Overhaus M, Raman KG, and Tzeng E**. Nitric oxide modulates vascular inflammation and intimal hyperplasia in insulin resistance and the metabolic syndrome. *Am J Physiol Heart Circ Physiol* 289: H228-236, 2005.

17. **Benoit JN, Zawieja DC, Goodman AH, and Granger HJ**. Characterization of intact mesenteric lymphatic pump and its responsiveness to acute edemagenic stress. *Am J Physiol* 257: H2059-2069, 1989.

18. **Berenji M, Kalani A, Kim J, Kelly K, and Wallack MK**. Massive localized lymphedema of the thigh in a morbidly obese patient. *Eur J Surg Oncol* 36: 104-106, 2010.

19. **Berg AH, and Scherer PE**. Adipose tissue, inflammation, and cardiovascular disease. *Circ Res* 96: 939-949, 2005.

20. **Bers DM, and Merrill DB**. The role of Ca influx in cardiac muscle excitation-contraction coupling. Assessment by extracellular Ca microelectrodes. *Advances in Myocardiology* 6: 49-57, 1985.

21. **Bigazzi R, and Bianchi S**. Insulin resistance, metabolic syndrome and endothelial dysfunction. *Journal of Nephrology* 20: 10-14, 2007.

22. **Bjorbaek C, El-Haschimi K, Frantz JD, and Flier JS**. The role of SOCS-3 in leptin signaling and leptin resistance. *J Biol Chem* 274: 30059-30065, 1999.

23. **Blankfield RP, Hudgel DW, Tapolyai AA, and Zyzanski SJ**. Bilateral leg edema, obesity, pulmonary hypertension, and obstructive sleep apnea. *Archives of Internal Medicine* 160: 2357-2362, 2000.

24. **Bloomgarden ZT**. World Congress on the insulin resistance syndrome, 2009: cellular mechanisms of insulin resistance. *Diabetes Care* 33: e103-108, 2010.

25. **Blum KS, Karaman S, Proulx ST, Ochsenbein AM, Luciani P, Leroux JC, Wolfrum C, and Detmar M**. Chronic high-fat diet impairs collecting lymphatic vessel function in mice. *PLoS One* 9: e94713, 2014.

26. **Bohlen HG, Gasheva OY, and Zawieja DC**. Nitric oxide formation by lymphatic bulb and valves is a major regulatory component of lymphatic pumping. *Am J Physiol Heart Circ Physiol* 301: H1897-1906, 2011.

27. **Bohlen HG, Wang W, Gashev A, Gasheva O, and Zawieja D**. Phasic contractions of rat mesenteric lymphatics increase basal and phasic nitric oxide generation in vivo. *Am J Physiol Heart Circ Physiol* 297: H1319-1328, 2009.

28. **Borgstrom B, and Laurell CB**. Studies of lymph and lymph-proteins during absorption of fat and saline by rats. *Acta Physiologica Scandinavica* 29: 264-280, 1953.

29. **Bowers MC, Hargrove LA, Kelly KA, Wu G, and Meininger CJ**. Tetrahydrobiopterin attenuates superoxide-induced reduction in nitric oxide. *Frontiers in Bioscience* 3: 1263-1272, 2011.

30. **Braun M, Ramracheya R, Bengtsson M, Zhang Q, Karanauskaite J, Partridge C, Johnson PR, and Rorsman P**. Voltage-gated ion channels in human

pancreatic beta-cells: electrophysiological characterization and role in insulin secretion. *Diabetes* 57: 1618-1628, 2008.

31. **Briand F, Thieblemont Q, Muzotte E, and Sulpice T**. High-fat and fructose intake induces insulin resistance, dyslipidemia, and liver steatosis and alters in vivo macrophage-to-feces reverse cholesterol transport in hamsters. *J Nutr* 142: 704-709, 2012.

32. **Brunzell JD, and Ayyobi AF**. Dyslipidemia in the metabolic syndrome and type 2 diabetes mellitus. *Am J Med* 115 Suppl 8A: 24S-28S, 2003.

33. **Buettner R, Bettermann I, Hechtl C, Gabele E, Hellerbrand C, Scholmerich J, and Bollheimer LC**. Dietary folic acid activates AMPK and improves insulin resistance and hepatic inflammation in dietary rodent models of the metabolic syndrome. *Hormone and Metabolic Research* 42: 769-774, 2010.

34. **Caballero AE**. Endothelial dysfunction, inflammation, and insulin resistance: a focus on subjects at risk for type 2 diabetes. *Curr Diab Rep* 4: 237-246, 2004.

35. **Cani PD, Amar J, Iglesias MA, Poggi M, Knauf C, Bastelica D, Neyrinck AM, Fava F, Tuohy KM, Chabo C, Waget A, Delmee E, Cousin B, Sulpice T, Chamontin B, Ferrieres J, Tanti JF, Gibson GR, Casteilla L, Delzenne NM, Alessi MC, and Burcelin R**. Metabolic endotoxemia initiates obesity and insulin resistance. *Diabetes* 56: 1761-1772, 2007.

36. **Cani PD, Bibiloni R, Knauf C, Waget A, Neyrinck AM, Delzenne NM, and Burcelin R**. Changes in gut microbiota control metabolic endotoxemia-induced

inflammation in high-fat diet-induced obesity and diabetes in mice. *Diabetes* 57: 1470-1481, 2008.

37. **Carvalho BM, and Saad MJ**. Influence of gut microbiota on subclinical inflammation and insulin resistance. *Mediators Inflamm* 2013: 986734, 2013.

38. **Chakraborty S, Zawieja S, Wang W, Zawieja DC, and Muthuchamy M**. Lymphatic system: a vital link between metabolic syndrome and inflammation. *Ann N Y Acad Sci* 1207 Suppl 1: E94-102, 2010.

39. **Channon KM**. Tetrahydrobiopterin: regulator of endothelial nitric oxide synthase in vascular disease. *Trends in Cardiovascular Medicine* 14: 323-327, 2004.

40. **Choi YJ, Shin HS, Choi HS, Park JW, Jo I, Oh ES, Lee KY, Lee BH, Johnson RJ, and Kang DH**. Uric acid induces fat accumulation via generation of endoplasmic reticulum stress and SREBP-1c activation in hepatocytes. *Laboratory Investigation; A Journal of Technical Methods and Pathology* 94: 1114-1125, 2014.

41. **Chopra K, Tadisina KK, Brewer M, Holton LH, Banda AK, and Singh DP**. Massive Localized Lymphedema Revisited: A Quickly Rising Complication of the Obesity Epidemic. *Ann Plast Surg* 2013.

42. **Cinti S, Mitchell G, Barbatelli G, Murano I, Ceresi E, Faloia E, Wang S, Fortier M, Greenberg AS, and Obin MS**. Adipocyte death defines macrophage localization and function in adipose tissue of obese mice and humans. *J Lipid Res* 46: 2347-2355, 2005.

43. **Collin HB**. The ultrastructure of conjunctival lymphatic anchoring filaments. *Experimental Eye Research* 8: 102-105, 1969.

44. **Cook DL, Satin LS, Ashford ML, and Hales CN**. ATP-sensitive K+ channels in pancreatic beta-cells. Spare-channel hypothesis. *Diabetes* 37: 495-498, 1988.

45. **Cosson E, Cohen-Boulakia F, Tarhzaoui K, Dabire H, Leger G, Charnaux N, Lestrade R, Behar A, and Valensi P**. Capillary endothelial but not lymphatic function is restored under rosiglitazone in Zucker diabetic fatty rats. *Microvasc Res* 77: 220-225, 2009.

46. **Cozma A, Orasan O, Sampelean D, Fodor A, Vlad C, Negrean V, Rednic N, and Zdrenghea D**. Endothelial dysfunction in metabolic syndrome. *Romanian Journal of Internal Medicine* 47: 133-140, 2009.

47. **Cromer WE, Mathis JM, Granger DN, Chaitanya GV, and Alexander JS**. Role of the endothelium in inflammatory bowel diseases. *World J Gastroenterol* 17: 578-593, 2011.

48. **Cromer WE, Zawieja SD, Tharakan B, Childs EW, Newell MK, and Zawieja DC**. The effects of inflammatory cytokines on lymphatic endothelial barrier function. *Angiogenesis* 17: 395-406, 2014.

49. **Czech MP, Tencerova M, Pedersen DJ, and Aouadi M**. Insulin signalling mechanisms for triacylglycerol storage. *Diabetologia* 56: 949-964, 2013.

50. **Dailey GE, 3rd, Noor MA, Park JS, Bruce S, and Fiedorek FT**. Glycemic control with glyburide/metformin tablets in combination with rosiglitazone in patients with type 2 diabetes: a randomized, double-blind trial. *Am J Med* 116: 223-229, 2004.

51. **Davidson M**. A review of the current status of the management of mixed dyslipidemia associated with diabetes mellitus and metabolic syndrome. *The American Journal of Cardiology* 102: 19L-27L, 2008.

52. **Davidson SM, and Duchen MR**. Endothelial mitochondria: contributing to vascular function and disease. *Circ Res* 100: 1128-1141, 2007.

53. **Davis MJ**. An improved, computer-based method to automatically track internal and external diameter of isolated microvessels. *Microcirculation* 12: 361-372, 2005.

54. **Davis MJ, Davis AM, Ku CW, and Gashev AA**. Myogenic constriction and dilation of isolated lymphatic vessels. *Am J Physiol Heart Circ Physiol* 296: H293-302, 2009.

55. **Davis MJ, Lane MM, Davis AM, Durtschi D, Zawieja DC, Muthuchamy M, and Gashev AA**. Modulation of lymphatic muscle contractility by the neuropeptide substance P. *Am J Physiol Heart Circ Physiol* 295: H587-597, 2008.

56. **Davis MJ, Meininger GA, and Zawieja DC**. Stretch-induced increases in intracellular calcium of isolated vascular smooth muscle cells. *Am J Physiol* 263: H1292-1299, 1992.

57. **Davis MJ, Scallan JP, Wolpers JH, Muthuchamy M, Gashev AA, and Zawieja DC**. Intrinsic increase in lymphangion muscle contractility in response to elevated afterload. *Am J Physiol Heart Circ Physiol* 303: H795-808, 2012.

58. **Davis MJ, Zawieja DC, and Gashev AA**. Automated measurement of diameter and contraction waves of cannulated lymphatic microvessels. *Lymphat Res Biol* 4: 3-10, 2006.

59. **de Ferranti S, and Mozaffarian D**. The perfect storm: obesity, adipocyte dysfunction, and metabolic consequences. *Clinical Chemistry* 54: 945-955, 2008.

60. **de Heredia FP, Gomez-Martinez S, and Marcos A**. Obesity, inflammation and the immune system. *The Proceedings Of The Nutrition Society* 71: 332-338, 2012.

61. **De Rosa V, Procaccini C, Cali G, Pirozzi G, Fontana S, Zappacosta S, La Cava A, and Matarese G**. A key role of leptin in the control of regulatory T cell proliferation. *Immunity* 26: 241-255, 2007.

62. **De Vos A, Heimberg H, Quartier E, Huypens P, Bouwens L, Pipeleers D, and Schuit F**. Human and rat beta cells differ in glucose transporter but not in glucokinase gene expression. *J Clin Invest* 96: 2489-2495, 1995.

63. **Dean SM, Zirwas MJ, and Horst AV**. Elephantiasis nostras verrucosa: an institutional analysis of 21 cases. *J Am Acad Dermatol* 64: 1104-1110, 2011.

64. **DeFronzo RA, and Tripathy D**. Skeletal muscle insulin resistance is the primary defect in type 2 diabetes. *Diabetes Care* 32 Suppl 2: S157-163, 2009.

65. **Deiuliis J, Shah Z, Shah N, Needleman B, Mikami D, Narula V, Perry K, Hazey J, Kampfrath T, Kollengode M, Sun Q, Satoskar AR, Lumeng C, Moffatt-Bruce S, and Rajagopalan S**. Visceral adipose inflammation in obesity is associated with critical alterations in tregulatory cell numbers. *PLoS One* 6: e16376, 2011.

66. **Delbosc S, Paizanis E, Magous R, Araiz C, Dimo T, Cristol JP, Cros G, and Azay J**. Involvement of oxidative stress and NADPH oxidase activation in the development of cardiovascular complications in a model of insulin resistance, the fructose-fed rat. *Atherosclerosis* 179: 43-49, 2005.

67. **Demark-Wahnefried W, Campbell KL, and Hayes SC**. Weight management and its role in breast cancer rehabilitation. *Cancer* 118: 2277-2287, 2012.

68. **Devaraj S, Singh U, and Jialal I**. Human C-reactive protein and the metabolic syndrome. *Current Opinion in Lipidology* 20: 182-189, 2009.

69. **Diamant M, and Tushuizen ME**. The metabolic syndrome and endothelial dysfunction: common highway to type 2 diabetes and CVD. *Curr Diab Rep* 6: 279-286, 2006.

70. **Dimmeler S, Fleming I, Fisslthaler B, Hermann C, Busse R, and Zeiher AM**. Activation of nitric oxide synthase in endothelial cells by Akt-dependent phosphorylation. *Nature* 399: 601-605, 1999.

71. **Diraison F, Yankah V, Letexier D, Dusserre E, Jones P, and Beylot M**. Differences in the regulation of adipose tissue and liver lipogenesis by carbohydrates in humans. *J Lipid Res* 44: 846-853, 2003.

72. **Dogan S, Celikbilek M, and Guven K**. High fructose consumption can induce endotoxemia. *Gastroenterology* 143: e29; author reply e29, 2012.

73. **Dougherty PJ, Davis MJ, Zawieja DC, and Muthuchamy M**. Calcium sensitivity and cooperativity of permeabilized rat mesenteric lymphatics. *Am J Physiol Regul Integr Comp Physiol* 294: R1524-1532, 2008.

74. **Dougherty PJ, Nepiyushchikh ZV, Chakraborty S, Wang W, Davis MJ, Zawieja DC, and Muthuchamy M**. PKC activation increases Ca(2)(+) sensitivity of permeabilized lymphatic muscle via myosin light chain 20 phosphorylation-dependent and -independent mechanisms. *Am J Physiol Heart Circ Physiol* 306: H674-683, 2014.

75. **Dranoff G, Crawford AD, Sadelain M, Ream B, Rashid A, Bronson RT, Dickersin GR, Bachurski CJ, Mark EL, Whitsett JA, and et al.** Involvement of granulocyte-macrophage colony-stimulating factor in pulmonary homeostasis. *Science* 264: 713-716, 1994.

76. **Drolet R, Richard C, Sniderman AD, Mailloux J, Fortier M, Huot C, Rheaume C, and Tchernof A**. Hypertrophy and hyperplasia of abdominal adipose tissues in women. *Int J Obes (Lond)* 32: 283-291, 2008.

77. **Duez H, Lamarche B, Uffelman KD, Valero R, Cohn JS, and Lewis GF**. Hyperinsulinemia is associated with increased production rate of intestinal apolipoprotein B-48-containing lipoproteins in humans. *Arterioscler Thromb Vasc Biol* 26: 1357-1363, 2006.

78. **Emanuela F, Grazia M, Marco de R, Maria Paola L, Giorgio F, and Marco B**. Inflammation as a Link between Obesity and Metabolic Syndrome. *Journal Of Nutrition and Metabolism* 2012: 476380, 2012.

79. **Erridge C, Attina T, Spickett CM, and Webb DJ**. A high-fat meal induces low-grade endotoxemia: evidence of a novel mechanism of postprandial inflammation. *Am J Clin Nutr* 86: 1286-1292, 2007.

80. **Eto M, Kitazawa T, and Brautigan DL**. Phosphoprotein inhibitor CPI-17 specificity depends on allosteric regulation of protein phosphatase-1 by regulatory subunits. *Proc Natl Acad Sci U S A* 101: 8888-8893, 2004.

81. **Farshid G, and Weiss SW**. Massive localized lymphedema in the morbidly obese: a histologically distinct reactive lesion simulating liposarcoma. *The American Journal of Surgical Pathology* 22: 1277-1283, 1998.

82. **Faure P, Rossini E, Lafond JL, Richard MJ, Favier A, and Halimi S**. Vitamin E improves the free radical defense system potential and insulin sensitivity of rats fed high fructose diets. *J Nutr* 127: 103-107, 1997.

83. **Faust IM, Johnson PR, Stern JS, and Hirsch J**. Diet-induced adipocyte number increase in adult rats: a new model of obesity. *Am J Physiol* 235: E279-286, 1978.

84. **Federico LM, Naples M, Taylor D, and Adeli K**. Intestinal insulin resistance and aberrant production of apolipoprotein B48 lipoproteins in an animal model of insulin resistance and metabolic dyslipidemia: evidence for activation of protein tyrosine phosphatase-1B, extracellular signal-related kinase, and sterol regulatory element-binding protein-1c in the fructose-fed hamster intestine. *Diabetes* 55: 1316-1326, 2006.

85. **Fife C**. Massive localized lymphedema, a disease unique to the morbidly obese: a case study. *Ostomy Wound Manage* 60: 30-35, 2014.

86. **Fife CE, Benavides S, and Carter MJ**. A patient-centered approach to treatment of morbid obesity and lower extremity complications: an overview and case studies. *Ostomy Wound Manage* 54: 20-22, 24-32, 2008.

87. **Fife CE, and Carter MJ**. Lymphedema in the morbidly obese patient: unique challenges in a unique population. *Ostomy Wound Manage* 54: 44-56, 2008.

88. **Filion KB, Joseph L, Boivin JF, Suissa S, and Brophy JM**. Thiazolidinediones and the risk of incident congestive heart failure among patients with type 2 diabetes mellitus. *Pharmacoepidemiology And Drug Safety* 20: 785-796, 2011.

89. **Finkelstein EA, Trogdon JG, Cohen JW, and Dietz W**. Annual medical spending attributable to obesity: payer-and service-specific estimates. *Health Affairs* 28: w822-831, 2009.

90. **Fiorentini S, Luganini A, Dell'Oste V, Lorusso B, Cervi E, Caccuri F, Bonardelli S, Landolfo S, Caruso A, and Gribaudo G**. Human cytomegalovirus productively infects lymphatic endothelial cells and induces a secretome that promotes angiogenesis and lymphangiogenesis through interleukin-6 and granulocyte-macrophage colony-stimulating factor. *The Journal Of General Virology* 92: 650-660, 2011.

91. **Fleetwood AJ, Lawrence T, Hamilton JA, and Cook AD**. Granulocyte-macrophage colony-stimulating factor (CSF) and macrophage CSF-dependent macrophage phenotypes display differences in cytokine profiles and transcription factor activities: implications for CSF blockade in inflammation. *J Immunol* 178: 5245-5252, 2007.

92. **Fleming I, and Busse R**. Molecular mechanisms involved in the regulation of the endothelial nitric oxide synthase. *Am J Physiol Regul Integr Comp Physiol* 284: R1-12, 2003.

93. **Foretz M, Guichard C, Ferre P, and Foufelle F**. Sterol regulatory element binding protein-1c is a major mediator of insulin action on the hepatic expression of

glucokinase and lipogenesis-related genes. *Proc Natl Acad Sci U S A* 96: 12737-12742, 1999.

94. **Francis SH, Busch JL, Corbin JD, and Sibley D**. cGMP-dependent protein kinases and cGMP phosphodiesterases in nitric oxide and cGMP action. *Pharmacological Reviews* 62: 525-563, 2010.

95. **Franks PW, Brage S, Luan J, Ekelund U, Rahman M, Farooqi IS, Halsall I, O'Rahilly S, and Wareham NJ**. Leptin predicts a worsening of the features of the metabolic syndrome independently of obesity. *Obesity Research* 13: 1476-1484, 2005.

96. **Frazier TH, DiBaise JK, and McClain CJ**. Gut microbiota, intestinal permeability, obesity-induced inflammation, and liver injury. *JPEN J Parenter Enteral Nutr* 35: 14S-20S, 2011.

97. **Fu J, Liu B, Liu P, Liu L, Li G, Wu B, and Liu X**. Substance P is associated with the development of obesity, chronic inflammation and type 2 diabetes mellitus. *Exp Clin Endocrinol Diabetes* 119: 177-181, 2011.

98. **Gainsford T, Willson TA, Metcalf D, Handman E, McFarlane C, Ng A, Nicola NA, Alexander WS, and Hilton DJ**. Leptin can induce proliferation, differentiation, and functional activation of hemopoietic cells. *Proc Natl Acad Sci U S A* 93: 14564-14568, 1996.

99. **Galassi A, Reynolds K, and He J**. Metabolic syndrome and risk of cardiovascular disease: a meta-analysis. *Am J Med* 119: 812-819, 2006.

100. **Gashev AA**. Lymphatic vessels: pressure- and flow-dependent regulatory reactions. *Ann N Y Acad Sci* 1131: 100-109, 2008.

101. **Gashev AA, Davis MJ, Delp MD, and Zawieja DC**. Regional variations of contractile activity in isolated rat lymphatics. *Microcirculation* 11: 477-492, 2004.

102. **Gashev AA, Davis MJ, and Zawieja DC**. Inhibition of the active lymph pump by flow in rat mesenteric lymphatics and thoracic duct. *J Physiol* 540: 1023-1037, 2002.

103. **Gasheva OY, Gashev AA, and Zawieja DC**. Cyclic guanosine monophosphate and the dependent protein kinase regulate lymphatic contractility in rat thoracic duct. *J Physiol* 591: 4549-4565, 2013.

104. **Gasheva OY, Zawieja DC, and Gashev AA**. Contraction-initiated NO-dependent lymphatic relaxation: a self-regulatory mechanism in rat thoracic duct. *J Physiol* 575: 821-832, 2006.

105. **Ghoshal S, Witta J, Zhong J, de Villiers W, and Eckhardt E**. Chylomicrons promote intestinal absorption of lipopolysaccharides. *J Lipid Res* 50: 90-97, 2009.

106. **Ginhoux F, and Jung S**. Monocytes and macrophages: developmental pathways and tissue homeostasis. *Nat Rev Immunol* 14: 392-404, 2014.

107. **Ginsberg HN, and Maccallum PR**. The obesity, metabolic syndrome, and type 2 diabetes mellitus pandemic: II. Therapeutic management of atherogenic dyslipidemia. *Journal of Clinical Hypertension* 11: 520-527, 2009.

108. **Ginsberg HN, and MacCallum PR**. The obesity, metabolic syndrome, and type 2 diabetes mellitus pandemic: Part I. Increased cardiovascular disease risk and the importance of atherogenic dyslipidemia in persons with the metabolic syndrome and type 2 diabetes mellitus. *Journal of the Cardiometabolic Syndrome* 4: 113-119, 2009.

109. **Goldberg RB**. Cytokine and cytokine-like inflammation markers, endothelial dysfunction, and imbalanced coagulation in development of diabetes and its complications. *The Journal of Clinical Endocrinology and Metabolism* 94: 3171-3182, 2009.

110. **Gollasch M**. Vasodilator signals from perivascular adipose tissue. *British Journal of Pharmacology* 165: 633-642, 2012.

111. **Goshtasby P, Dawson J, and Agarwal N**. Pseudosarcoma: massive localized lymphedema of the morbidly obese. *Obesity Surgery* 16: 88-93, 2006.

112. **Greene AK, Grant FD, and Slavin SA**. Lower-extremity lymphedema and elevated body-mass index. *N Engl J Med* 366: 2136-2137, 2012.

113. **Gross K, Karagiannides I, Thomou T, Koon HW, Bowe C, Kim H, Giorgadze N, Tchkonia T, Pirtskhalava T, Kirkland JL, and Pothoulakis C**. Substance P promotes expansion of human mesenteric preadipocytes through proliferative and antiapoptotic pathways. *Am J Physiol Gastrointest Liver Physiol* 296: G1012-1019, 2009.

114. **Grundy SM**. Obesity, metabolic syndrome, and cardiovascular disease. *J Clin Endocrinol Metab* 89: 2595-2600, 2004.

115. **Grundy SM, Brewer HB, Jr., Cleeman JI, Smith SC, Jr., Lenfant C, National Heart L, Blood I, and American Heart A**. Definition of metabolic syndrome: report of the National Heart, Lung, and Blood Institute/American Heart Association conference on scientific issues related to definition. *Arterioscler Thromb Vasc Biol* 24: e13-18, 2004.

116. **Grunfeld C, and Feingold KR**. Endotoxin in the gut and chylomicrons: translocation or transportation? *J Lipid Res* 50: 1-2, 2009.

117. **Guo S**. Insulin signaling, resistance, and the metabolic syndrome: insights from mouse models into disease mechanisms. *The Journal of Endocrinology* 220: T1-T23, 2014.

118. **Haemmerle M, Keller T, Egger G, Schachner H, Steiner CW, Stokic D, Neumayer C, Brown MK, Kerjaschki D, and Hantusch B**. Enhanced lymph vessel density, remodeling, and inflammation are reflected by gene expression signatures in dermal lymphatic endothelial cells in type 2 diabetes. *Diabetes* 62: 2509-2529, 2013.

119. **Haidari M, Leung N, Mahbub F, Uffelman KD, Kohen-Avramoglu R, Lewis GF, and Adeli K**. Fasting and postprandial overproduction of intestinally derived lipoproteins in an animal model of insulin resistance. Evidence that chronic fructose feeding in the hamster is accompanied by enhanced intestinal de novo lipogenesis and ApoB48-containing lipoprotein overproduction. *J Biol Chem* 277: 31646-31655, 2002.

120. **Hall KL, Volk-Draper LD, Flister MJ, and Ran S**. New model of macrophage acquisition of the lymphatic endothelial phenotype. *PLoS One* 7: e31794, 2012.

121. **Hargens AR, and Zweifach BW**. Contractile stimuli in collecting lymph vessels. *Am J Physiol* 233: H57-65, 1977.

122. **Hartge MM, Unger T, and Kintscher U**. The endothelium and vascular inflammation in diabetes. *Diab Vasc Dis Res* 4: 84-88, 2007.

123. **Harvey NL**. The link between lymphatic function and adipose biology. *Ann N Y Acad Sci* 1131: 82-88, 2008.

124. **Harvey NL**. The link between lymphatic function and adipose biology. *Annals of the New York Academy of Sciences* 1131: 82-88, 2008.

125. **Harvey NL, Srinivasan RS, Dillard ME, Johnson NC, Witte MH, Boyd K, Sleeman MW, and Oliver G**. Lymphatic vascular defects promoted by Prox1 haploinsufficiency cause adult-onset obesity. *Nat Genet* 37: 1072-1081, 2005.

126. **Helyer LK, Varnic M, Le LW, Leong W, and McCready D**. Obesity is a risk factor for developing postoperative lymphedema in breast cancer patients. *The Breast Journal* 16: 48-54, 2010.

127. **Hernandez AV, Usmani A, Rajamanickam A, and Moheet A**. Thiazolidinediones and risk of heart failure in patients with or at high risk of type 2 diabetes mellitus: a meta-analysis and meta-regression analysis of placebo-controlled randomized clinical trials. *American Journal of Cardiovascular Drugs : Drugs, Devices, and Other Interventions* 11: 115-128, 2011.

128. **Himes RW, and Smith CW**. Tlr2 is critical for diet-induced metabolic syndrome in a murine model. *FASEB J* 24: 731-739, 2010.

129. **Hirano K, Derkach DN, Hirano M, Nishimura J, and Kanaide H**. Protein kinase network in the regulation of phosphorylation and dephosphorylation of smooth muscle myosin light chain. *Molecular and Cellular Biochemistry* 248: 105-114, 2003.

130. **Hirano K, Hirano M, and Kanaide H**. Regulation of myosin phosphorylation and myofilament Ca2+ sensitivity in vascular smooth muscle. *Journal of Smooth Muscle Research* 40: 219-236, 2004.

131. **Hirosumi J, Tuncman G, Chang L, Gorgun CZ, Uysal KT, Maeda K, Karin M, and Hotamisligil GS**. A central role for JNK in obesity and insulin resistance. *Nature* 420: 333-336, 2002.

132. **Hoang HH, Padgham SV, and Meininger CJ**. L-arginine, tetrahydrobiopterin, nitric oxide and diabetes. *Current Opinion in Clinical Nutrition and Metabolic Care* 16: 76-82, 2013.

133. **Hosaka K, Mizuno R, and Ohhashi T**. Rho-Rho kinase pathway is involved in the regulation of myogenic tone and pump activity in isolated lymph vessels. *Am J Physiol Heart Circ Physiol* 284: H2015-2025, 2003.

134. **Hotamisligil GS**. Inflammation and metabolic disorders. *Nature* 444: 860-867, 2006.

135. **Hotamisligil GS**. The role of TNFalpha and TNF receptors in obesity and insulin resistance. *Journal of Internal Medicine* 245: 621-625, 1999.

136. **Hotamisligil GS, Peraldi P, Budavari A, Ellis R, White MF, and Spiegelman BM**. IRS-1-mediated inhibition of insulin receptor tyrosine kinase activity in TNF-alpha- and obesity-induced insulin resistance. *Science* 271: 665-668, 1996.

137. **Hotamisligil GS, Shargill NS, and Spiegelman BM**. Adipose expression of tumor necrosis factor-alpha: direct role in obesity-linked insulin resistance. *Science* 259: 87-91, 1993.

138. **Huang KC, Lin RC, Kormas N, Lee LT, Chen CY, Gill TP, and Caterson ID**. Plasma leptin is associated with insulin resistance independent of age, body mass index, fat mass, lipids, and pubertal development in nondiabetic adolescents.

International Journal of Obesity and Related Metabolic Disorders : Journal of the International Association for the Study of Obesity 28: 470-475, 2004.

139. **Huttunen R, and Syrjanen J**. Obesity and the risk and outcome of infection. *Int J Obes (Lond)* 37: 333-340, 2013.

140. **Ikeoka D, Mader JK, and Pieber TR**. Adipose tissue, inflammation and cardiovascular disease. *Revista Da Associacao Medica Brasileira* 56: 116-121, 2010.

141. **Ilan Y, Maron R, Tukpah AM, Maioli TU, Murugaiyan G, Yang K, Wu HY, and Weiner HL**. Induction of regulatory T cells decreases adipose inflammation and alleviates insulin resistance in ob/ob mice. *Proc Natl Acad Sci U S A* 107: 9765-9770, 2010.

142. **Irjala H, Johansson EL, Grenman R, Alanen K, Salmi M, and Jalkanen S**. Mannose receptor is a novel ligand for L-selectin and mediates lymphocyte binding to lymphatic endothelium. *J Exp Med* 194: 1033-1042, 2001.

143. **Jaguin M, Houlbert N, Fardel O, and Lecureur V**. Polarization profiles of human M-CSF-generated macrophages and comparison of M1-markers in classically activated macrophages from GM-CSF and M-CSF origin. *Cellular Immunology* 281: 51-61, 2013.

144. **Jensen V, Witte MH, and Latifi R**. Massive localized lipolymphedema pseudotumor in a morbidly obese patient. *Lymphology* 39: 181-184, 2006.

145. **Jin J, Zhang X, Lu Z, Perry DM, Li Y, Russo SB, Cowart LA, Hannun YA, and Huang Y**. Acid sphingomyelinase plays a key role in palmitic acid-amplified

inflammatory signaling triggered by lipopolysaccharide at low concentrations in macrophages. *Am J Physiol Endocrinol Metab* 305: E853-867, 2013.

146. **Jocken JW, Langin D, Smit E, Saris WH, Valle C, Hul GB, Holm C, Arner P, and Blaak EE**. Adipose triglyceride lipase and hormone-sensitive lipase protein expression is decreased in the obese insulin-resistant state. *J Clin Endocrinol Metab* 92: 2292-2299, 2007.

147. **Jones JR, Barrick C, Kim KA, Lindner J, Blondeau B, Fujimoto Y, Shiota M, Kesterson RA, Kahn BB, and Magnuson MA**. Deletion of PPARgamma in adipose tissues of mice protects against high fat diet-induced obesity and insulin resistance. *Proc Natl Acad Sci U S A* 102: 6207-6212, 2005.

148. **Jorgensen SB, O'Neill HM, Sylow L, Honeyman J, Hewitt KA, Palanivel R, Fullerton MD, Oberg L, Balendran A, Galic S, van der Poel C, Trounce IA, Lynch GS, Schertzer JD, and Steinberg GR**. Deletion of skeletal muscle SOCS3 prevents insulin resistance in obesity. *Diabetes* 62: 56-64, 2013.

149. **Jung CH, Lee WJ, Hwang JY, Yu JH, Shin MS, Lee MJ, Jang JE, Leem J, Park JY, and Kim HK**. Assessment of the fatty liver index as an indicator of hepatic steatosis for predicting incident diabetes independently of insulin resistance in a Korean population. *Diabetic Medicine : A Journal of the British Diabetic Association* 30: 428-435, 2013.

150. **Kadowaki T, and Yamauchi T**. Adiponectin and adiponectin receptors. *Endocrine Reviews* 26: 439-451, 2005.

151. **Kajikawa Y, Ikeda M, Takemoto S, Tomoda J, Ohmaru N, and Kusachi S**. Association of circulating levels of leptin and adiponectin with metabolic syndrome and coronary heart disease in patients with various coronary risk factors. *International Heart Journal* 52: 17-22, 2011.

152. **Kalima TV**. Experimental lymphatic obstruction in the ileum. *Ann Chir Gynaecol Fenn* 59: 187-201, 1970.

153. **Kalofoutis C, Piperi C, Kalofoutis A, Harris F, Phoenix D, and Singh J**. Type II diabetes mellitus and cardiovascular risk factors: Current therapeutic approaches. *Experimental And Clinical Cardiology* 12: 17-28, 2007.

154. **Kang DH, Park SK, Lee IK, and Johnson RJ**. Uric acid-induced C-reactive protein expression: implication on cell proliferation and nitric oxide production of human vascular cells. *Journal of the American Society of Nephrology : JASN* 16: 3553-3562, 2005.

155. **Kang S, Lee SP, Kim KE, Kim HZ, Memet S, and Koh GY**. Toll-like receptor 4 in lymphatic endothelial cells contributes to LPS-induced lymphangiogenesis by chemotactic recruitment of macrophages. *Blood* 113: 2605-2613, 2009.

156. **Karagiannides I, and Pothoulakis C**. Substance P, obesity, and gut inflammation. *Curr Opin Endocrinol Diabetes Obes* 16: 47-52, 2009.

157. **Kavanagh K, Wylie AT, Tucker KL, Hamp TJ, Gharaibeh RZ, Fodor AA, and Cullen JM**. Dietary fructose induces endotoxemia and hepatic injury in calorically controlled primates. *Am J Clin Nutr* 98: 349-357, 2013.

158. **Keast DH, Despatis M, Allen JO, and Brassard A**. Chronic oedema/lymphoedema: under-recognised and under-treated. *International Wound Journal* 2014.

159. **Kerjaschki D**. The crucial role of macrophages in lymphangiogenesis. *J Clin Invest* 115: 2316-2319, 2005.

160. **Khanna M, Naraghi AM, Salonen D, Bhumbra R, Dickson BC, Kransdorf MJ, and White LM**. Massive localised lymphoedema: clinical presentation and MR imaging characteristics. *Skeletal Radiol* 40: 647-652, 2011.

161. **Kim F, Pham M, Maloney E, Rizzo NO, Morton GJ, Wisse BE, Kirk EA, Chait A, and Schwartz MW**. Vascular inflammation, insulin resistance, and reduced nitric oxide production precede the onset of peripheral insulin resistance. *Arterioscler Thromb Vasc Biol* 28: 1982-1988, 2008.

162. **Kim JH, Kim JE, Liu HY, Cao W, and Chen J**. Regulation of interleukin-6-induced hepatic insulin resistance by mammalian target of rapamycin through the STAT3-SOCS3 pathway. *J Biol Chem* 283: 708-715, 2008.

163. **Kim JI, Urban M, Young GD, and Eto M**. Reciprocal regulation controlling the expression of CPI-17, a specific inhibitor protein for the myosin light chain phosphatase in vascular smooth muscle cells. *American Journal of Physiology Cell Physiology* 303: C58-68, 2012.

164. **Kim KE, Koh YJ, Jeon BH, Jang C, Han J, Kataru RP, Schwendener RA, Kim JM, and Koh GY**. Role of CD11b+ macrophages in intraperitoneal

lipopolysaccharide-induced aberrant lymphangiogenesis and lymphatic function in the diaphragm. *Am J Pathol* 175: 1733-1745, 2009.

165. **Kobayashi M, Jeschke MG, Shigematsu K, Asai A, Yoshida S, Herndon DN, and Suzuki F**. M2b monocytes predominated in peripheral blood of severely burned patients. *J Immunol* 185: 7174-7179, 2010.

166. **Kocak Z, and Overgaard J**. Risk factors of arm lymphedema in breast cancer patients. *Acta Oncol* 39: 389-392, 2000.

167. **Kohjima M, Higuchi N, Kato M, Kotoh K, Yoshimoto T, Fujino T, Yada M, Yada R, Harada N, Enjoji M, Takayanagi R, and Nakamuta M**. SREBP-1c, regulated by the insulin and AMPK signaling pathways, plays a role in nonalcoholic fatty liver disease. *International Journal of Molecular Medicine* 21: 507-511, 2008.

168. **Kolehmainen M, Vidal H, Alhava E, and Uusitupa MI**. Sterol regulatory element binding protein 1c (SREBP-1c) expression in human obesity. *Obesity Research* 9: 706-712, 2001.

169. **Komajda M, McMurray JJ, Beck-Nielsen H, Gomis R, Hanefeld M, Pocock SJ, Curtis PS, Jones NP, and Home PD**. Heart failure events with rosiglitazone in type 2 diabetes: data from the RECORD clinical trial. *Eur Heart J* 31: 824-831, 2010.

170. **Korenblat KM, Fabbrini E, Mohammed BS, and Klein S**. Liver, muscle, and adipose tissue insulin action is directly related to intrahepatic triglyceride content in obese subjects. *Gastroenterology* 134: 1369-1375, 2008.

171. **Koteish A, and Diehl AM**. Animal models of steatosis. *Seminars in Liver Disease* 21: 89-104, 2001.

172. **Koyama K, Chen G, Lee Y, and Unger RH**. Tissue triglycerides, insulin resistance, and insulin production: implications for hyperinsulinemia of obesity. *Am J Physiol* 273: E708-713, 1997.

173. **Kruis T, Batra A, and Siegmund B**. Bacterial translocation - impact on the adipocyte compartment. *Frontiers in Immunology* 4: 510, 2014.

174. **Lacey DC, Achuthan A, Fleetwood AJ, Dinh H, Roiniotis J, Scholz GM, Chang MW, Beckman SK, Cook AD, and Hamilton JA**. Defining GM-CSF- and macrophage-CSF-dependent macrophage responses by in vitro models. *J Immunol* 188: 5752-5765, 2012.

175. **Lakka HM, Laaksonen DE, Lakka TA, Niskanen LK, Kumpusalo E, Tuomilehto J, and Salonen JT**. The metabolic syndrome and total and cardiovascular disease mortality in middle-aged men. *JAMA* 288: 2709-2716, 2002.

176. **Lanaspa MA, Cicerchi C, Garcia G, Li N, Roncal-Jimenez CA, Rivard CJ, Hunter B, Andres-Hernando A, Ishimoto T, Sanchez-Lozada LG, Thomas J, Hodges RS, Mant CT, and Johnson RJ**. Counteracting roles of AMP deaminase and AMP kinase in the development of fatty liver. *PLoS One* 7: e48801, 2012.

177. **Lanaspa MA, Sanchez-Lozada LG, Choi YJ, Cicerchi C, Kanbay M, Roncal-Jimenez CA, Ishimoto T, Li N, Marek G, Duranay M, Schreiner G, Rodriguez-Iturbe B, Nakagawa T, Kang DH, Sautin YY, and Johnson RJ**. Uric acid induces hepatic steatosis by generation of mitochondrial oxidative stress: potential role in fructose-dependent and -independent fatty liver. *J Biol Chem* 287: 40732-40744, 2012.

178. **Landmesser U, Dikalov S, Price SR, McCann L, Fukai T, Holland SM, Mitch WE, and Harrison DG**. Oxidation of tetrahydrobiopterin leads to uncoupling of endothelial cell nitric oxide synthase in hypertension. *J Clin Invest* 111: 1201-1209, 2003.

179. **Langton P, Ward SM, Carl A, Norell MA, and Sanders KM**. Spontaneous electrical activity of interstitial cells of Cajal isolated from canine proximal colon. *Proc Natl Acad Sci U S A* 86: 7280-7284, 1989.

180. **Laplante M, and Sabatini DM**. mTORC1 activates SREBP-1c and uncouples lipogenesis from gluconeogenesis. *Proc Natl Acad Sci U S A* 107: 3281-3282, 2010.

181. **Large V, Reynisdottir S, Langin D, Fredby K, Klannemark M, Holm C, and Arner P**. Decreased expression and function of adipocyte hormone-sensitive lipase in subcutaneous fat cells of obese subjects. *J Lipid Res* 40: 2059-2066, 1999.

182. **Lawrence JA, Bryant D, Roberts KB, and Barrowman JA**. Effect of secretin on intestinal lymph flow and composition in the rat. *Quarterly Journal of Experimental Physiology* 66: 297-305, 1981.

183. **Leak LV, and Burke JF**. Ultrastructural studies on the lymphatic anchoring filaments. *The Journal of Cell Biology* 36: 129-149, 1968.

184. **Lee S, and Kwak HB**. Role of adiponectin in metabolic and cardiovascular disease. *Journal Of Exercise Rehabilitation* 10: 54-59, 2014.

185. **Leibowitz A, Rehman A, Paradis P, and Schiffrin EL**. Role of T regulatory lymphocytes in the pathogenesis of high-fructose diet-induced metabolic syndrome. *Hypertension* 61: 1316-1321, 2013.

186. **Li Z, Zhao ZJ, Zhu XQ, Ren QS, Nie FF, Gao JM, Gao XJ, Yang TB, Zhou WL, Shen JL, Wang Y, Lu FL, Chen XG, Hide G, Ayala FJ, and Lun ZR**. Differences in iNOS and arginase expression and activity in the macrophages of rats are responsible for the resistance against T. gondii infection. *PLoS One* 7: e35834, 2012.

187. **Liao S, Cheng G, Conner DA, Huang Y, Kucherlapati RS, Munn LL, Ruddle NH, Jain RK, Fukumura D, and Padera TP**. Impaired lymphatic contraction associated with immunosuppression. *PNAS* 108: 18784-18789, 2011.

188. **Lim S, Lee HK, Kimm KC, Park C, Shin C, and Cho NH**. C-reactive protein level as an independent risk factor of metabolic syndrome in the Korean population. CRP as risk factor of metabolic syndrome. *Diabetes Research and Clinical Practice* 70: 126-133, 2005.

189. **Lincoln TM, and Cornwell TL**. Towards an understanding of the mechanism of action of cyclic AMP and cyclic GMP in smooth muscle relaxation. *Blood Vessels* 28: 129-137, 1991.

190. **Liu M, and Liu F**. Regulation of adiponectin multimerization, signaling and function. *Best Practice & Research Clinical Endocrinology & Metabolism* 28: 25-31, 2014.

191. **Lobov GI, and Kubyshkina NA**. Mechanisms underlying the effect of E. coli endotoxin on contractile function of lymphatic vessels. *Bull Exp Biol Med* 137: 114-116, 2004.

192. **Loffreda S, Yang SQ, Lin HZ, Karp CL, Brengman ML, Wang DJ, Klein AS, Bulkley GB, Bao C, Noble PW, Lane MD, and Diehl AM**. Leptin regulates proinflammatory immune responses. *FASEB J* 12: 57-65, 1998.

193. **Loughlin V**. Massive obesity simulating lymphedema. *N Engl J Med* 328: 1496, 1993.

194. **Lteif AA, Han K, and Mather KJ**. Obesity, insulin resistance, and the metabolic syndrome: determinants of endothelial dysfunction in whites and blacks. *Circulation* 112: 32-38, 2005.

195. **Lumeng CN, Bodzin JL, and Saltiel AR**. Obesity induces a phenotypic switch in adipose tissue macrophage polarization. *J Clin Invest* 117: 175-184, 2007.

196. **Lumeng CN, DelProposto JB, Westcott DJ, and Saltiel AR**. Phenotypic switching of adipose tissue macrophages with obesity is generated by spatiotemporal differences in macrophage subtypes. *Diabetes* 57: 3239-3246, 2008.

197. **Maenpaa PH, Raivio KO, and Kekomaki MP**. Liver adenine nucleotides: fructose-induced depletion and its effect on protein synthesis. *Science* 161: 1253-1254, 1968.

198. **Magne J, Mariotti F, Fischer R, Mathe V, Tome D, and Huneau JF**. Early postprandial low-grade inflammation after high-fat meal in healthy rats: possible involvement of visceral adipose tissue. *J Nutr Biochem* 21: 550-555, 2010.

199. **Malik S, Wong ND, Franklin SS, Kamath TV, L'Italien GJ, Pio JR, and Williams GR**. Impact of the metabolic syndrome on mortality from coronary heart

disease, cardiovascular disease, and all causes in United States adults. *Circulation* 110: 1245-1250, 2004.

200. **Mantovani A, Sica A, Sozzani S, Allavena P, Vecchi A, and Locati M**. The chemokine system in diverse forms of macrophage activation and polarization. *Trends Immunol* 25: 677-686, 2004.

201. **Marken Lichtenbelt WD, and Fogelholm M**. Increased extracellular water compartment, relative to intracellular water compartment, after weight reduction. *Journal of Applied Physiology* 87: 294-298, 1999.

202. **Marttila-Ichihara F, Turja R, Miiluniemi M, Karikoski M, Maksimow M, Niemela J, Martinez-Pomares L, Salmi M, and Jalkanen S**. Macrophage mannose receptor on lymphatics controls cell trafficking. *Blood* 112: 64-72, 2008.

203. **Matarese G, Moschos S, and Mantzoros CS**. Leptin in immunology. *J Immunol* 174: 3137-3142, 2005.

204. **Mathias R, and von der Weid PY**. Involvement of the NO-cGMP-K(ATP) channel pathway in the mesenteric lymphatic pump dysfunction observed in the guinea pig model of TNBS-induced ileitis. *Am J Physiol Gastrointest Liver Physiol* 304: G623-634, 2013.

205. **Matsubara M, Maruoka S, and Katayose S**. Inverse relationship between plasma adiponectin and leptin concentrations in normal-weight and obese women. *European Journal of Endocrinology*147: 173-180, 2002.

206. **Maurice DH**. Cyclic nucleotide phosphodiesterase-mediated integration of cGMP and cAMP signaling in cells of the cardiovascular system. *Frontiers in Bioscience : A Journal and Virtual Library* 10: 1221-1228, 2005.

207. **McHale NG, and Meharg MK**. Co-ordination of pumping in isolated bovine lymphatic vessels. *J Physiol* 450: 503-512, 1992.

208. **Mehrara BJ, and Greene AK**. Lymphedema and obesity: is there a link? *Plastic and Reconstructive Surgery* 134: 154e-160e, 2014.

209. **Meijssen S, Cabezas MC, Ballieux CG, Derksen RJ, Bilecen S, and Erkelens DW**. Insulin mediated inhibition of hormone sensitive lipase activity in vivo in relation to endogenous catecholamines in healthy subjects. *J Clin Endocrinol Metab* 86: 4193-4197, 2001.

210. **Meyer MR, Fredette NC, Barton M, and Prossnitz ER**. Regulation of vascular smooth muscle tone by adipose-derived contracting factor. *PLoS One* 8: e79245, 2013.

211. **Miller NE, Michel CC, Nanjee MN, Olszewski WL, Miller IP, Hazell M, Olivecrona G, Sutton P, Humphreys SM, and Frayn KN**. Secretion of adipokines by human adipose tissue in vivo: partitioning between capillary and lymphatic transport. *American Journal of Physiology Endocrinology and Metabolism* 301: E659-667, 2011.

212. **Mislin H**. Active contractility of the lymphangion and coordination of lymphangion chains. *Experientia* 32: 820-822, 1976.

213. **Miura K, and Ohnishi H**. Role of gut microbiota and Toll-like receptors in nonalcoholic fatty liver disease. *World J Gastroenterol* 20: 7381-7391, 2014.

214. **Modolin ML, Cintra W, Jr., Paggiaro AO, Faintuch J, Gemperli R, and Ferreira MC**. Massive localized lymphedema (MLL) in bariatric candidates. *Obesity Surgery* 16: 1126-1130, 2006.

215. **Modolin ML, Cintra W, Jr., Paggiaro AO, Faintuch J, Gemperli R, and Ferreira MC**. Massive localized lymphedema (MLL) in bariatric candidates. *Obes Surg* 16: 1126-1130, 2006.

216. **Molofsky AB, Nussbaum JC, Liang HE, Van Dyken SJ, Cheng LE, Mohapatra A, Chawla A, and Locksley RM**. Innate lymphoid type 2 cells sustain visceral adipose tissue eosinophils and alternatively activated macrophages. *J Exp Med* 210: 535-549, 2013.

217. **Montagnani M, Chen H, Barr VA, and Quon MJ**. Insulin-stimulated activation of eNOS is independent of Ca2+ but requires phosphorylation by Akt at Ser(1179). *J Biol Chem* 276: 30392-30398, 2001.

218. **Mosser DM**. The many faces of macrophage activation. *Journal of Leukocyte Biology* 73: 209-212, 2003.

219. **Mosser DM, and Edwards JP**. Exploring the full spectrum of macrophage activation. *Nat Rev Immunol* 8: 958-969, 2008.

220. **Mosser DM, and Karp CL**. Receptor mediated subversion of macrophage cytokine production by intracellular pathogens. *Current Opinion in Immunology* 11: 406-411, 1999.

221. **Mullner N, Lazar A, and Hrabak A**. Enhanced utilization and altered metabolism of arginine in inflammatory macrophages caused by raised nitric oxide

synthesis. *The International Journal of Biochemistry & Cell Biology* 34: 1080-1090, 2002.

222. **Murano I, Barbatelli G, Parisani V, Latini C, Muzzonigro G, Castellucci M, and Cinti S**. Dead adipocytes, detected as crown-like structures, are prevalent in visceral fat depots of genetically obese mice. *J Lipid Res* 49: 1562-1568, 2008.

223. **Murthy KS, Zhou H, Grider JR, and Makhlouf GM**. Inhibition of sustained smooth muscle contraction by PKA and PKG preferentially mediated by phosphorylation of RhoA. *Am J Physiol Gastrointest Liver Physiol* 284: G1006-1016, 2003.

224. **Murumalla RK, Gunasekaran MK, Padhan JK, Bencharif K, Gence L, Festy F, Cesari M, Roche R, and Hoareau L**. Fatty acids do not pay the toll: effect of SFA and PUFA on human adipose tissue and mature adipocytes inflammation. *Lipids in Health and Disease* 11: 175, 2012.

225. **Musil D, Kaletova M, and Herman J**. Age, body mass index and severity of primary chronic venous disease. *Biomedical Papers of the Medical Faculty of the University Palacky, Olomouc, Czechoslovakia* 155: 367-371, 2011.

226. **Muthuchamy M, Gashev A, Boswell N, Dawson N, and Zawieja D**. Molecular and functional analyses of the contractile apparatus in lymphatic muscle. *FASEB J* 17: 920-922, 2003.

227. **Muthuchamy M, Rethinasamy P, and Wieczorek DF**. Tropomyosin structure and function new insights. *Trends in Cardiovascular Medicine* 7: 124-128, 1997.

228. **Muthuchamy M, and Zawieja D**. Molecular regulation of lymphatic contractility. *Ann N Y Acad Sci* 1131: 89-99, 2008.

229. **Nagai Y, Nishio Y, Nakamura T, Maegawa H, Kikkawa R, and Kashiwagi A**. Amelioration of high fructose-induced metabolic derangements by activation of PPARalpha. *Am J Physiol Endocrinol Metab* 282: E1180-1190, 2002.

230. **Nagaoka T, Kuo L, Ren Y, Yoshida A, and Hein TW**. C-reactive protein inhibits endothelium-dependent nitric oxide-mediated dilation of retinal arterioles via enhanced superoxide production. *Investigative Ophthalmology & Visual Science* 49: 2053-2060, 2008.

231. **Nakano S, Kuboki K, Matsumoto T, Nishimura C, and Yoshino G**. Small, dense LDL and high-sensitivity C-reactive protein (hs-CRP) in metabolic syndrome with type 2 diabetes mellitus. *Journal of Atherosclerosis and Thrombosis* 17: 410-415, 2010.

232. **Natali A, Toschi E, Baldeweg S, Ciociaro D, Favilla S, Sacca L, and Ferrannini E**. Clustering of insulin resistance with vascular dysfunction and low-grade inflammation in type 2 diabetes. *Diabetes* 55: 1133-1140, 2006.

233. **Nesto RW, Bell D, Bonow RO, Fonseca V, Grundy SM, Horton ES, Le Winter M, Porte D, Semenkovich CF, Smith S, Young LH, and Kahn R**. Thiazolidinedione use, fluid retention, and congestive heart failure: a consensus statement from the American Heart Association and American Diabetes Association. *Diabetes Care* 27: 256-263, 2004.

234. **Nomura F, Akashi S, Sakao Y, Sato S, Kawai T, Matsumoto M, Nakanishi K, Kimoto M, Miyake K, Takeda K, and Akira S**. Cutting edge: endotoxin tolerance

in mouse peritoneal macrophages correlates with down-regulation of surface toll-like receptor 4 expression. *J Immunol* 164: 3476-3479, 2000.

235. **Nussbaum JC, Van Dyken SJ, von Moltke J, Cheng LE, Mohapatra A, Molofsky AB, Thornton EE, Krummel MF, Chawla A, Liang HE, and Locksley RM**. Type 2 innate lymphoid cells control eosinophil homeostasis. *Nature* 502: 245-248, 2013.

236. **Oda E**. C-Reactive protein cutoff-point of 0.65 mg/L may be appropriate not only as a component of metabolic syndrome but also as a risk predictor of cardiovascular disease. *Circulation Journal : Official Journal of the Japanese Circulation Society* 71: 1501; author reply 1502, 2007.

237. **Ogden CL, Carroll MD, Kit BK, and Flegal KM**. Prevalence of childhood and adult obesity in the United States, 2011-2012. *JAMA* 311: 806-814, 2014.

238. **Ohhashi T, and Azuma T**. Electrical activity and ultrastructure of bovine mesenteric lymphatics. *Lymphology* 12: 4-6, 1979.

239. **Owen JL, Zhang Y, Bae SH, Farooqi MS, Liang G, Hammer RE, Goldstein JL, and Brown MS**. Insulin stimulation of SREBP-1c processing in transgenic rat hepatocytes requires p70 S6-kinase. *Proc Natl Acad Sci U S A* 109: 16184-16189, 2012.

240. **Owen MK, Witzmann FA, McKenney ML, Lai X, Berwick ZC, Moberly SP, Alloosh M, Sturek M, and Tune JD**. Perivascular adipose tissue potentiates contraction of coronary vascular smooth muscle: influence of obesity. *Circulation* 128: 9-18, 2013.

241. **Padgett EL, and Pruett SB**. Evaluation of nitrite production by human monocyte-derived macrophages. *Biochemical and Biophysical Research Communications* 186: 775-781, 1992.

242. **Padwal R**. Thiazolidinediones increased risk for heart failure, myocardial infarction, and death in older patients with type 2 diabetes. *ACP Journal Club* 148: 13, 2008.

243. **Palanivel R, Fullerton MD, Galic S, Honeyman J, Hewitt KA, Jorgensen SB, and Steinberg GR**. Reduced Socs3 expression in adipose tissue protects female mice against obesity-induced insulin resistance. *Diabetologia* 55: 3083-3093, 2012.

244. **Paskett ED, Dean JA, Oliveri JM, and Harrop JP**. Cancer-related lymphedema risk factors, diagnosis, treatment, and impact: a review. *J Clin Oncol* 30: 3726-3733, 2012.

245. **Pegu A, Qin S, Fallert Junecko BA, Nisato RE, Pepper MS, and Reinhart TA**. Human lymphatic endothelial cells express multiple functional TLRs. *J Immunol* 180: 3399-3405, 2008.

246. **Perheentupa J, and Raivio K**. Fructose-induced hyperuricaemia. *Lancet* 2: 528-531, 1967.

247. **Pettinelli P, Del Pozo T, Araya J, Rodrigo R, Araya AV, Smok G, Csendes A, Gutierrez L, Rojas J, Korn O, Maluenda F, Diaz JC, Rencoret G, Braghetto I, Castillo J, Poniachik J, and Videla LA**. Enhancement in liver SREBP-1c/PPAR-alpha ratio and steatosis in obese patients: correlations with insulin resistance and n-3 long-

chain polyunsaturated fatty acid depletion. *Biochimica et Biophysica Acta* 1792: 1080-1086, 2009.

248. **Quick CM, Venugopal AM, Gashev AA, Zawieja DC, and Stewart RH**. Intrinsic pump-conduit behavior of lymphangions. *Am J Physiol Regul Integr Comp Physiol* 292: R1510-1518, 2007.

249. **Randolph GJ**. Dendritic cell migration to lymph nodes: cytokines, chemokines, and lipid mediators. *Semin Immunol* 13: 267-274, 2001.

250. **Randolph GJ, Angeli V, and Swartz MA**. Dendritic-cell trafficking to lymph nodes through lymphatic vessels. *Nat Rev Immunol* 5: 617-628, 2005.

251. **Recek C**. Venous pressure gradients in the lower extremity and the hemodynamic consequences. *Vasa* 39: 292-297, 2010.

252. **Ridker PM, Buring JE, Cook NR, and Rifai N**. C-reactive protein, the metabolic syndrome, and risk of incident cardiovascular events: an 8-year follow-up of 14 719 initially healthy American women. *Circulation* 107: 391-397, 2003.

253. **Rivera CA, Adegboyega P, van Rooijen N, Tagalicud A, Allman M, and Wallace M**. Toll-like receptor-4 signaling and Kupffer cells play pivotal roles in the pathogenesis of non-alcoholic steatohepatitis. *J Hepatol* 47: 571-579, 2007.

254. **Rockson SG**. Causes and consequences of lymphatic disease. *Annals of the New York Academy of Sciences* 1207 Suppl 1: E2-6, 2010.

255. **Rockson SG**. The lymphatics and the inflammatory response: lessons learned from human lymphedema. *Lymphat Res Biol* 11: 117-120, 2013.

256. **Rockson SG**. Lymphedema. *Current Treatment Options in Cardiovascular Medicine* 8: 129-136, 2006.

257. **Rockson SG**. Lymphedema, at the forefront. *Lymphat Res Biol* 7: 1-2, 2009.

258. **Rockson SG**. Update on the biology and treatment of lymphedema. *Current Treatment Options in Cardiovascular Medicine* 14: 184-192, 2012.

259. **Ruderman NB, Carling D, Prentki M, and Cacicedo JM**. AMPK, insulin resistance, and the metabolic syndrome. *J Clin Invest* 123: 2764-2772, 2013.

260. **Rybalkin SD, Yan C, Bornfeldt KE, and Beavo JA**. Cyclic GMP phosphodiesterases and regulation of smooth muscle function. *Circ Res* 93: 280-291, 2003.

261. **Sakurai M, Takamura T, Ota T, Ando H, Akahori H, Kaji K, Sasaki M, Nakanuma Y, Miura K, and Kaneko S**. Liver steatosis, but not fibrosis, is associated with insulin resistance in nonalcoholic fatty liver disease. *Journal of Gastroenterology* 42: 312-317, 2007.

262. **Savetsky IL, Torrisi JS, Cuzzone DA, Ghanta S, Albano NJ, Gardenier JC, Joseph WJ, and Mehrara BJ**. Obesity increases inflammation and impairs lymphatic function in a mouse model of lymphedema. *Am J Physiol Heart Circ Physiol* 307: H165-172, 2014.

263. **Sawa Y, Ueki T, Hata M, Iwasawa K, Tsuruga E, Kojima H, Ishikawa H, and Yoshida S**. LPS-induced IL-6, IL-8, VCAM-1, and ICAM-1 expression in human lymphatic endothelium. *J Histochem Cytochem* 56: 97-109, 2008.

264. **Scallan JP, and Davis MJ**. Genetic removal of basal nitric oxide enhances contractile activity in isolated murine collecting lymphatic vessels. *J Physiol* 591: 2139-2156, 2013.

265. **Schaer DJ, Boretti FS, Schoedon G, and Schaffner A**. Induction of the CD163-dependent haemoglobin uptake by macrophages as a novel anti-inflammatory action of glucocorticoids. *British Journal of Haematology* 119: 239-243, 2002.

266. **Scheinfeld NS**. Obesity and dermatology. *Clin Dermatol* 22: 303-309, 2004.

267. **Schmid-Schonbein GW**. Nitric oxide (NO) side of lymphatic flow and immune surveillance. *PNAS* 109: 3-4, 2012.

268. **Schneemann M, and Schoeden G**. Macrophage biology and immunology: man is not a mouse. *Journal of Leukocyte Biology* 81: 579; discussion 580, 2007.

269. **Schneemann M, Schoedon G, Hofer S, Blau N, Guerrero L, and Schaffner A**. Nitric oxide synthase is not a constituent of the antimicrobial armature of human mononuclear phagocytes. *The Journal of Infectious Diseases* 167: 1358-1363, 1993.

270. **Schubert R, Lidington D, and Bolz SS**. The emerging role of Ca2+ sensitivity regulation in promoting myogenic vasoconstriction. *Cardiovasc Res* 77: 8-18, 2008.

271. **Schwartz EA, Zhang WY, Karnik SK, Borwege S, Anand VR, Laine PS, Su Y, and Reaven PD**. Nutrient modification of the innate immune response: a novel mechanism by which saturated fatty acids greatly amplify monocyte inflammation. *Arterioscler Thromb Vasc Biol* 30: 802-808, 2010.

272. **Seidel A, Belczak C, Campos M, Campos R, and Harada D**. The impact of obesity on venous insufficiency. *Phlebology / Venous Forum Of The Royal Society Of Medicine* 2014.

273. **Sewter C, Berger D, Considine RV, Medina G, Rochford J, Ciaraldi T, Henry R, Dohm L, Flier JS, O'Rahilly S, and Vidal-Puig AJ**. Human obesity and type 2 diabetes are associated with alterations in SREBP1 isoform expression that are reproduced ex vivo by tumor necrosis factor-alpha. *Diabetes* 51: 1035-1041, 2002.

274. **Shankar SS, and Steinberg HO**. Obesity and endothelial dysfunction. *Seminars in Vascular Medicine* 5: 56-64, 2005.

275. **Shao B, Lu M, Katz SC, Varley AW, Hardwick J, Rogers TE, Ojogun N, Rockey DC, Dematteo RP, and Munford RS**. A host lipase detoxifies bacterial lipopolysaccharides in the liver and spleen. *J Biol Chem* 282: 13726-13735, 2007.

276. **Sharabi Y, Oron-Herman M, Kamari Y, Avni I, Peleg E, Shabtay Z, Grossman E, and Shamiss A**. Effect of PPAR-gamma agonist on adiponectin levels in the metabolic syndrome: lessons from the high fructose fed rat model. *Am J Hypertens* 20: 206-210, 2007.

277. **Shi H, Kokoeva MV, Inouye K, Tzameli I, Yin H, and Flier JS**. TLR4 links innate immunity and fatty acid-induced insulin resistance. *J Clin Invest* 116: 3015-3025, 2006.

278. **Shimabukuro M, Higa N, Tagawa T, Yamakawa K, Sata M, and Ueda S**. Defects of vascular nitric oxide bioavailability in subjects with impaired glucose

tolerance: a potential link to insulin resistance. *International Journal of Cardiology* 167: 298-300, 2013.

279. **Shinozaki K, Kashiwagi A, Nishio Y, Okamura T, Yoshida Y, Masada M, Toda N, and Kikkawa R**. Abnormal biopterin metabolism is a major cause of impaired endothelium-dependent relaxation through nitric oxide/O2- imbalance in insulin-resistant rat aorta. *Diabetes* 48: 2437-2445, 1999.

280. **Shinozaki K, Nishio Y, Okamura T, Yoshida Y, Maegawa H, Kojima H, Masada M, Toda N, Kikkawa R, and Kashiwagi A**. Oral administration of tetrahydrobiopterin prevents endothelial dysfunction and vascular oxidative stress in the aortas of insulin-resistant rats. *Circ Res* 87: 566-573, 2000.

281. **Shirasawa Y, Ikomi F, and Ohhashi T**. Physiological roles of endogenous nitric oxide in lymphatic pump activity of rat mesentery in vivo. *Am J Physiol Gastrointest Liver Physiol* 278: G551-556, 2000.

282. **Shoelson SE, Lee J, and Goldfine AB**. Inflammation and insulin resistance. *J Clin Invest* 116: 1793-1801, 2006.

283. **Shulman GI**. Cellular mechanisms of insulin resistance. *J Clin Invest* 106: 171-176, 2000.

284. **Simmonds WJ**. The effect of fluid, electrolyte and food intake on thoracic duct lymph flow in unanaesthetized rats. *The Australian Journal of Experimental Biology And Medical Science* 32: 285-299, 1954.

285. **Singh U, Devaraj S, Vasquez-Vivar J, and Jialal I**. C-reactive protein decreases endothelial nitric oxide synthase activity via uncoupling. *J Mol Cell Cardiol* 43: 780-791, 2007.

286. **Skurk T, Alberti-Huber C, Herder C, and Hauner H**. Relationship between adipocyte size and adipokine expression and secretion. *J Clin Endocrinol Metab* 92: 1023-1033, 2007.

287. **Smith AG, Sheridan PA, Harp JB, and Beck MA**. Diet-induced obese mice have increased mortality and altered immune responses when infected with influenza virus. *J Nutr* 137: 1236-1243, 2007.

288. **Spalding KL, Arner E, Westermark PO, Bernard S, Buchholz BA, Bergmann O, Blomqvist L, Hoffstedt J, Naslund E, Britton T, Concha H, Hassan M, Ryden M, Frisen J, and Arner P**. Dynamics of fat cell turnover in humans. *Nature* 453: 783-787, 2008.

289. **Spooner PM, Chernick SS, Garrison MM, and Scow RO**. Insulin regulation of lipoprotein lipase activity and release in 3T3-L1 adipocytes. Separation and dependence of hormonal effects on hexose metabolism and synthesis of RNA and protein. *J Biol Chem* 254: 10021-10029, 1979.

290. **Spruss A, and Bergheim I**. Dietary fructose and intestinal barrier: potential risk factor in the pathogenesis of nonalcoholic fatty liver disease. *J Nutr Biochem* 20: 657-662, 2009.

291. **Spruss A, Kanuri G, Wagnerberger S, Haub S, Bischoff SC, and Bergheim I**. Toll-like receptor 4 is involved in the development of fructose-induced hepatic steatosis in mice. *Hepatology* 50: 1094-1104, 2009.

292. **Steinberg GR**. Inflammation in obesity is the common link between defects in fatty acid metabolism and insulin resistance. *Cell Cycle* 6: 888-894, 2007.

293. **Strissel KJ, DeFuria J, Shaul ME, Bennett G, Greenberg AS, and Obin MS**. T-cell recruitment and Th1 polarization in adipose tissue during diet-induced obesity in C57BL/6 mice. *Obesity (Silver Spring)* 18: 1918-1925, 2010.

294. **Suzuki T, Hirata K, Elkind MS, Jin Z, Rundek T, Miyake Y, Boden-Albala B, Di Tullio MR, Sacco R, and Homma S**. Metabolic syndrome, endothelial dysfunction, and risk of cardiovascular events: the Northern Manhattan Study (NOMAS). *American Heart Journal* 156: 405-410, 2008.

295. **Tagzirt M, Corseaux D, Pasquesoone L, Mouquet F, Roma-Lavisse C, Ung A, Lorenzi R, Jude B, Elkalioubie A, Van Belle E, Susen S, and Dupont A**. Alterations in neutrophil production and function at an early stage in the high-fructose rat model of metabolic syndrome. *Am J Hypertens* 27: 1096-1104, 2014.

296. **Tamakoshi K, Yatsuya H, Kondo T, Hori Y, Ishikawa M, Zhang H, Murata C, Otsuka R, Zhu S, and Toyoshima H**. The metabolic syndrome is associated with elevated circulating C-reactive protein in healthy reference range, a systemic low-grade inflammatory state. *International Journal of Obesity and Related Metabolic Disorders : Journal of the International Association for the Study of Obesity* 27: 443-449, 2003.

297. **Tanti JF, and Jager J**. Cellular mechanisms of insulin resistance: role of stress-regulated serine kinases and insulin receptor substrates (IRS) serine phosphorylation. *Curr Opin Pharmacol* 9: 753-762, 2009.

298. **Thangaswamy S, Bridenbaugh EA, and Gashev AA**. Evidence of increased oxidative stress in aged mesenteric lymphatic vessels. *Lymphat Res Biol* 10: 53-62, 2012.

299. **Thuy S, Ladurner R, Volynets V, Wagner S, Strahl S, Konigsrainer A, Maier KP, Bischoff SC, and Bergheim I**. Nonalcoholic fatty liver disease in humans is associated with increased plasma endotoxin and plasminogen activator inhibitor 1 concentrations and with fructose intake. *J Nutr* 138: 1452-1455, 2008.

300. **Tian YF, He CT, Chen YT, and Hsieh PS**. Lipoic acid suppresses portal endotoxemia-induced steatohepatitis and pancreatic inflammation in rats. *World J Gastroenterol* 19: 2761-2771, 2013.

301. **Turner SG, and Barrowman JA**. Intestinal lymph flow and lymphatic transport of protein during fat absorption. *Quarterly Journal of Experimental Physiology and Cognate Medical Sciences* 62: 175-180, 1977.

302. **Ueki K, Kondo T, Tseng YH, and Kahn CR**. Central role of suppressors of cytokine signaling proteins in hepatic steatosis, insulin resistance, and the metabolic syndrome in the mouse. *Proc Natl Acad Sci U S A* 101: 10422-10427, 2004.

303. **Unger BS, and Patil BM**. Apocynin improves endothelial function and prevents the development of hypertension in fructose fed rat. *Indian Journal of Pharmacology* 41: 208-212, 2009.

304. **van de Woestijne AP, Monajemi H, Kalkhoven E, and Visseren FL**. Adipose tissue dysfunction and hypertriglyceridemia: mechanisms and management. *Obesity Reviews : An Official Journal of the International Association for the Study of Obesity* 12: 829-840, 2011.

305. **van den Oever IA, Raterman HG, Nurmohamed MT, and Simsek S**. Endothelial dysfunction, inflammation, and apoptosis in diabetes mellitus. *Mediators Inflamm* 2010: 792393, 2010.

306. **van Hees AM, Jocken JW, Essers Y, Roche HM, Saris WH, and Blaak EE**. Adipose triglyceride lipase and hormone-sensitive lipase protein expression in subcutaneous adipose tissue is decreased after an isoenergetic low-fat high-complex carbohydrate diet in the metabolic syndrome. *Metabolism* 61: 1404-1412, 2012.

307. **Van Helden DF**. Pacemaker potentials in lymphatic smooth muscle of the guinea-pig mesentery. *J Physiol* 471: 465-479, 1993.

308. **van Rij AM, De Alwis CS, Jiang P, Christie RA, Hill GB, Dutton SJ, and Thomson IA**. Obesity and impaired venous function. *Eur J Vasc Endovasc Surg* 35: 739-744, 2008.

309. **Vander Haar E, Lee SI, Bandhakavi S, Griffin TJ, and Kim DH**. Insulin signalling to mTOR mediated by the Akt/PKB substrate PRAS40. *Nature Cell Biology* 9: 316-323, 2007.

310. **Vasileiou AM, Bull R, Kitou D, Alexiadou K, Garvie NJ, and Coppack SW**. Oedema in obesity; role of structural lymphatic abnormalities. *Int J Obes (Lond)* 35: 1247-1250, 2011.

311. **Veremeyko T, Siddiqui S, Sotnikov I, Yung A, and Ponomarev ED**. IL-4/IL-13-dependent and independent expression of miR-124 and its contribution to M2 phenotype of monocytic cells in normal conditions and during allergic inflammation. *PLoS One* 8: e81774, 2013.

312. **Verma S, Bhanot S, Yao L, and McNeill JH**. Vascular insulin resistance in fructose-hypertensive rats. *European Journal of Pharmacology* 322: R1-2, 1997.

313. **Vidal-Puig AJ, Considine RV, Jimenez-Linan M, Werman A, Pories WJ, Caro JF, and Flier JS**. Peroxisome proliferator-activated receptor gene expression in human tissues. Effects of obesity, weight loss, and regulation by insulin and glucocorticoids. *J Clin Invest* 99: 2416-2422, 1997.

314. **Vilar L, Canadas V, Arruda MJ, Arahata C, Agra R, Pontes L, Montenegro L, Vilar CF, Silva LM, Albuquerque JL, and Gusmao A**. Comparison of metformin, gliclazide MR and rosiglitazone in monotherapy and in combination for type 2 diabetes. *Arquivos Brasileiros de Endocrinologia e Metabologia* 54: 311-318, 2010.

315. **von der Weid PY**. ATP-sensitive K+ channels in smooth muscle cells of guinea-pig mesenteric lymphatics: role in nitric oxide and beta-adrenoceptor agonist-induced hyperpolarizations. *British Journal Of Pharmacology* 125: 17-22, 1998.

316. **von der Weid PY**. Review article: lymphatic vessel pumping and inflammation--the role of spontaneous constrictions and underlying electrical pacemaker potentials. *Aliment Pharmacol Ther* 15: 1115-1129, 2001.

317. **von der Weid PY, Crowe MJ, and Van Helden DF**. Endothelium-dependent modulation of pacemaking in lymphatic vessels of the guinea-pig mesentery. *J Physiol* 493 (Pt 2): 563-575, 1996.

318. **von der Weid PY, Lee S, Imtiaz MS, Zawieja DC, and Davis MJ**. Electrophysiological properties of rat mesenteric lymphatic vessels and their regulation by stretch. *Lymphat Res Biol* 12: 66-75, 2014.

319. **von der Weid PY, and Muthuchamy M**. Regulatory mechanisms in lymphatic vessel contraction under normal and inflammatory conditions. *Pathophysiology* 17: 263-276, 2010.

320. **von der Weid PY, Rahman M, Imtiaz MS, and van Helden DF**. Spontaneous transient depolarizations in lymphatic vessels of the guinea pig mesentery: pharmacology and implication for spontaneous contractility. *Am J Physiol Heart Circ Physiol* 295: H1989-2000, 2008.

321. **von der Weid PY, Rehal S, Dyrda P, Lee S, Mathias R, Rahman M, Roizes S, and Imtiaz MS**. Mechanisms of VIP-induced inhibition of the lymphatic vessel pump. *J Physiol* 590: 2677-2691, 2012.

322. **von der Weid PY, and Zawieja DC**. Lymphatic smooth muscle: the motor unit of lymph drainage. *The International Journal of Biochemistry & Cell Biology* 36: 1147-1153, 2004.

323. **von der Weid PY, Zhao J, and Van Helden DF**. Nitric oxide decreases pacemaker activity in lymphatic vessels of guinea pig mesentery. *Am J Physiol Heart Circ Physiol* 280: H2707-2716, 2001.

324. **Waki M, Kral JG, Mazariegos M, Wang J, Pierson RN, Jr., and Heymsfield SB**. Relative expansion of extracellular fluid in obese vs. nonobese women. *The American Journal of Physiology* 261: E199-203, 1991.

325. **Wang HJ, Zakhari S, and Jung MK**. Alcohol, inflammation, and gut-liver-brain interactions in tissue damage and disease development. *World J Gastroenterol* 16: 1304-1313, 2010.

326. **Wang W, Nepiyushchikh Z, Zawieja DC, Chakraborty S, Zawieja SD, Gashev AA, Davis MJ, and Muthuchamy M**. Inhibition of myosin light chain phosphorylation decreases rat mesenteric lymphatic contractile activity. *American Journal of Physiology Heart and Circulatory Physiology* 297: H726-734, 2009.

327. **Wang X, Nie J, Jia Z, Feng M, Zheng Z, Chen W, Li X, Peng W, Zhang S, Sun L, Mao H, Lan HY, and Yu X**. Impaired TGF-beta signalling enhances peritoneal inflammation induced by E. coli in rats. *Nephrology, Dialysis, Transplantation : Official Publication of the European Dialysis and Transplant Association - European Renal Association* 25: 399-412, 2010.

328. **Wang Y, Ghoshal S, Ward M, de Villiers W, Woodward J, and Eckhardt E**. Chylomicrons promote intestinal absorption and systemic dissemination of dietary antigen (ovalbumin) in mice. *PLoS One* 4: e8442, 2009.

329. **Wang Y, and Oliver G**. Current views on the function of the lymphatic vasculature in health and disease. *Genes Dev* 24: 2115-2126, 2010.

330. **Weitman ES, Aschen SZ, Farias-Eisner G, Albano N, Cuzzone DA, Ghanta S, Zampell JC, Thorek D, and Mehrara BJ**. Obesity impairs lymphatic fluid transport and dendritic cell migration to lymph nodes. *PLoS One* 8: e70703, 2013.

331. **Wesselman JP, Spaan JA, van der Meulen ET, and VanBavel E**. Role of protein kinase C in myogenic calcium-contraction coupling of rat cannulated mesenteric small arteries. *Clin Exp Pharmacol Physiol* 28: 848-855, 2001.

332. **West M**. Dead adipocytes and metabolic dysfunction: recent progress. *Curr Opin Endocrinol Diabetes Obes* 16: 178-182, 2009.

333. **White UA, and Stephens JM**. Transcriptional factors that promote formation of white adipose tissue. *Molecular and Cellular Endocrinology* 318: 10-14, 2010.

334. **Wijesundera KK, Izawa T, Murakami H, Tennakoon AH, Golbar HM, Kato-Ichikawa C, Tanaka M, Kuwamura M, and Yamate J**. M1- and M2-macrophage polarization in thioacetamide (TAA)-induced rat liver lesions; a possible analysis for hepato-pathology. *Histology and Histopathology* 29: 497-511, 2014.

335. **Wijesundera KK, Izawa T, Tennakoon AH, Murakami H, Golbar HM, Katou-Ichikawa C, Tanaka M, Kuwamura M, and Yamate J**. M1- and M2-macrophage polarization in rat liver cirrhosis induced by thioacetamide (TAA), focusing on Iba1 and galectin-3. *Experimental and Molecular Pathology* 96: 382-392, 2014.

336. **Willenberg T, Schumacher A, Amann-Vesti B, Jacomella V, Thalhammer C, Diehm N, Baumgartner I, and Husmann M**. Impact of obesity on venous hemodynamics of the lower limbs. *Journal of Vascular Surgery* 52: 664-668, 2010.

337. **Wu D, Molofsky AB, Liang HE, Ricardo-Gonzalez RR, Jouihan HA, Bando JK, Chawla A, and Locksley RM**. Eosinophils sustain adipose alternatively activated macrophages associated with glucose homeostasis. *Science* 332: 243-247, 2011.

338. **Wu G, and Meininger CJ**. Nitric oxide and vascular insulin resistance. *BioFactors* 35: 21-27, 2009.

339. **Wu Q, Ortegon AM, Tsang B, Doege H, Feingold KR, and Stahl A**. FATP1 is an insulin-sensitive fatty acid transporter involved in diet-induced obesity. *Molecular and Cellular Biology* 26: 3455-3467, 2006.

340. **Wu TF, Carati CJ, Macnaughton WK, and von der Weid PY**. Contractile activity of lymphatic vessels is altered in the TNBS model of guinea pig ileitis. *Am J Physiol Gastrointest Liver Physiol* 291: G566-574, 2006.

341. **Xu H, Barnes GT, Yang Q, Tan G, Yang D, Chou CJ, Sole J, Nichols A, Ross JS, Tartaglia LA, and Chen H**. Chronic inflammation in fat plays a crucial role in the development of obesity-related insulin resistance. *J Clin Invest* 112: 1821-1830, 2003.

342. **Yamauchi T, Kamon J, Minokoshi Y, Ito Y, Waki H, Uchida S, Yamashita S, Noda M, Kita S, Ueki K, Eto K, Akanuma Y, Froguel P, Foufelle F, Ferre P, Carling D, Kimura S, Nagai R, Kahn BB, and Kadowaki T**. Adiponectin stimulates glucose utilization and fatty-acid oxidation by activating AMP-activated protein kinase. *Nat Med* 8: 1288-1295, 2002.

343. **Yang SQ, Lin HZ, Lane MD, Clemens M, and Diehl AM**. Obesity increases sensitivity to endotoxin liver injury: implications for the pathogenesis of steatohepatitis. *Proc Natl Acad Sci U S A* 94: 2557-2562, 1997.

344. **Yao LC, Baluk P, Srinivasan RS, Oliver G, and McDonald DM**. Plasticity of button-like junctions in the endothelium of airway lymphatics in development and inflammation. *Am J Pathol* 180: 2561-2575, 2012.

345. **Yoon MJ, Lee GY, Chung JJ, Ahn YH, Hong SH, and Kim JB**. Adiponectin increases fatty acid oxidation in skeletal muscle cells by sequential activation of AMP-activated protein kinase, p38 mitogen-activated protein kinase, and peroxisome proliferator-activated receptor alpha. *Diabetes* 55: 2562-2570, 2006.

346. **Yuan G, Zhou L, Tang J, Yang Y, Gu W, Li F, Hong J, Gu Y, Li X, Ning G, and Chen M**. Serum CRP levels are equally elevated in newly diagnosed type 2 diabetes and impaired glucose tolerance and related to adiponectin levels and insulin sensitivity. *Diabetes Research and Clinical Practice* 72: 244-250, 2006.

347. **Yudkin JS, Stehouwer CD, Emeis JJ, and Coppack SW**. C-reactive protein in healthy subjects: associations with obesity, insulin resistance, and endothelial dysfunction: a potential role for cytokines originating from adipose tissue? *Arterioscler Thromb Vasc Biol* 19: 972-978, 1999.

348. **Zaccolo M, and Movsesian MA**. cAMP and cGMP signaling cross-talk: role of phosphodiesterases and implications for cardiac pathophysiology. *Circ Res* 100: 1569-1578, 2007.

349. **Zampell JC, Aschen S, Weitman ES, Yan A, Elhadad S, De Brot M, and Mehrara BJ**. Regulation of adipogenesis by lymphatic fluid stasis: part I. Adipogenesis, fibrosis, and inflammation. *Plastic And Reconstructive Surgery* 129: 825-834, 2012.

350. **Zampell JC, Yan A, Avraham T, Andrade V, Malliaris S, Aschen S, Rockson SG, and Mehrara BJ**. Temporal and spatial patterns of endogenous danger signal expression after wound healing and in response to lymphedema. *Am J Physiol Cell Physiol* 300: C1107-1121, 2011.

351. **Zawieja D**. Lymphatic biology and the microcirculation: past, present and future. *Microcirculation* 12: 141-150, 2005.

352. **Zawieja DC**. Contractile physiology of lymphatics. *Lymphat Res Biol* 7: 87-96, 2009.

353. **Zawieja DC, and Davis KL**. Inhibition of the active lymph pump in rat mesenteric lymphatics by hydrogen peroxide. *Lymphology* 26: 135-142, 1993.

354. **Zawieja DC, Davis KL, Schuster R, Hinds WM, and Granger HJ**. Distribution, propagation, and coordination of contractile activity in lymphatics. *Am J Physiol* 264: H1283-1291, 1993.

355. **Zawieja DC, Garcia C, and Granger HJ**. Oxygen radicals, enzymes, and fluid transport through pericardial interstitium. *Am J Physiol* 262: H136-143, 1992.

356. **Zawieja DC, Greiner ST, Davis KL, Hinds WM, and Granger HJ**. Reactive oxygen metabolites inhibit spontaneous lymphatic contractions. *Am J Physiol* 260: H1935-1943, 1991.

357. **Zawieja SD, Wang W, Wu X, Nepiyushchikh ZV, Zawieja DC, and Muthuchamy M**. Impairments in the intrinsic contractility of mesenteric collecting lymphatics in a rat model of metabolic syndrome. *Am J Physiol Heart Circ Physiol* 302: H643-653, 2012.

358. **Zhang Y, and Xing J**. Effect of transforming growth factor-beta1 on monocyte Toll-like receptor 4 expression in septic rats. *World Journal of Emergency Medicine* 2: 228-231, 2011.

359. **Zou H, Ratz PH, and Hill MA**. Role of myosin phosphorylation and [Ca2+]i in myogenic reactivity and arteriolar tone. *Am J Physiol* 269: H1590-1596, 1995.

APPENDIX

APSS	Albumin Physiological Saline Solution
CCL1	Chemokine Ligand 1
CCL2	Monocyte Chemoattractant Protein 1
CVD	Cardiovascular Disease
eNOS	Endothelial NOS
GMCSF	Granulocyte / Monocyte Colony Stimulating Factor
i.p	Intra-peritoneal
IL-6	Interleukin 6
iNOS	Inducible NOS
K_{ATP}	ATP Sensitive Potassium Channels
LNAME	L-N^G-Nitro Arginine Methyl Ester
LPS	Lipopolysaccharide
MCSF	Monocyte Colony Stimulating Factor
MetSyn	Metabolic Syndrome
MHCII	Major Histocompatibility Complex II
MLL	Massive Localized Lymphedema
MLV	Mesenteric Lymphatic Vessel
NO	Nitric Oxide
PSS	Physiological Saline Solution
QPCR	Quantitative Polymerase Chain Reaction

SNAP	S-Nitro-*N*-Acetylpenicillamine
TGFβ	Transforming Growth Factor β
TIIDM	Type II Diabetes Mellitus
TNFα	Tumor Necrosis Factor α